The Influence of Short Embedment and

Close Spacing on the Strength of

Hooked Bar Anchorages

By

LARRY A. JOHNSON

and

JAMES O. JIRSA

DEPARTMENT OF CIVIL ENGINEERING / Phil M. Ferguson Structural
                                        Engineering Laboratory
THE UNIVERSITY OF TEXAS AT AUSTIN

THE INFLUENCE OF SHORT EMBEDMENT AND CLOSE SPACING ON

THE STRENGTH OF HOOKED BAR ANCHORAGES

by

Larry A. Johnson and James O. Jirsa

Report on a Research Project

Sponsored by

The Reinforced Concrete Research Council--Project 33

and

U. S. Army Corps of Engineers Contract DACW39-78-M-2441

Phil M. Ferguson Structural Engineering Laboratory
Department of Civil Engineering
The University of Texas at Austin

April 1981

SUMMARY OF REPORT

The development of bars in reinforced concrete beams and/or slabs framing into relatively thin walls presents a special design problem. In anchoring bars in walls, standard 90° hooked bars are generally used. In some cases, the wall thickness will be sufficient to permit a short straight embedment between the hook and wall face. In thin walls the hook may start at the face (critical section) of the supporting wall. Full development of yield is highly unlikely in either case. Currently, no data concerning the efficiency of hooked anchorages with short embedment lengths exists. Design recommendations for such embedments are needed to cover the broad range of design situations encountered.

From the data obtained in earlier investigations conducted under Reinforced Concrete Research Council Project 33, equations were developed for the capacity or the required embedment length for a hooked bar failing in a side splitting mode.

In this investigation the behavior of hooked bar anchorages with short embedment lengths was evaluated. The specimens were intended to simulate (in full scale) typical anchorages in walls. In the study, the range of variables previously investigated under Project 33 was extended and design recommendations developed previously were examined to determine applicability to short embedments. The bar diameter, concrete strength, beam depth, lead embedment, transverse reinforcement, unbonded straight lead lengths, and spacing between hooked bars were varied.

ACKNOWLEDGMENTS

CONTENTS

LIST OF FIGURES

LIST OF TABLES

1. INTRODUCTION

1.1 Object and Scope

In this investigation, the behavior of hooked bar anchorages with short embedment lengths was evaluated. The specimens were intended to simulate (in full scale) typical anchorages in walls. In the study, the range of variables previously investigated under Reinforced Concrete Research Council Project 33 was extended and design recommendations developed previously were examined to determine applicability to short embedments. The bar diameter, concrete strength, beam depth, lead embedment, transverse reinforcement, unbonded straight lead lengths, and spacing between hooked bars were varied.

1.2 Definition of the Problem

The development of bars in reinforced concrete beams and/or slabs framing into relatively thin walls pose a serious design problem. In anchoring bars in walls, standard 90° hooked bars are generally used. In some cases, the wall thickness will be suffi-cient to permit a short straight embedment between the hook and wall face. In thin walls the hook may start at the face (critical section) of the supporting wall. Full development of yield is highly unlikely in either case.

Currently, no data concerning the efficiency of hooked anchorages with short embedment lengths exists. Design recommenda-tions for such embedments are needed to cover the broad range of design situations encountered.

1.3 Previous Studies

The investigation reported by Pinc, Watkins, and Jirsa [3] extended two earlier investigations [1,2] and led to a refinement

1

of design recommendations in Ref. 2. The strength of hooked bar
anchorages in beam-column joints was examined in Refs. 2 and 3
following work by Minor [1], which dealt with parameters influencing
the anchorage capacity of bent bars. For anchorages with equal
bonded length to bar diameter ratios (see Fig. 1.1), the trends
reported by Minor [1] can be summarized as follows:

(1) Bent bar anchorages slipped more at a given bar stress
than straight bars and the larger the angle of bend, the
greater the slip at a given bar stress.

(2) The smaller the radius of bend, the greater the slip at a
given bar stress.

(3) In a bent bar anchorage consisting of straight and curved
sections, most of the slip was developed in the curved
section.

(4) Hooks had little effect on ultimate strength except for
very short bond lengths.
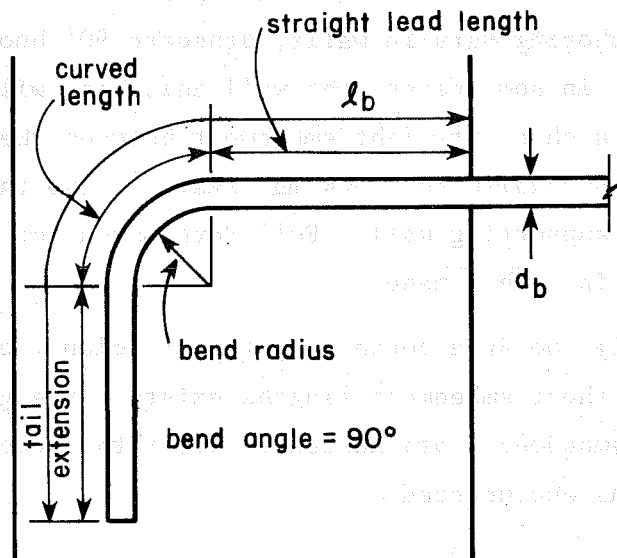
Fig. 1.1   Detail defining bond length ℓ_b and
hook geometry

The studies of hooked bar anchorages in beam-column joints [2,3] led to the following conclusions.

(1) Failure of a hooked bar was governed primarily by a loss of cover due to side splitting along a plane coinciding with the plane of the hooked bar (as shown in Fig. 1.2) rather than pulling out.

(2) At failure of the concrete, very little stress was transferred to the concrete along the straight lead embedment (Fig. 1.1) for small ratios of lead embedment to bar diameter.

(3) Length of embedment and the degree of lateral confinement of the joint seemed to be the principal factors affecting anchorage capacity.

Based on tests [2,3], the following equations were proposed for the capacity or the required embedment length for a hooked bar failing in a side splitting mode.

$$f_h = \frac{\sqrt{f'_c} \cdot \ell_{dh} \cdot \psi}{0.02 \cdot d_b} \tag{1.1}$$

and
$$\ell_{dh} = \frac{0.02 \, d_b f_h}{\psi \cdot \sqrt{f'_c}} \geq 8d_b \text{ or 6 in.} \tag{1.2}$$

whichever greater

The variables in Eqs. 1.1 and 1.2 are defined as follows:

d_b = bar diameter

ψ = one or more of the following factors as applicable:

(a) 1.0 unless the following conditions are satisfied.

(b) 1.4 for #11 bars or smaller where side cover normal to the plane of the hooked bar is not less than 2.5 in. and cover on the tail extension of 90° hooks is not less than 2 in.

(c) 1.8 if the conditions (b) are met and additional confinement by closed stirrups or hoops at a spacing of $3d_b$ (d_b of anchored bar) or less is provided.
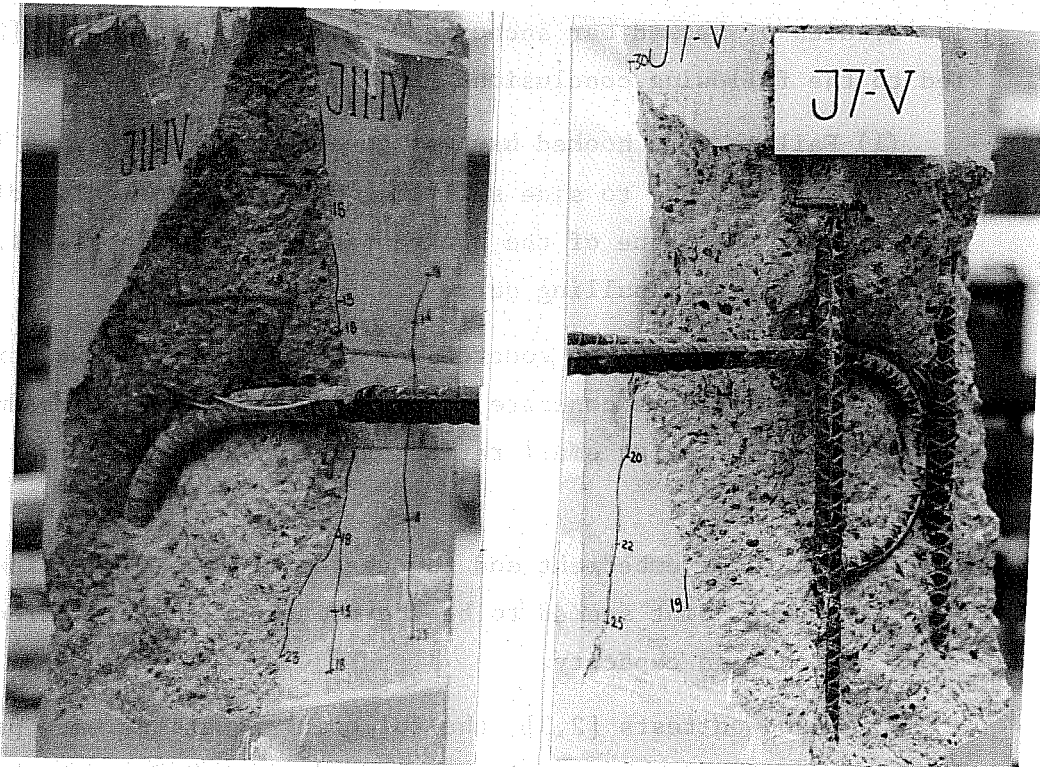
Fig. 1.2 Typical side cover splitting of columns (from Ref. 2)
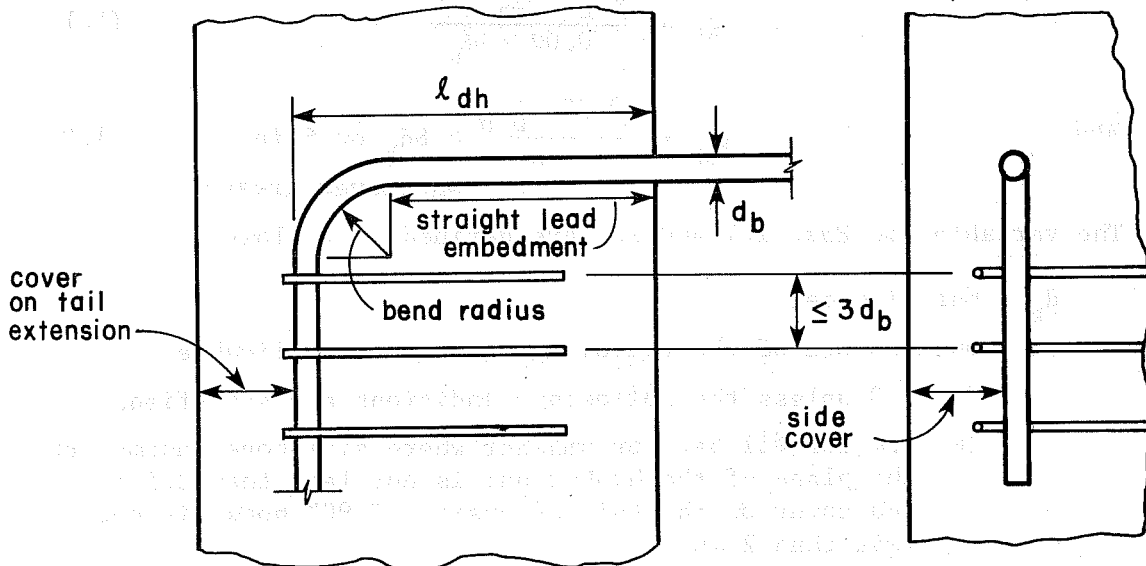
Fig. 1.3 Detail defining ℓ_{dh}

(d) $60000/f_y$ for reinforcement having yield strength other than 60000 psi.

(e) 0.83 for lightweight aggregate replacing all or a portion of the aggregate.

(f) A_{sp}/A_{sr} for reinforcement in flexural members in excess of that required,
where A_{sr} = area of reinforcement required
and A_{sp} = area of reinforcement provided.

Equations 1.1 and 1.2 reflect a greater number of variables than are considered in previous design provisions for hooked bars. However, the lack of data for hooked anchorages with short embedment lengths led to the investigation described in this report.

2. EXPERIMENTAL PROGRAM

2.1 Introduction

In the previous investigations supported by Reinforced Concrete Research Council Project 33 [2,3], tests were conducted on full-scale models of beam-column joints. Failure was generally governed by spalling or splitting of the column side cover. Side cover failure was not expected with hooked bar anchorages having a very short or no straight lead embedment. Short anchorages are most likely to occur in walls where there is adequate side cover on the hooked anchorages to prevent side spalling. The most obvious type of failure of a hooked bar anchorage with a short lead embedment is some type of a cone failure (similar to headed stud or anchor bolt failures) as shown in Fig. 2.1(a). For this reason, a specimen was designed in which the wall thickness could be varied and in which the width was sufficient to ensure the face splitting (cone) type of failure expected for a hooked bar anchored in a wall.

2.2 Specimen Geometry

Single Bar Specimens. The single bar specimens had a width of 24 in., a height of 52 in., and a single hooked bar protruding from the face. The thickness of the walls ranged from 3.5 to 8.5 in., depending primarily on the size of the hooked bar to be anchored (see Fig. 2.2). For instance, 3.5 in. was the minimum wall thickness for a standard ACI #4 hooked bar with 1.5 in. of concrete cover over the tail extension. Likewise, a 5 in. wall was needed for a #7 hooked bar with 1.5 in. cover over the tail extension. For a #11 bar, an 8.5 in. thick wall was used (see Table 2.1). A cover of 1.5 in. on the tail extension of the hooked bar anchorages was used to prevent an early splitting failure of the back cover which might occur due to prying of the tail extension on the back cover as the hook

7
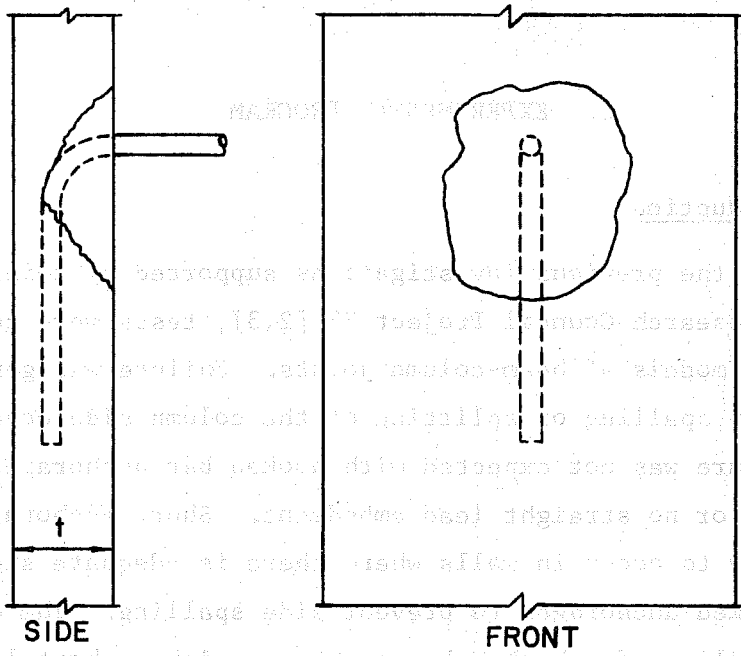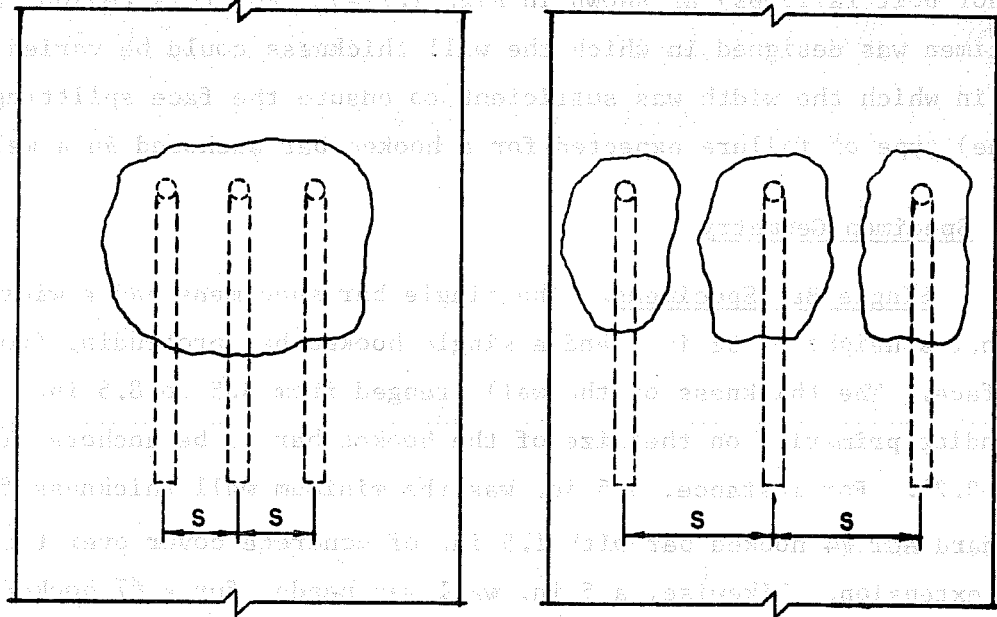
(a) Single bar specimen

(b) Multiple bar specimens

Fig. 2.1 Expected mode of failure for wall anchorages

STRAIGHT LEAD
EMBEDMENT

D

d

12 d

TAIL
EXTENSION

D= 6d FOR #4 & #7
D= 8d FOR #9 & #11
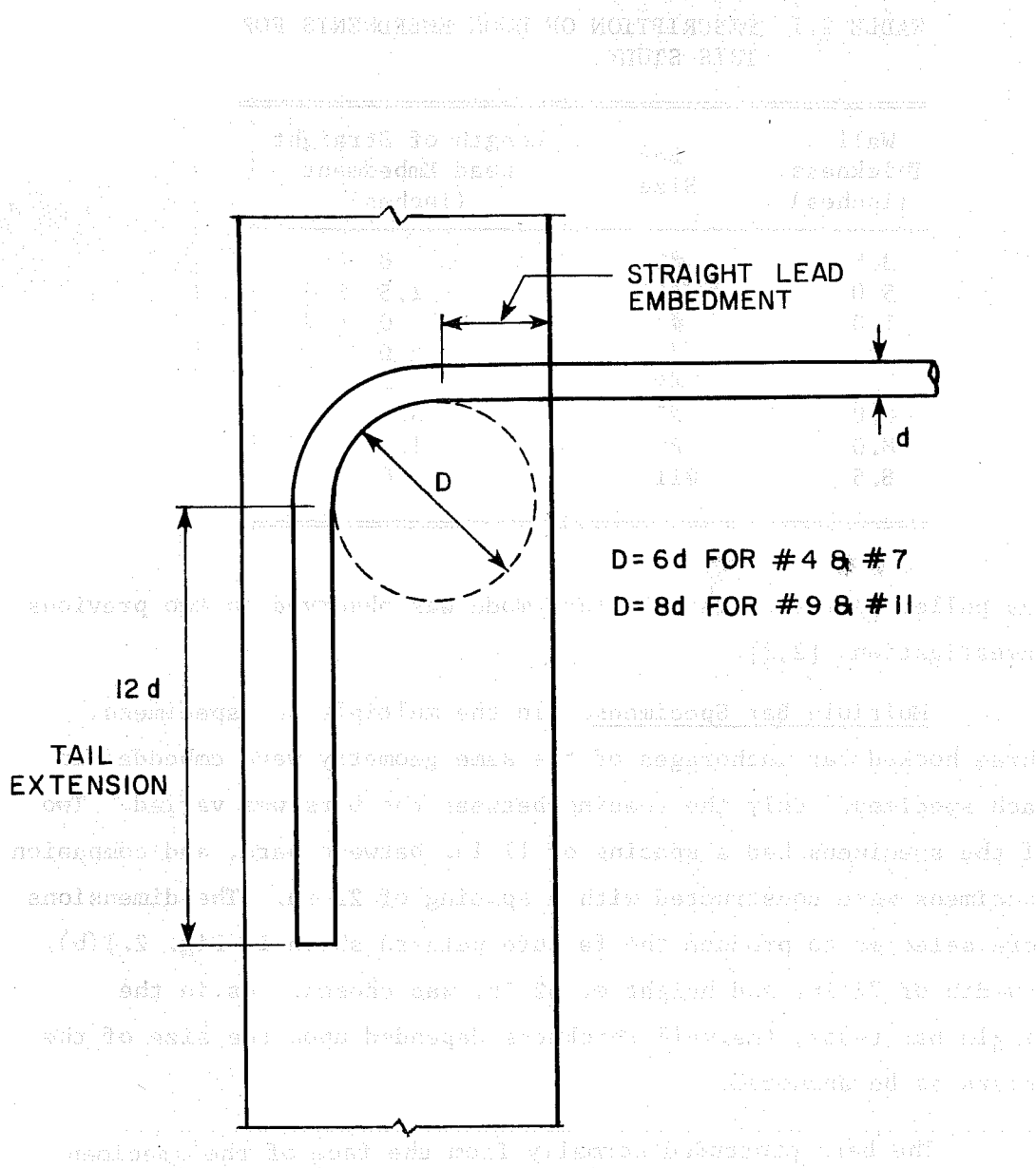
Fig. 2.2   Typical ACI Standard 90° Hook in a wall

10

TABLE 2.1   DESCRIPTION OF HOOK EMBEDMENTS FOR
             THIS STUDY

Wall Thickness (inches)	Bar Size	Length of Straight Lead Embedment (inches)
3.5	#4	0
5.0	#4	1.5
5.0	#7	0
7.0	#7	2.0
7.0	#9	0
8.0	#7	3.0
8.0	#9	1.0
8.5	#11	0

was pulled forward. This failure mode was observed in two previous investigations [2,3].

Multiple Bar Specimens. In the multiple bar specimens, three hooked bar anchorages of the same geometry were embedded in each specimen. Only the spacing between the bars was varied. Two of the specimens had a spacing of 11 in. between bars, and companion specimens were constructed with a spacing of 22 in. The dimensions were selected to produce the failure pattern shown in Fig. 2.1(b). A width of 72 in. and height of 52 in. was chosen. As in the single bar tests, the wall thickness depended upon the size of the rebars to be anchored.

The bars protruded normally from the face of the specimen at a height of 28 in. above the base. The bars were positioned as close to midheight as possible. The tail extensions of all the hooked bars fit within the 28 in. vertical distance between the base of the wall and the center of the protruding bar.

2.3 Reinforcement Details

Figure 2.3 shows a typical reinforcement layout for a single bar specimen. Grade 60 reinforcement was used throughout. The moment capacity of the walls was substantially greater than required to preclude an early flexural failure. In some cases the vertical wall reinforcement was determined by the minimum requirements of the ACI 318-77 Building Code. In all cases, the horizontal reinforcement was controlled by minimum code requirements for horizontal steel in walls. Concrete cover of 3/4 in. was maintained on all vertical reinforcement with the horizontal steel placed inside the vertical. To limit the influence of the vertical and horizontal steel on anchorage strength, the wall reinforcement was placed at least 6 in. from the protruding bar. No horizontal reinforcement was placed in front of the hook or tail extension, except in two special tests in which the effect of transverse bars was examined.

2.4 Variables

The major portion of this investigation was concerned with the effect of four variables on the strength and failure pattern of the single hooked bar anchorages. The variables studied include: (1) diameter of the hooked bar, (2) straight lead embedment (wall thickness), (3) lever arm, denoted as Z (see Fig. 2.3), and (4) concrete compressive strength (f_c').

Size of Hooked Bar Anchorage. Four bar sizes were used in the investigation: #4, #7, #9, and #11 in the single bar specimens, and #7 and #11 bars in the triple bar specimens. It is unlikely that #9 and #11 hooked anchorages with short lead embedment would be used in practice. The #4 and #7 hooked bars are probably more realistic, especially when the start of the hook is close to the face of the wall.

Straight Lead Embedment (Wall Thickness). By varying the wall thickness and fixing the concrete cover on the tail extension

GENERAL
REINFORCEMENT SCHEDULE

Wall Thickness	Size Anchor	Vert. Steel	Horz. Steel
3.5in.	#4	#3	#3
5.0	#4	#3	#3
5.0	#7	#5	#3
7.0	#7	#4	#4
7.0	#9	#6	#4
8.0	#7	#4	#4
8.0	#9	#6	#4
8.5	#11	#7	#4

1·1/2" CONCRETE COVER ON
TAIL EXTENSION OF HOOK

3/4" CONCRETE COVER ON
VERTICAL STEEL
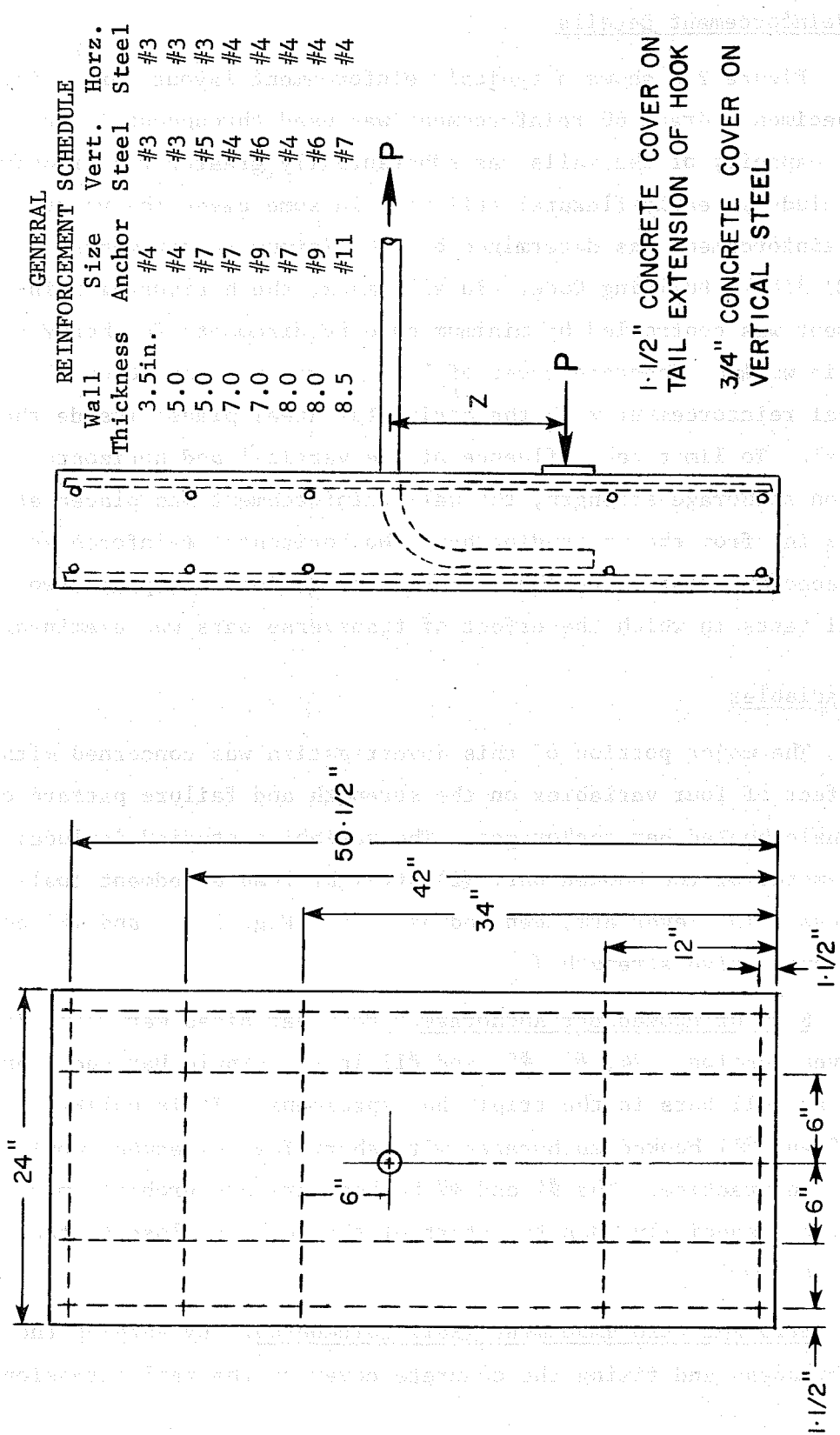
Fig. 2.3   Typical specimen reinforcement details

of the hook, the amount of straight lead embedment in front of the hook was varied from a minimum of zero (the start of the hook coincided with the face of the wall) to a maximum of about 3 in. (a #7 hooked bar embedded in an 8 in. wall).

Lever Arm (Z). An important objective of this investigation was to study the effect of different beam or slab depths framing into the wall. It was felt that the lever arm, or distance between the centroid of the tensile reinforcement in the beam or slab and the centroid of the compressive zone as shown in Fig. 2.4, would be instrumental in determining the hooked anchorage strength and failure pattern.

Concrete Compressive Strength (f_c'). In order to investigate the influence of different concrete strengths, a series of 12 tests with varying f_c' was conducted: four of relatively low strength concrete (2500 psi), four of moderate strength concrete (4500 psi), and four of relatively high strength concrete (5800 psi).

2.5 Specimen Notation

Thirty-six specimens were tested during the course of this project. To identify the variables in each specimen, a simple notation was developed. For each specimen the notation consisted of four symbols. The first symbol indicates the diameter of the hooked bar. The second gives the wall thickness in inches. The third symbol provides the lever arm length (Z) in inches. A fourth letter (L, M, or H) indicates the nominal concrete strength at the time of testing--L for a low f_c' of about 2500 psi, M for a medium strength concrete of about 4500 psi, and H for a high strength concrete of about 5800 psi. For example, specimen 7-5-14-M had a #7 hooked bar embedded in a 5 in. thick wall. The internal lever arm was 14 in. and f_c' at the time of testing was in the mid-range of values tested.
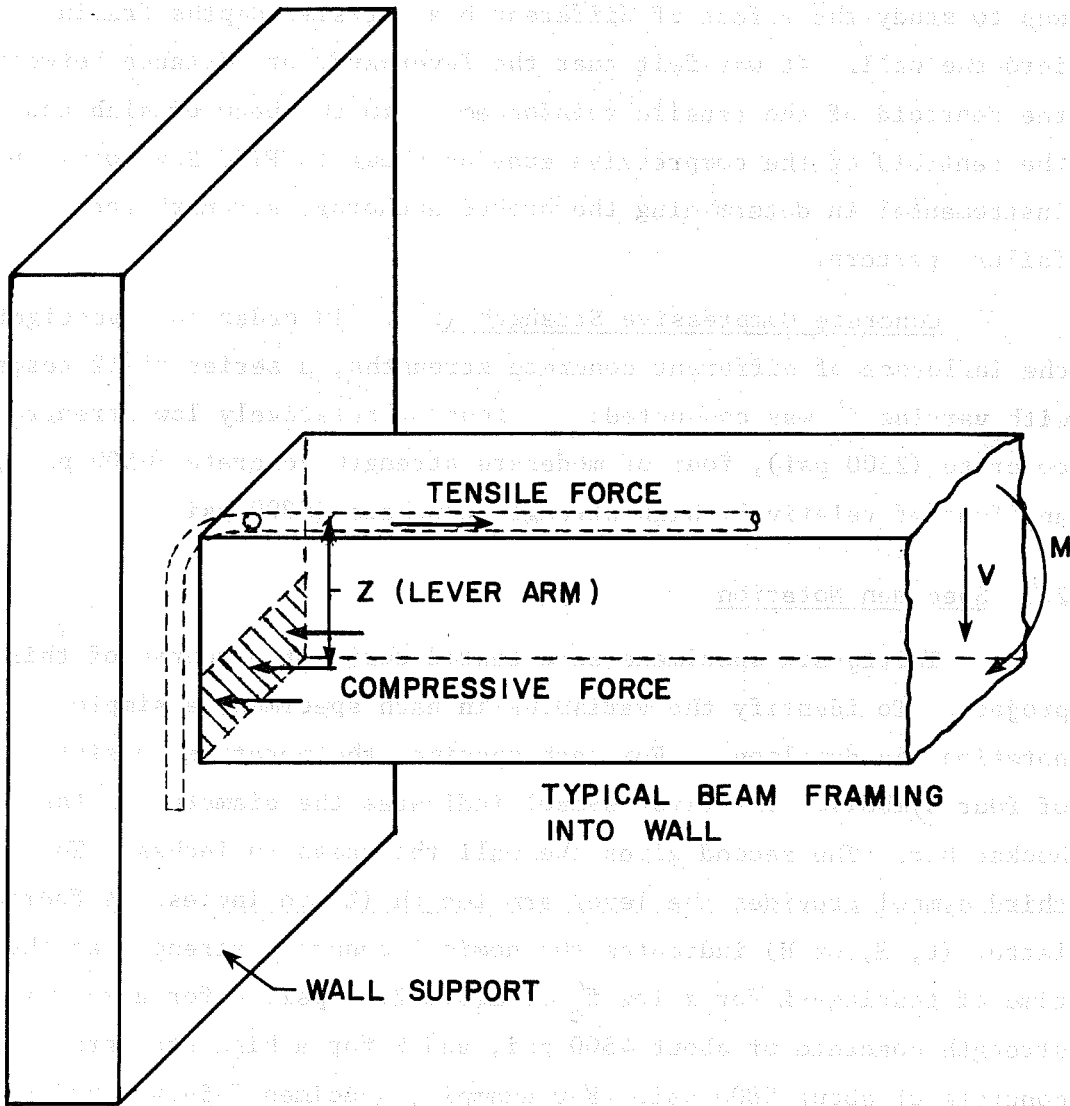
Fig. 2.4 Internal lever arm (Z)

2.6 Materials

All hooked bars used in this study conformed with the requirements of ACI 318-77 for standard hooked bars with 90° bends. The bar were all of Grade 60 steel and lead embedment bar stresses greater than 60 ksi never occurred during any of the tests. The #4 bar of Specimen 4-5-11-M did reach a tensile stress of 60 ksi; however, a later tension test on the bar revealed yield to be 67.5 ksi.

The 3/4 in. concrete cover on the vertical reinforcement limited the maximum size aggregate to 5/8 in. For thin walls, a fairly high slump mix was used. Mixes with slumps ranging between 6 in. and 9 in. worked very well and were used throughout the program. In order to attain the desired strengths with such high slumps, a water-reducing additive (Airsene) was added to each mix at a rate of 6 oz/sack/yd^3.

2.7 Fabrication

In designing the formwork, several factors were considered: (1) the formwork was to be adjustable to permit changing the wall thicknesses; (2) several specimens were to be cast at the same time, and (3) the forms were to be reusable throughout the project. The final design permitted the casting of four specimens at once. A different wall thickness could be set for each pair of specimens in a given casting (Fig. 2.5). The forms could be easily assembled and disassembled.

Reinforcement cages for the specimens were fabricated and placed in the form. The vertical as well as the horizontal steel was the same in both faces of each specimen. Horizontal steel bent into the "hairpin" shape shown in Fig. 2.6 held the vertical steel in both forces and made the cages easier to handle. Spacers (3/4 in. chairs) were tied to the vertical steel bars to maintain the desired concrete cover.
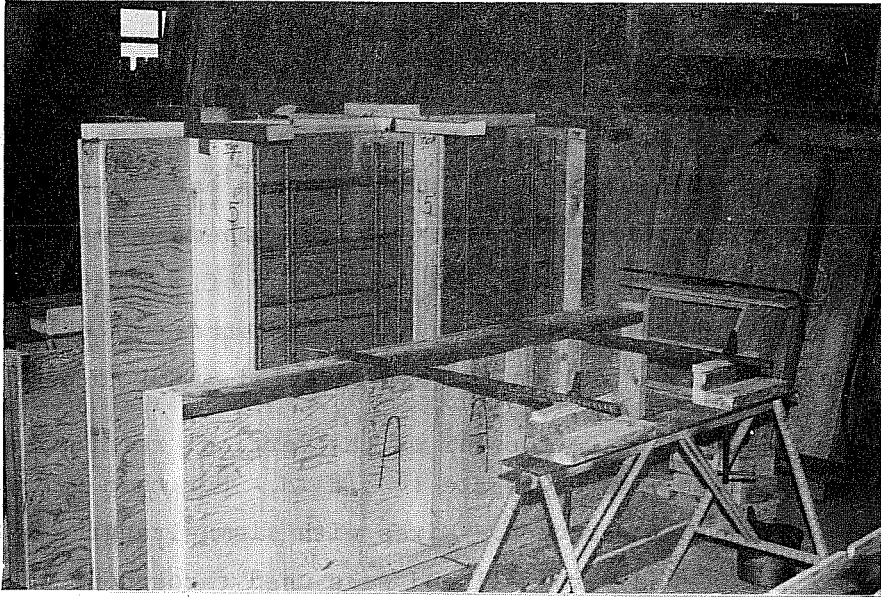
Fig. 2.5 Formwork construction in progress

Fig. 2.6 Horizontal "hairpin" reinforcement

The front face form was split at the level of the protruding bar for facilitating placement of the hooked bar anchorages and for ease of stripping the forms. Two of the four steel cages can be seen in place against the common back wall in Fig. 2.5. A hooked bar anchorage is supported in a slot at the top of the bottom face form (labeled A). After all of the reinforcement and instrumentation was in place, the top face form was added.

The concrete was placed vertically from the top of the form. In the thin walls, careful placement and vibration was required to prevent honeycombing. Initially, each of the four specimens was filled to the level of the hook and mechanically vibrated. A second lift was placed and vibrated to complete the wall.

Ten 6×12 in. control cylinders were cast with each group of four specimens so that the compressive strength at testing could be determined. The specimens as well as the control cylinders were covered with a plastic sheet for 4 to 5 days to prevent excessive moisture loss. After removal of all forms the specimens were allowed to cure for at least four weeks.

2.8 Loading System

Figure 2.4 showed schematically the forces applied to the wall in a beam-wall joint. In the test specimens the loading was simulated with a tensile or pullout force applied to the hooked bar while an equal compressive force was applied at a distance Z below the bar. Figure 2.7 shows a sketch of the loading system. A rigid frame was welded to one end of a steel beam to allow a centerhole hydraulic ram to be mounted on the loading beam, as shown in Fig. 2.8. Holes were drilled at desired distances (Z) below the center of the ram, as can be seen in Fig. 2.8. The holes allowed a 1×4×8 in. steel plate to be bolted to the face of the loading beam, providing a defined compressive area. In order for a couple

SIDE VIEW

LOADING RAM

P

LEVER ARM (Z)

P

LOADING BEAM

SUPPORT
BLOCK

REACTION WALL

SPECIMEN

HOOKED
ANCHORAGE

COMPRESSION
STRUT
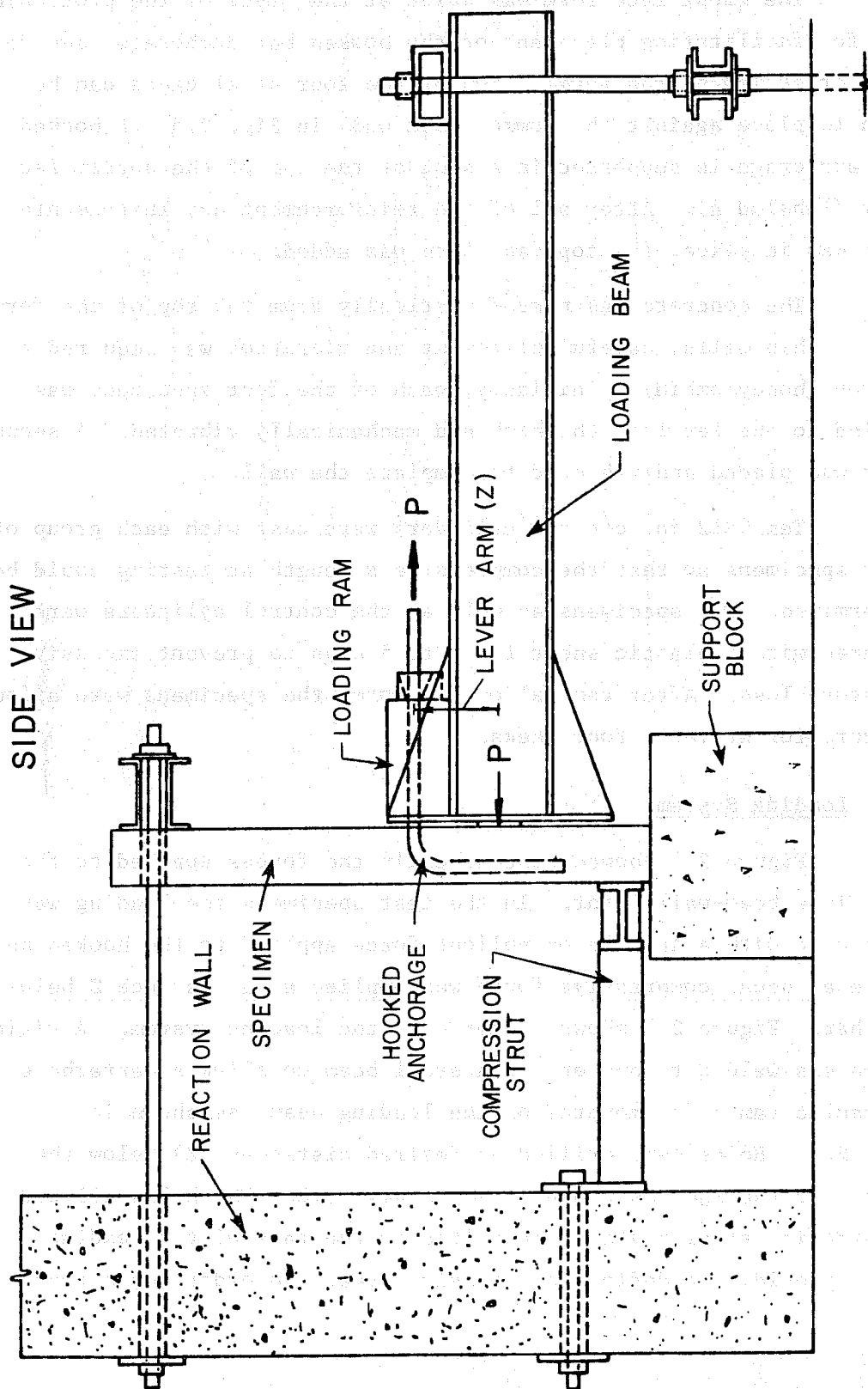
Fig. 2.7 Detail of loading system

Fig. 2.8 Adjustable compression plate
on the loading beam

to be produced, the end of the loading beam was tied to the laboratory floor by means of anchors in the slab, as seen in Figs. 2.7 and 2.9.

Three loading beams (shown in Fig. 2.9(b) were used in the triple bar tests. By connecting the hydraulic lines of the three centerhole rams to a common manifold, the same force was applied simultaneously to each of the three hooked anchorages.

Figures 2.7 and 2.9 show the two steel bolts which pass through the top of the specimen and through a pair of composite channel sections to tie the top of the specimen to the laboratory reaction wall. A compression strut was provided at the bottom to prevent rotation of the specimen as the couple was applied.

Each anchorage was loaded by means of a hydraulic hand pump connected to the centerhole ram shown in Fig. 2.10. A steel chuck having a cone-shaped hole was placed over the bar ahead of the hydraulic ram. Three grooved wedges (Fig. 2.11) gripped the bar. A pressure transducer placed in the hydraulic system allowed applied loads to be monitored with a digital strain indicator.

2.9 Slip Measurement

To establish the effect of the variables described in Sec. 2.4 on the load-deformation characteristics of the hooked bars, slip measurements were made. Slip refers to a movement of the bar relative to the concrete.

In previous hook tests by Jirsa and Marques [2], and by Pinc, Watkins, and Jirsa [3], it was found that movement of the tail extension in the direction of applied force was insignificant. Therefore, slip measurements along the tail extension of the bars in this study were not made. Since the hook began at or very near the face of each specimen, slip was measured only at two locations along the embedded bar: (1) the lead point of tangency of the hook (not
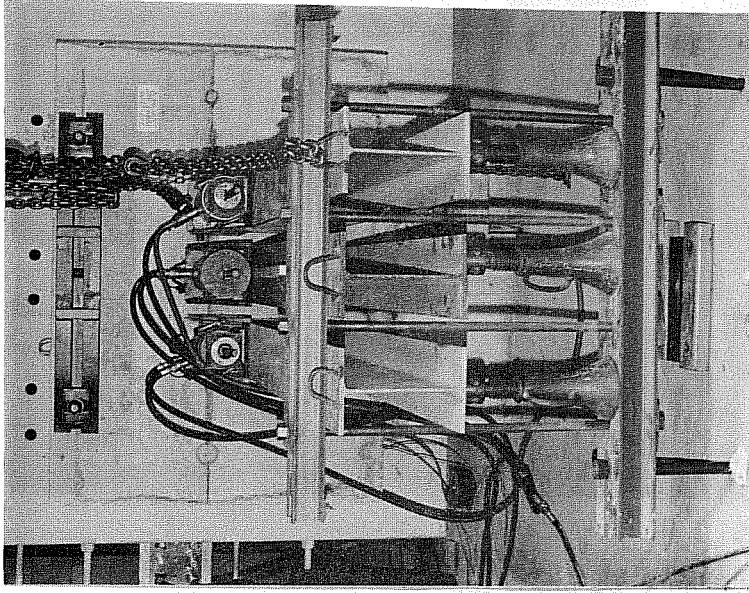
(b) Multiple bar specimen
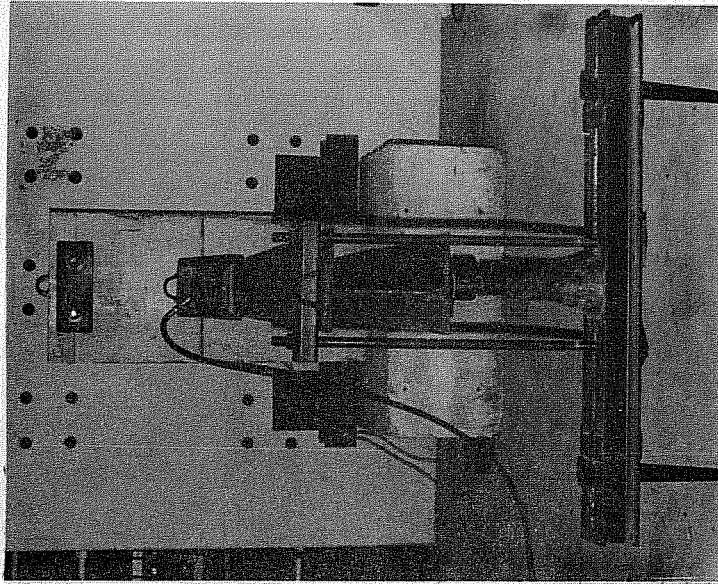
(a) Single bar specimen

Fig. 2.9 Loading beams in position
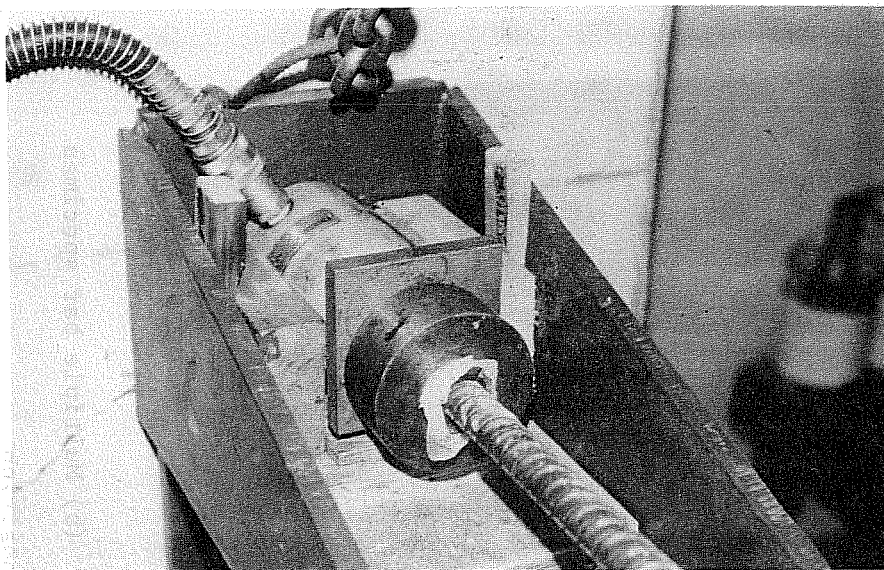
Fig. 2.10 Centerhole ram with hydraulic line and bar chuck in position
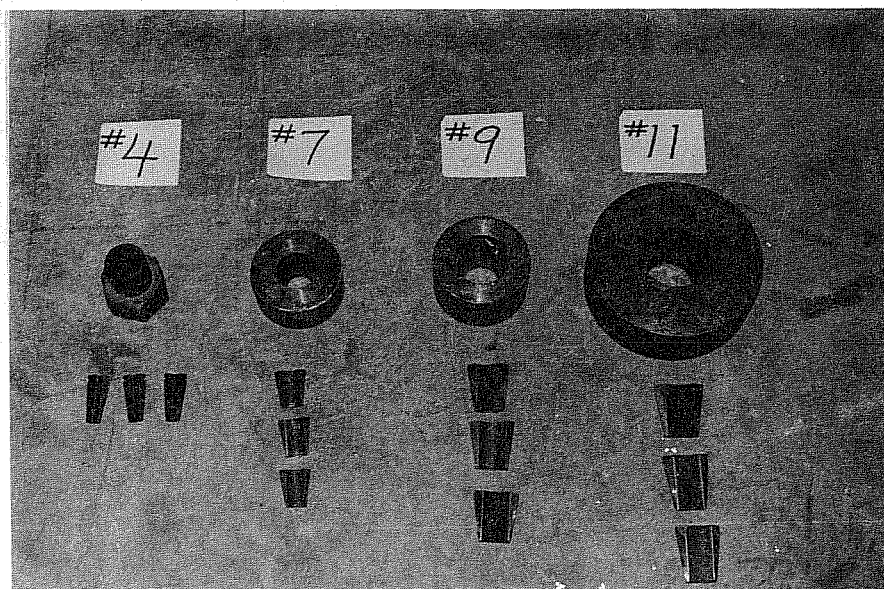
Fig. 2.11 Chucks and wedges used to grip the bars

necessarily at the face of the wall), and (2) the point of tangency between the lead and the tail, as shown in Fig. 2.12.

The method of slip measurement developed by Minor [1] and used in previous investigations [2,3] was used in this study. A 1/4 in. 90° bend was made on one end on an adequate length of a small diameter (0.059 in.) piano wire. The slip wire was then attached to the bar by placing the 1/4 in. length in a hole of the same wire diameter, drilled at the point of desired slip measurement. A 1/8 in. diameter soft plastic tube was then slipped over the piano wire to prevent bond between the wire and concrete. The connection between each wire and the bar was covered with a small amount of waterproofing to ensure that cement paste would not enter the plastic tube (Fig. 2.13).

The wires were cut to extend horizontally 1.5 in. from the concrete surface. Each slip wire was subjected to a slight tensile force by the use of a small spring placed between a thin metal plate (glued to the concrete surface) and an aluminum plug (fastened to the slip wire with a set screw), as shown in Fig. 2.14. Each transducer was mounted using inserts embedded on the back side of the specimen to decrease the influence that cracking and spalling might have on the relative slip readings.

2.10 Test Procedure

Since no previous data on hooked bars with very short lead embedments were available, prediction of anchorage strength was difficult at the outset of this study. However, with each successive test strength could be estimated more accurately. In order to reduce the effect of time dependent factors on the response, the period between initial loading and failure for all the test specimens was about the same, 50 to 60 minutes. Load increments were applied at 2 min. intervals. After each load increment was applied,
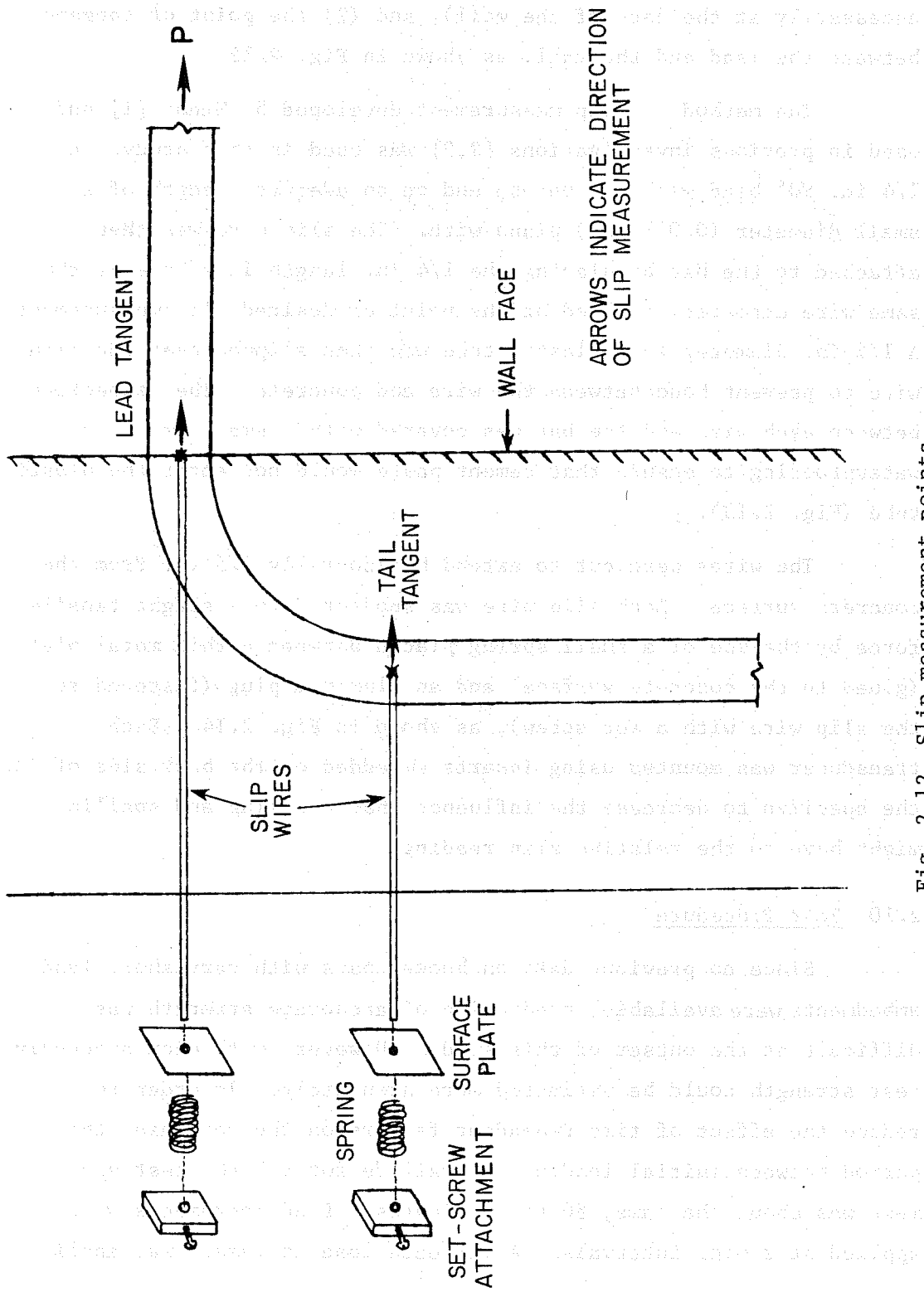
Fig. 2.12 Slip measurement points
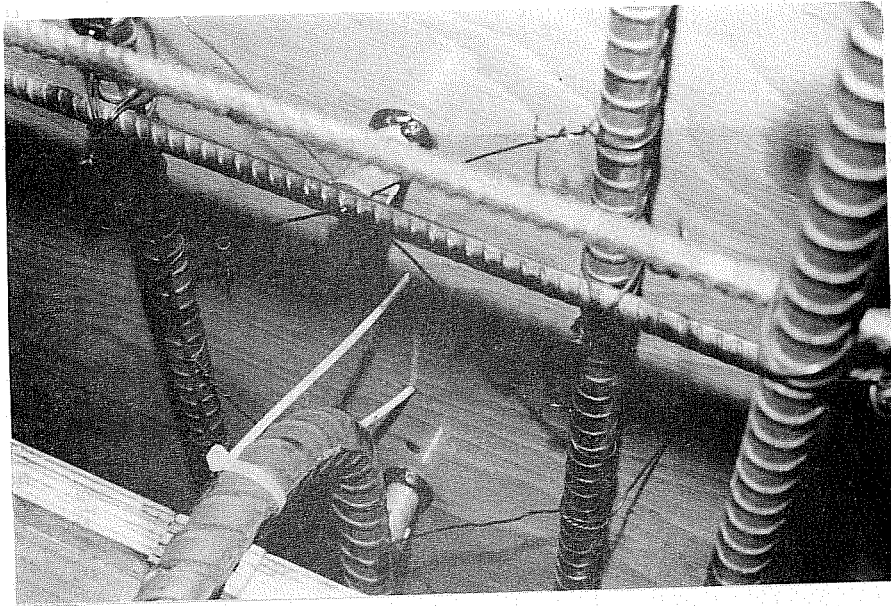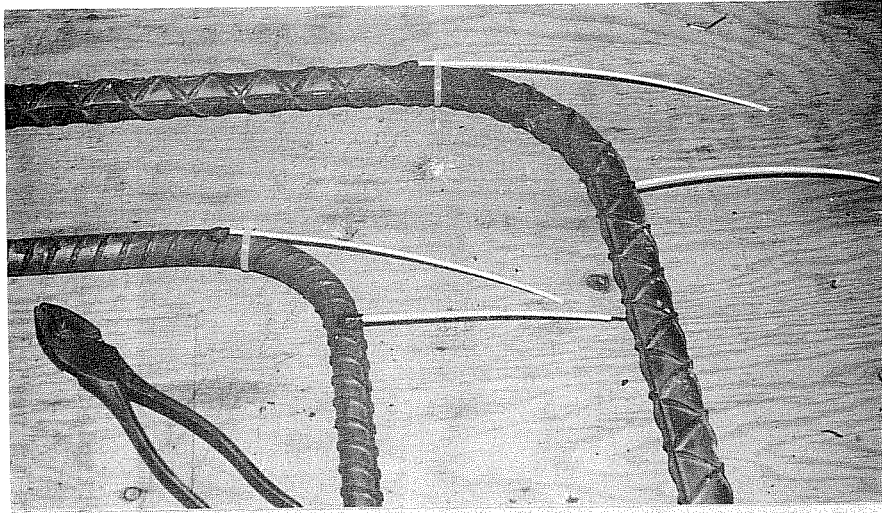
Fig. 2.13   Slip wire mounting and placement in forms
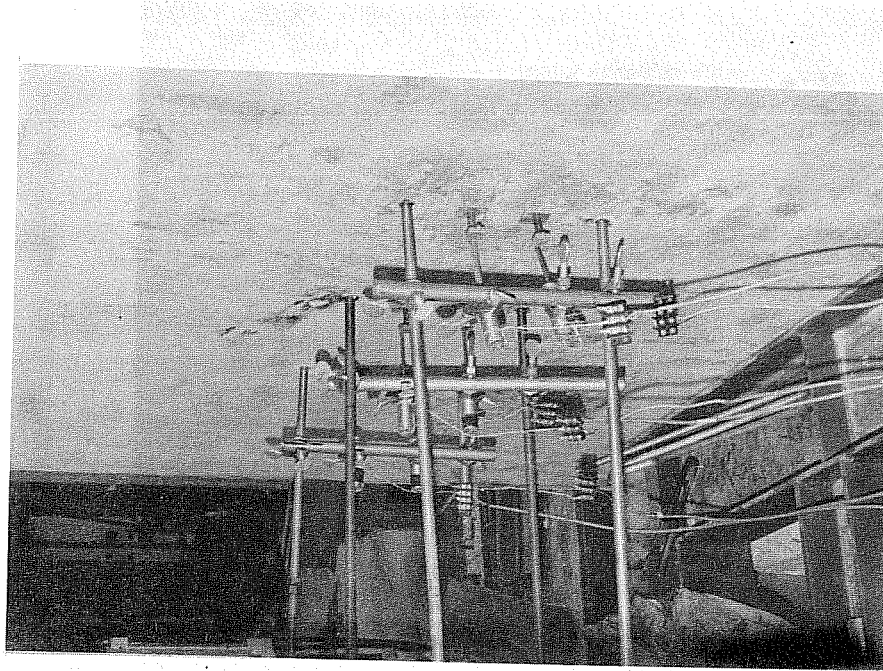
Multiple bar specimen
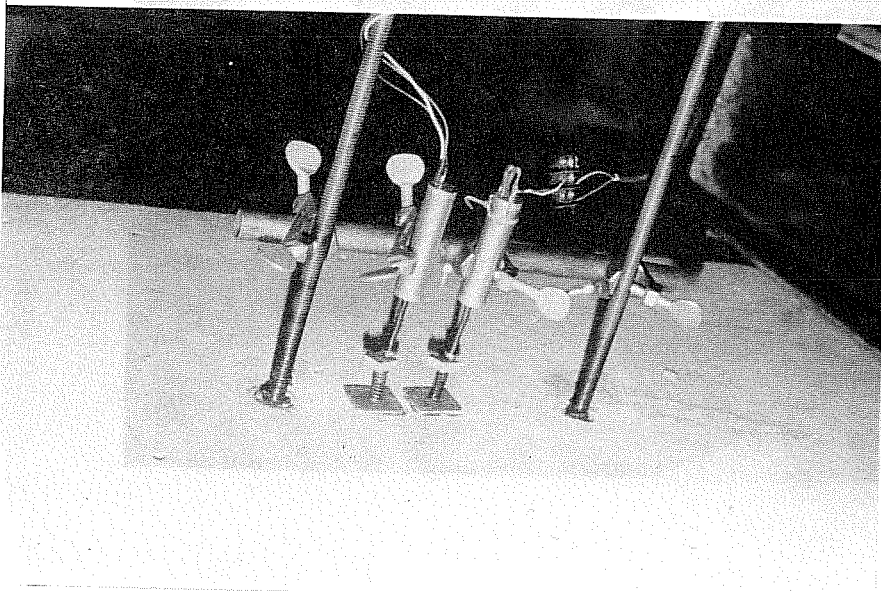
Single bar specimen

Fig. 2.14 Linear displacement potentiometers in position

slip readings were taken. While maintaining the load, a second set of slip readings was taken at the 1.5 min. mark, so that an average slip value could later be calculated for each load level.

The specimen was inspected to determine the initiation of cracking. Cracking patterns were marked as the test progressed. As maximum load was reached, it became increasingly difficult to maintain a constant load for the 2 min. interval. Failure was reached when the load suddenly dropped to a fraction of the level that the bar had been holding. No further load increases beyond this level were possible. In the multiple bar tests, all three anchorages did not fail at the same time. As each anchorage failed, the hydraulic lines leading to the ram on the bar which failed were disconnected and the loading was continued on the remaining bars until failure of all anchorages was complete.

Upon removal of the loading beams the failure zone and crack patterns were marked and photographed. Loose concrete in the failure zone was removed so that the failure surface could be observed and photographed.

3. TEST RESULTS

3.1 Introduction

A total of 36 specimens were tested. The observed trends are discussed in this chapter. The slip measurements at the points shown in Fig. 2.12 were plotted against the stress applied to the hooked anchorage. A typical set of curves is shown in Fig. 3.1. Because the slip measurements at the tail point of tangency were insignificant in all tests, only the lead tangent slip will be presented. In the discussion, "companion specimens" refer to specimens with the same wall thickness and bar diameter.

3.2 General Mode of Failure

The crack formation and failure pattern was similar in all the tests. Initial cracking always began on the specimen face, just above the bar, and radiated horizontally as higher loads were applied. Generally, the cracks extended to both sides of the specimen, and as failure approached slip generally increased at a higher rate and it became increasingly difficult to maintain the high load level on the bar. Failure was always sudden, marked by the load dropping to a small percentage of its previous level. The size of the zone of failure was controlled by the lever arm length. The concrete fractured at the top edge of the compression block (unless the lever arm was very large) and sometimes cracking extended diagonally from the upper corners of the compression block toward the bottom corners of the specimen, as shown by Fig. 3.2. The horizontal extension of the failure zone seemed to be directly related to the lever arm distance. That is, a test with a lever arm of 8 in. generally produced a failure zone extending approximately 8 in. on both sides of the bar, as shown in Fig. 3.3. The failure

29

30
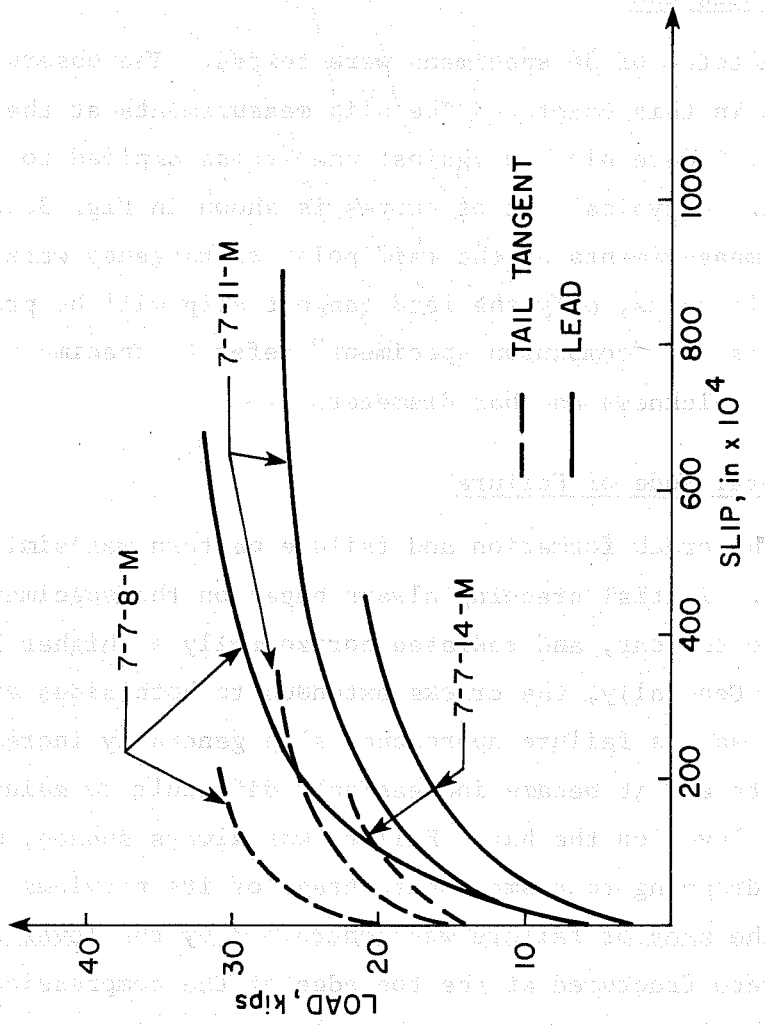
Fig. 3.1 Load-slip curves for #7 hooked bars in 7 in. walls
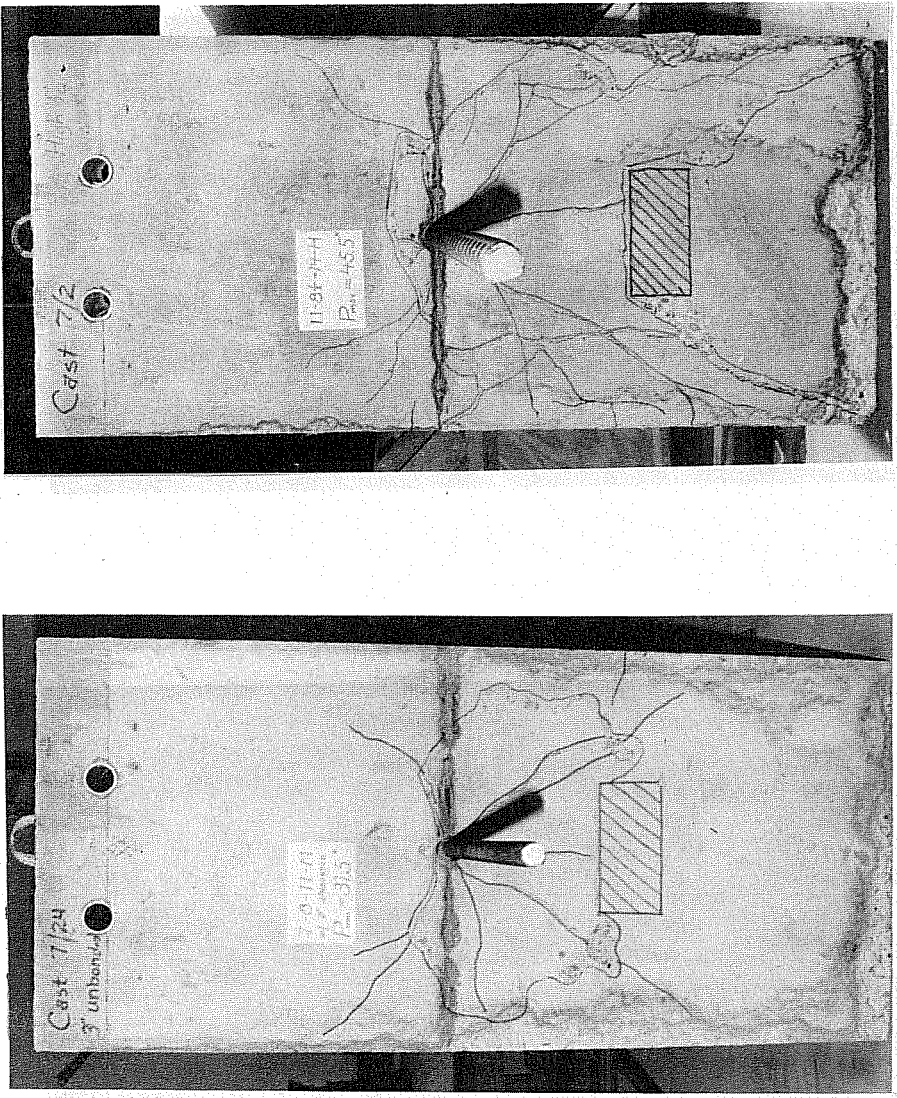
Fig. 3.2 Typical crack patterns
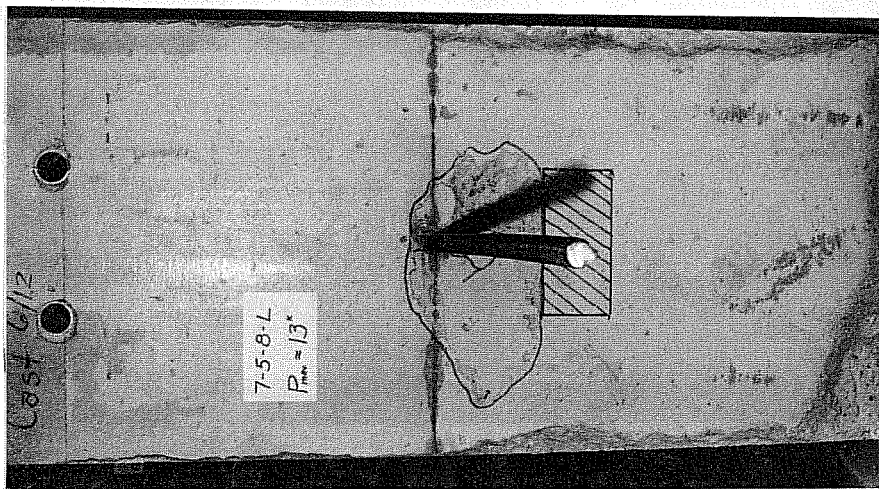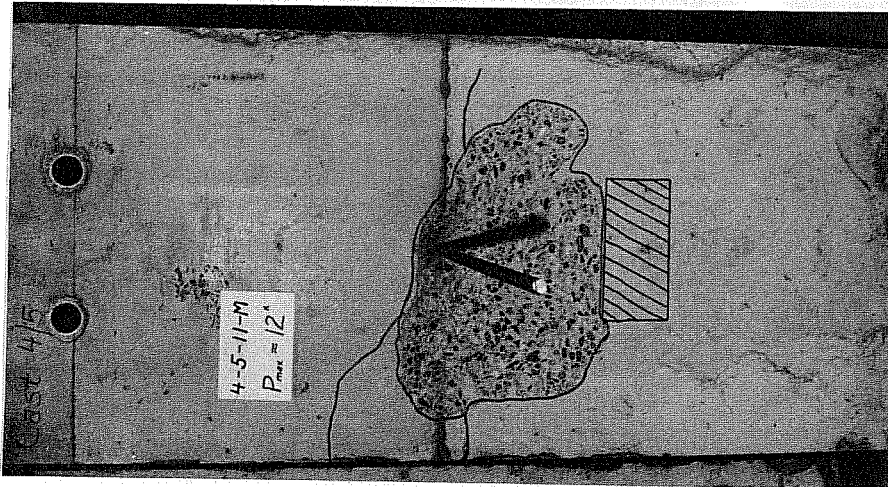
Fig. 3.3 Failure patterns contained entirely on the face

zone of a specimen with a lever arm of 11 in. generally extended about 11 in. on either side of the bar. The largest lever arm lengths investigated (14 in. and 18 in.) generally led to failure zones that extended to the vertical edges of the specimen.

Removal of the fractured concrete exposed part or all of the curved portion of the hooked anchor. A cone type of failure beginning at the bend was observed in each specimen. The failures in the multiple bar specimens can be seen in Figs. 3.4 to 3.7. Note that the bars spaced at 11 in. appeared to fail as a unit, while those spaced at 22 in. fractured the concrete individually.

Figure 3.8 shows cracking on the back of Specimens 9-8-14-M and 11-8.5-14-L. These cracks are typical of most of the specimens with #9 or #11 hooked bar anchors. The stiff large diameter bars tended to pry against the back cover as previously described [2,3]. Since the prying cracks formed just prior to failure, they did not influence slip measurements.

3.3 Influence of Concrete Strength

Concrete compressive strength at date of testing is presented in Table 3.1. Observed loads and stresses are given to indicate the variation in load between companion specimens with different values of f'_c. The stress-slip curves in Fig. 3.9 show that the highest anchorage capacity was reached in specimens with the highest values of f'_c. The influence of concrete strength on observed ultimate slip was quite varied; however, with low f'_c greater slip was observed at comparable stress levels.

Previous research in bond and anchorage and in the evaluation of the tensile characteristics of concrete have shown that the response is proportional to $\sqrt{f'_c}$. Therefore, normalized loads and stresses, based on a nominal f'_c of 4500 psi, have been
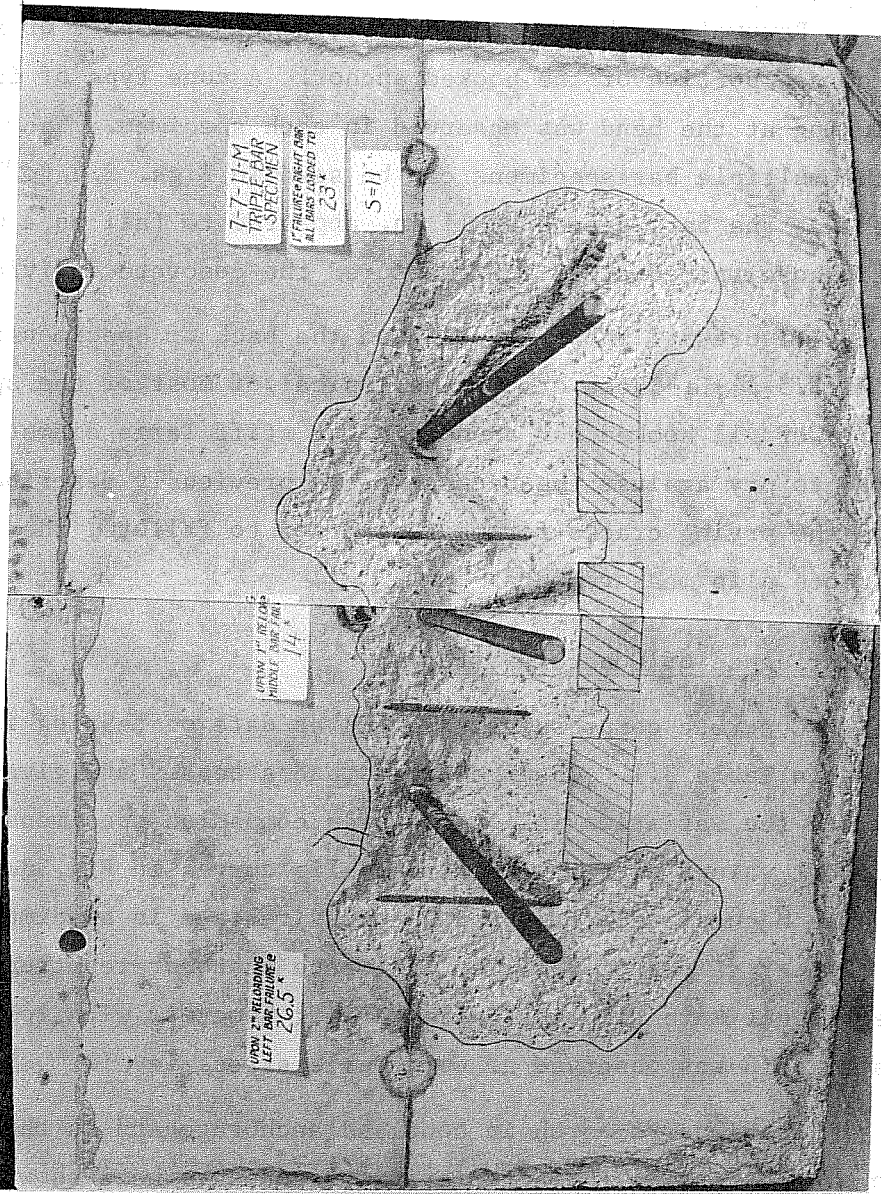
Fig. 3.4 Fractured surface of a multiple bar specimen, #7 bars, 11 in. spacing

7-7-11-L
TRIPLE BAR SPEC
S=22"

1" FAILURE @ RIGHT BAR
EACH BAR LOADED TO
22 ᴷ

UPON 2" RELOADING
MIDDLE BAR FAILURE
@ 24 ᴷ

UPON 1" RELOADING
LEFT BAR FAILURE @
22 1/4 ᴷ
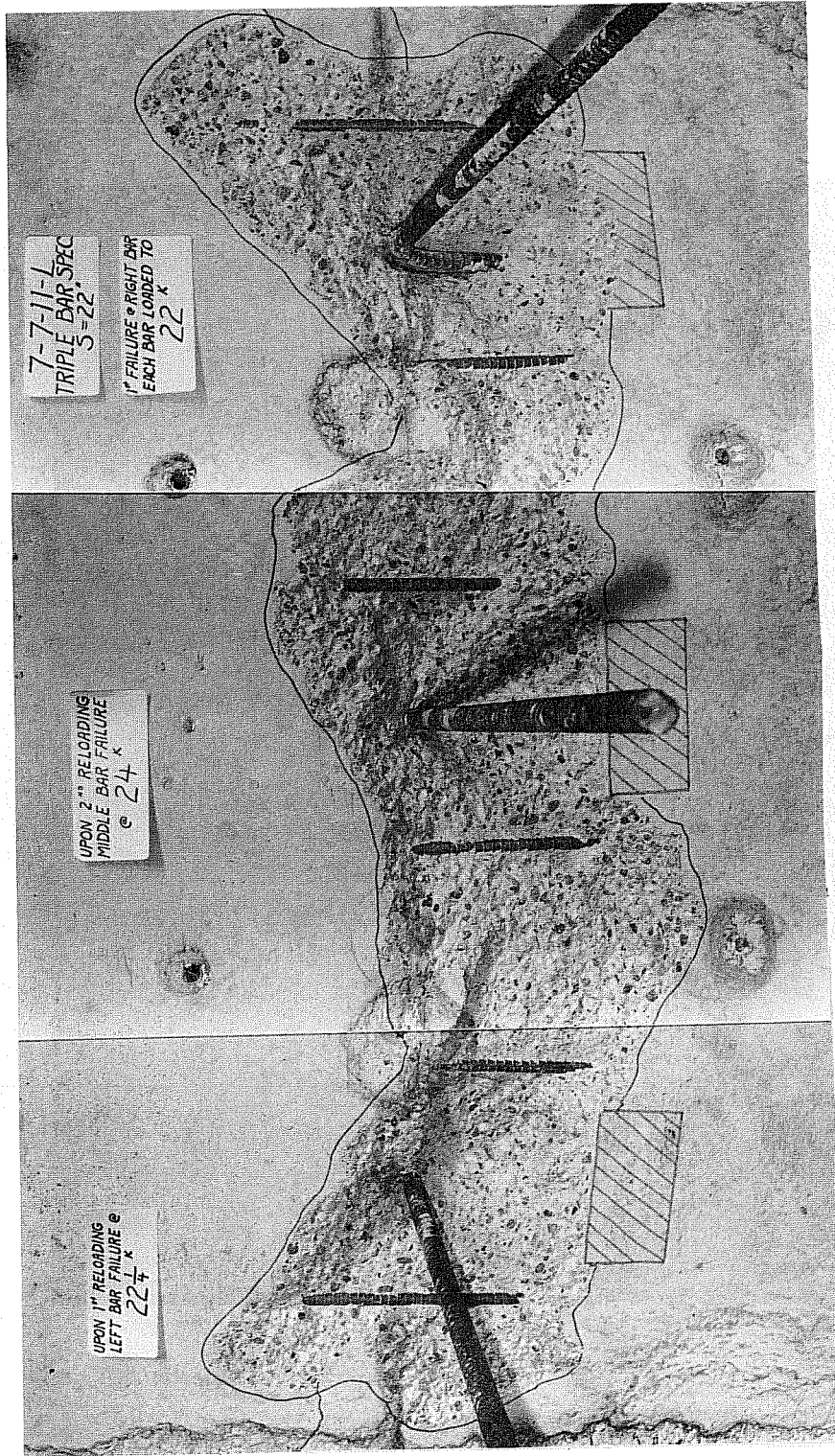
Fig. 3.5 Fractured surface of a multiple bar specimen, #7 bars, 22 in. spacing
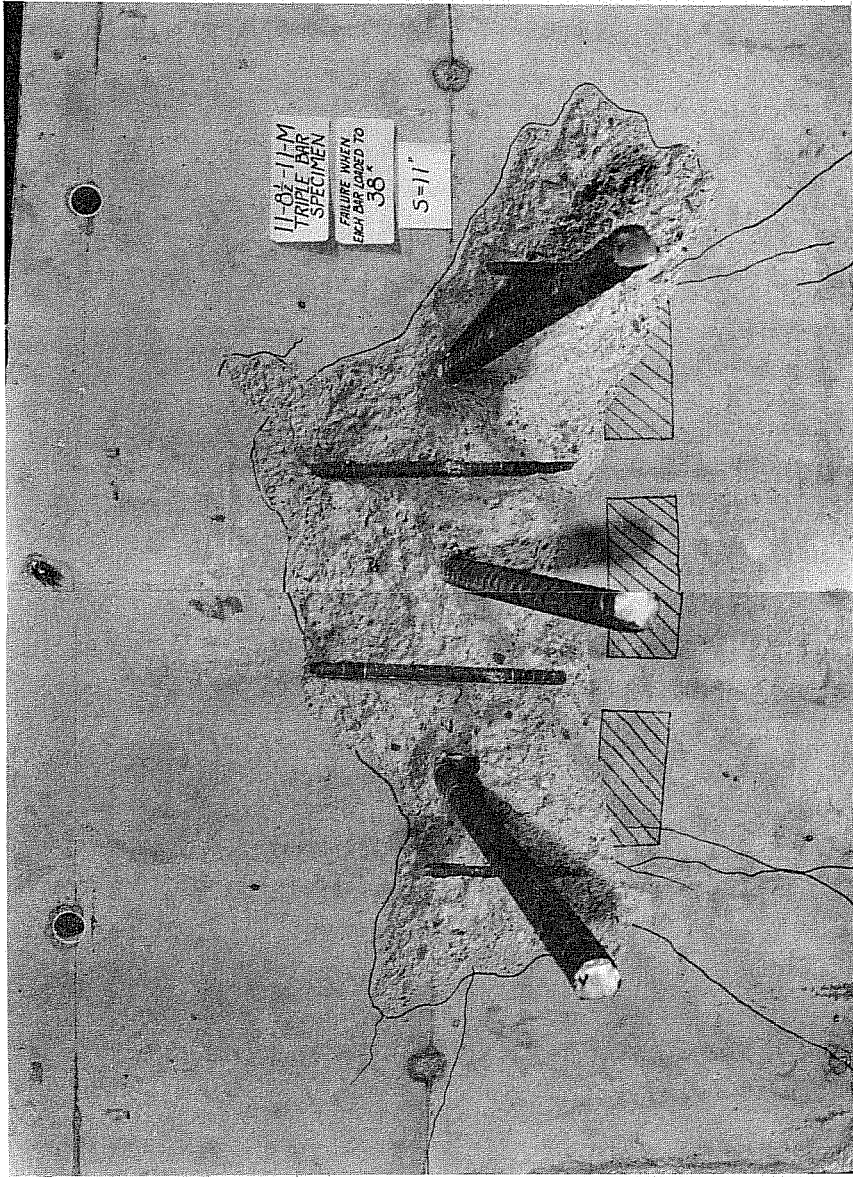
Fig. 3.6 Fractured surface of a multiple bar specimen, #11 bars, 11 in. spacing
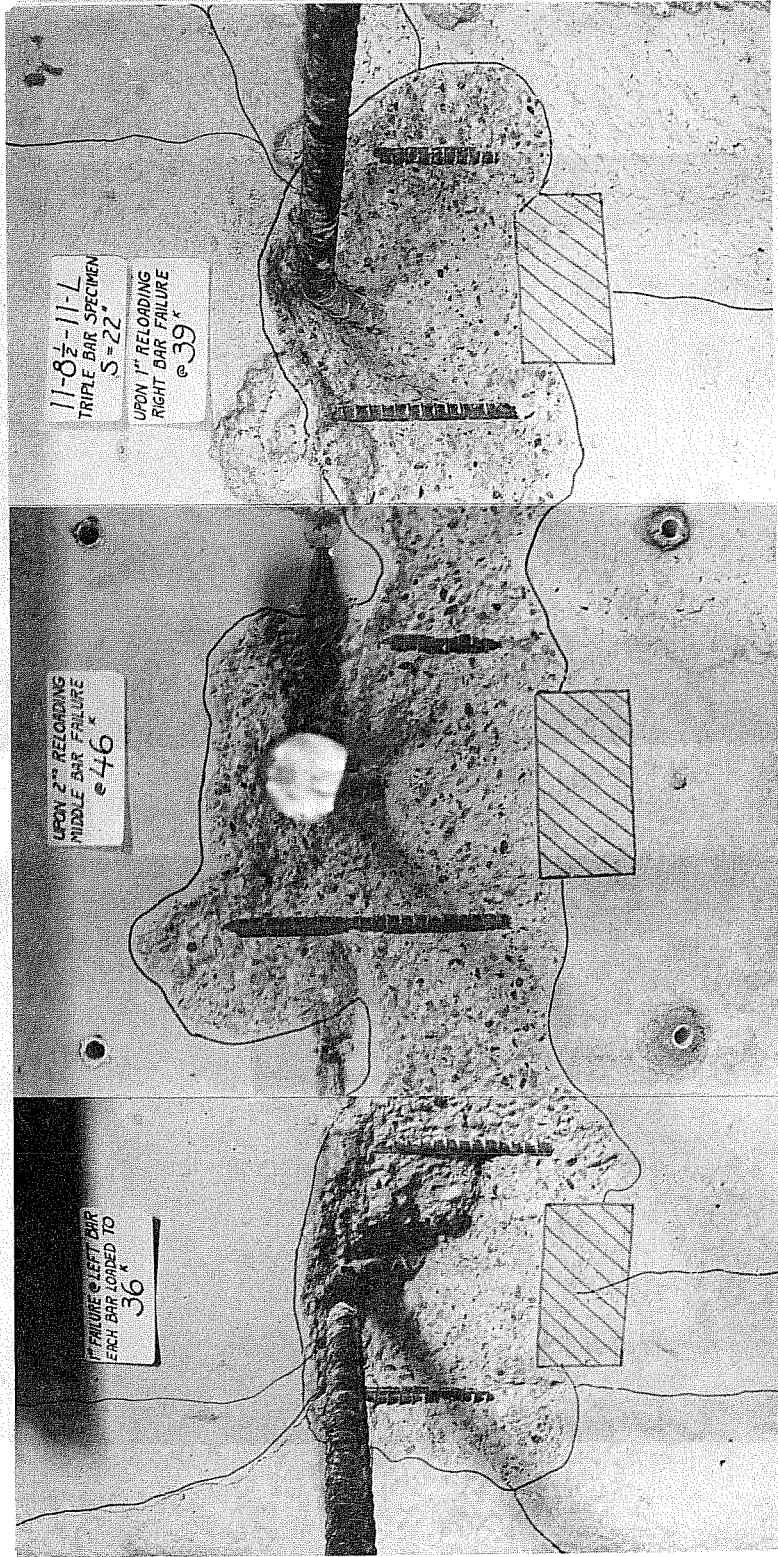
Fig. 3.7 Fractured surface of a multiple bar specimen, #11 bars, 22 in. spacing

38
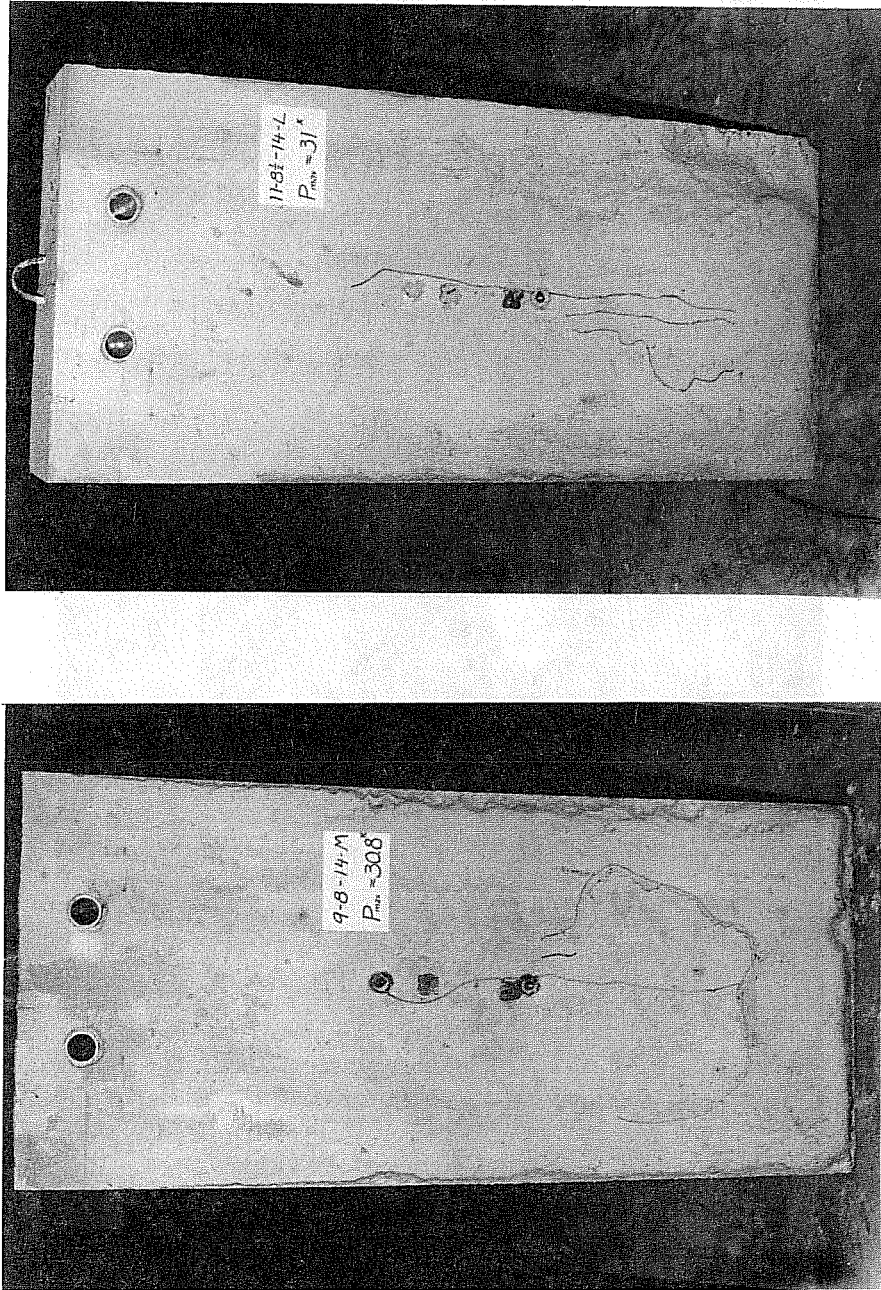
Fig. 3.8 Cracking on the back of specimens with large diameter bars
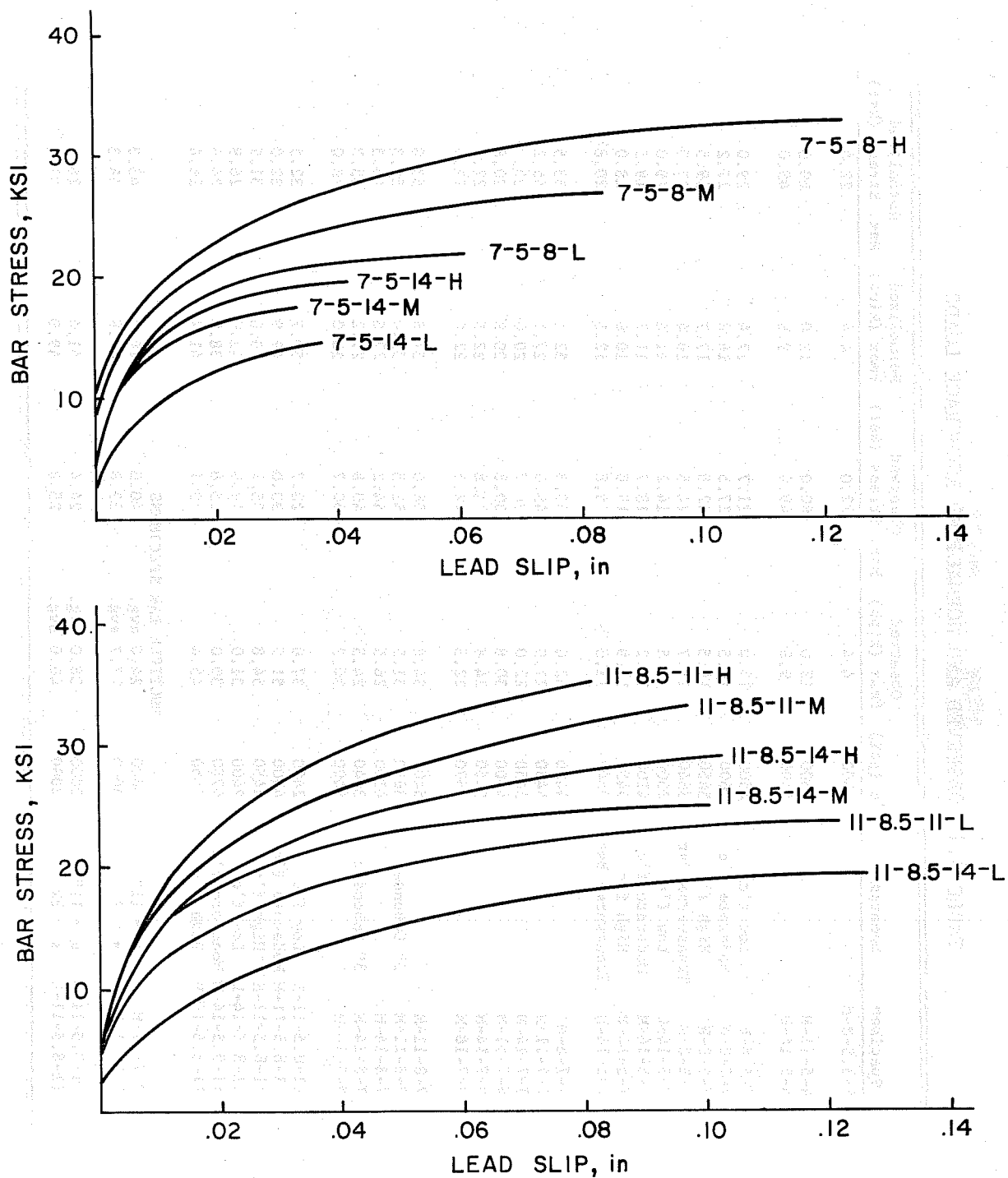
Fig. 3.9   Influence of concrete strength

TABLE 3.1 OBSERVED AND NORMALIZED ANCHORAGE LOADS

Specimen	Remarks	f'c (psi)	Observed Pmax (kips)	Observed Max. Stress (ksi)	Normalized Pmax (kips)	Normalized Max. Stress (ksi)
4-3.5-8-M		4500	4.4	22.0	4.4	22.0
4-5-11-M		4500	12.0	60.0	12.0	60.0
4-5-14-M		4500	9.8	49.0	9.8	49.0
7-5-8-L	Low f'c	2500	13.0	21.7	17.4	29.0
7-5-8-M	Moderate f'c	4600	16.5	27.5	16.3	27.2
7-5-8-H	High f'c	5450	19.5	32.5	17.7	29.5
7-5-8-M	Transverse Bar	3640	14.7	24.5	16.4	27.3
7-5-14-L	Low f'c	2500	8.5	14.2	11.4	19.0
7-5-14-M	Moderate f'c	4100	11.2	18.7	11.7	19.5
7-5-14-H	High f'c	5450	11.9	19.8	10.8	18.0
7-5-14-M	Transverse Bar	3640	11.3	18.8	12.5	20.8
7-7-8-M		4480	32.0	53.3	32.1	53.5
7-7-11-M		4480	27.0	45.0	27.1	45.2
7-7-14-M		5450	22.0	36.7	20.0	33.3
9-7-11-M		4500	30.8	30.8	30.8	30.8
9-7-14-M		5450	24.8	24.8	22.5	22.5
9-7-18-M		4570	22.3	22.3	22.0	22.0
7-8-11-M		5400	34.8	58.0	31.8	53.0
7-8-11-M	3" Unbonded	3640	31.5	52.5	35.0	58.3
7-8-14-M		4100	26.5	44.2	27.8	46.3
7-8-14-M	3" Unbonded	3640	24.5	40.8	27.2	45.3
9-8-14-M		5400	30.7	30.7	28.0	28.0
11-8.5-11-L	Low f'c	2400	37.0	23.7	50.7	32.5
11-8.5-11-M	Moderate f'c	4800	51.5	33.0	49.9	32.0
11-8.5-11-H	High f'c	5450	54.8	35.1	49.8	31.9
11-8.5-14-L	Low f'c	2400	31.0	19.9	42.0	26.9
11-8.5-14-M	Moderate f'c	4750	39.0	25.0	38.0	24.4
11-8.5-14-H	High f'c	5450	45.4	29.1	41.2	26.4
MULTIPLE BAR SPECIMENS						
7-7-11-M	s = 11"	3800	24.0 avg.	40.0	26.0	43.3
7-7-11-L	s = 22"	3000	22.7 avg.	37.8	27.8	46.3
11-8.5-11-M	s = 11"	3800	38.0 avg.	24.4	41.4	26.5
11-8.5-11-L	s = 22"	3000	40.0 avg.	25.6	49.0	31.4

determined for each specimen. These values were calculated by taking the product of the observed ultimate load or stress and the normalization factor, $\sqrt{4500/f_c'}$. Comparable specimens with low, medium, and high strength concrete illustrate the validity of the normalization factor. For instance, Specimens 11-8.5-11-L, 11-8.5-11-M, and 11-8.5-11-H had observed ultimate loads of 37k, 51.5k, and 54.8k, respectively. The normalized loads become 50.7k, 49.9k, and 49.8k, respectively. By using normalized values, the variable material strength is eliminated in making comparisons between tests.

3.4 Influence of Lever Arm (Z)

The lever arm distance shown in Fig. 2.3 was the most significant variable influencing the results of each test. A series of stress-slip curves for three 7 in. walls is presented in Fig. 3.10. Each of the three walls had a #7 hooked anchorage. Only the lever arm lengths (8, 11, and 14 in.) were different in the three specimens. The appearance of each specimen after failure can be seen in Fig. 3.11. Note the increase in the extent of the fractured areas below the bar as Z increases from 8 to 14 in. Shortening of the lever arm increases the confinement on the hook so that a larger stress can be developed by the anchor. The decrease in load capacity with increasing Z reaches a limit, as shown by the stress-slip curves for Specimens 9-7-11-M, 9-7-14-M, and 9-7-18-M (Fig. 3.12). The ultimate stress decreases when Z increases from 11 in. to 14 in. but stays about the same for lever arm lengths of 14 in. and 18 in. It can be concluded that no further reduction in ultimate will be realized for lever arms greater than about 14 in. for a #9 hooked bar embedded in a 7 in. wall. Figure 3.13 shows the failure pattern for each of the three specimens of the 9-7-Z-M series. The cracking zone extends down to and across the top of the compression area on the specimens with 11 and 14 in. lever arm lengths. However, the failure surface of Specimen
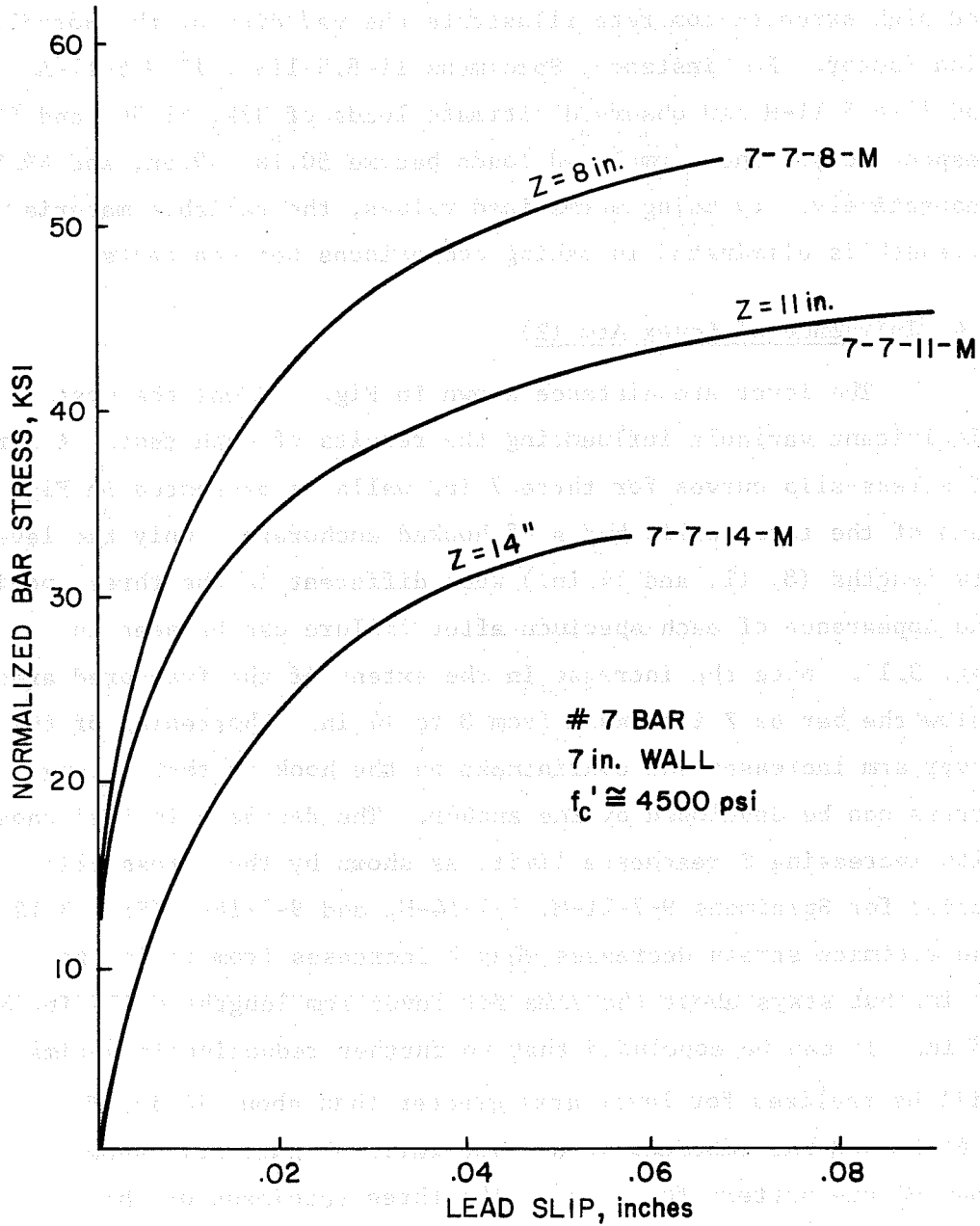
Fig. 3.10 Influence of lever arm
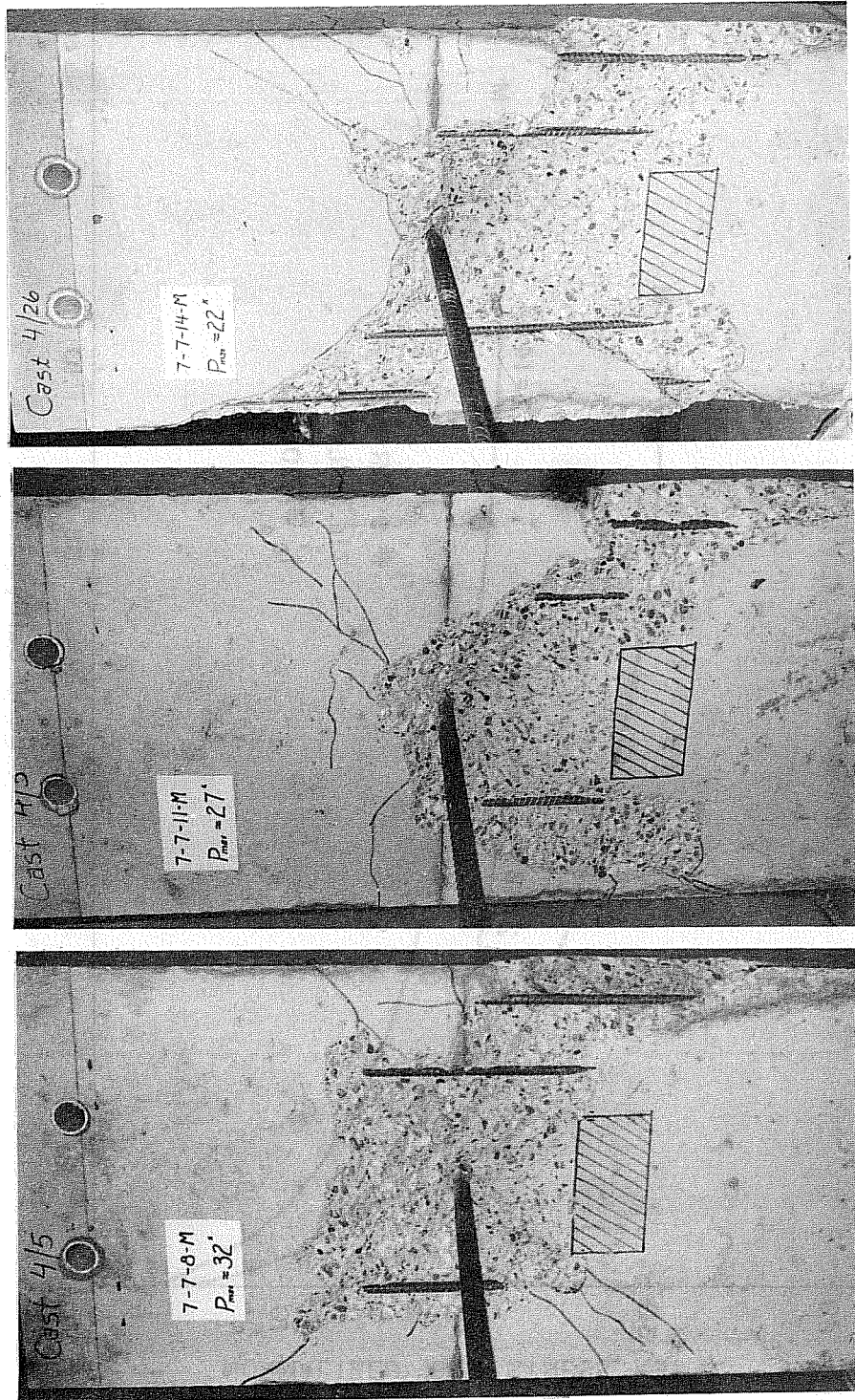
Fig. 3.11 Influence of lever arm on failure patterns, #7 bars
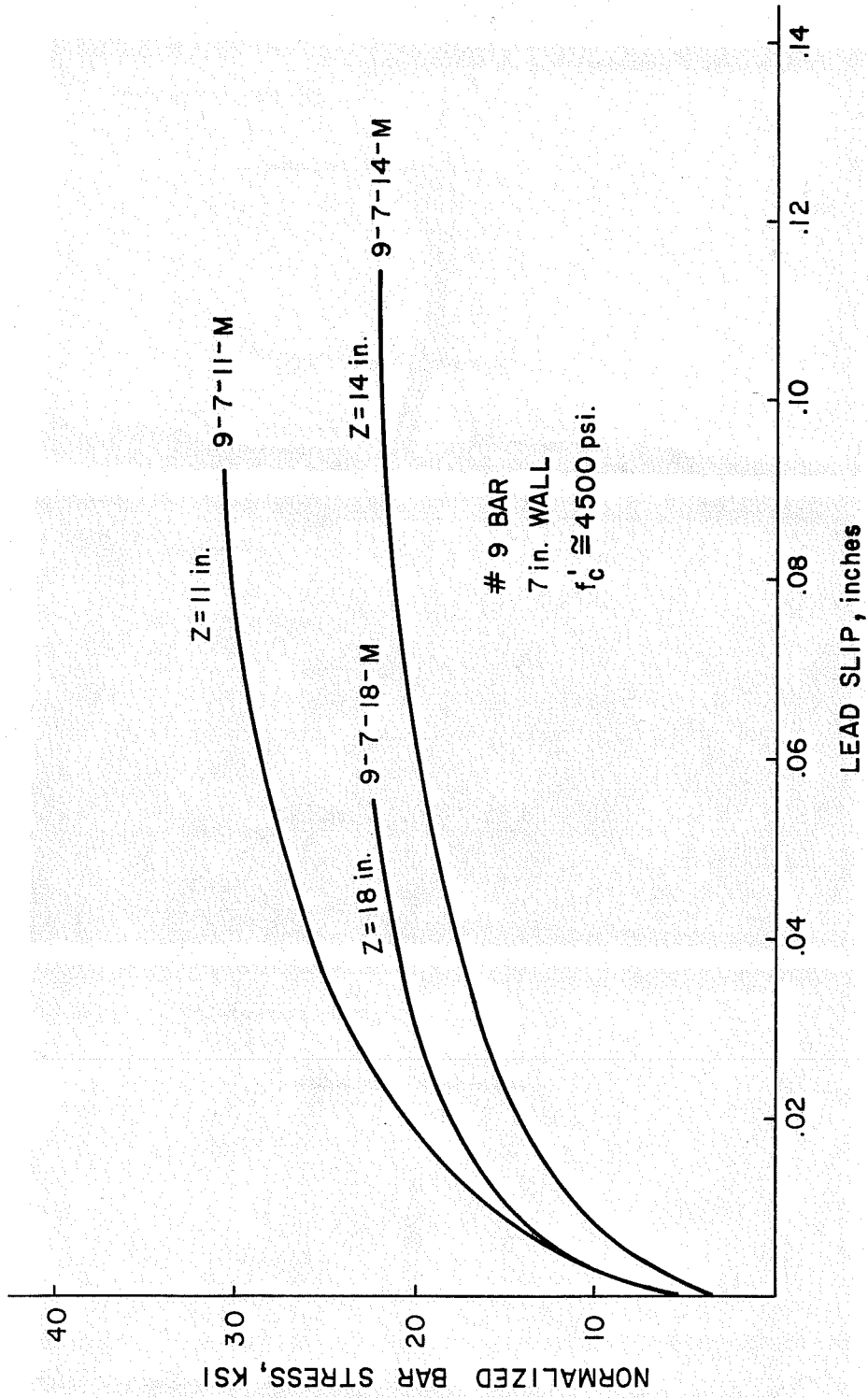
Fig. 3.12 Influence of lever arm
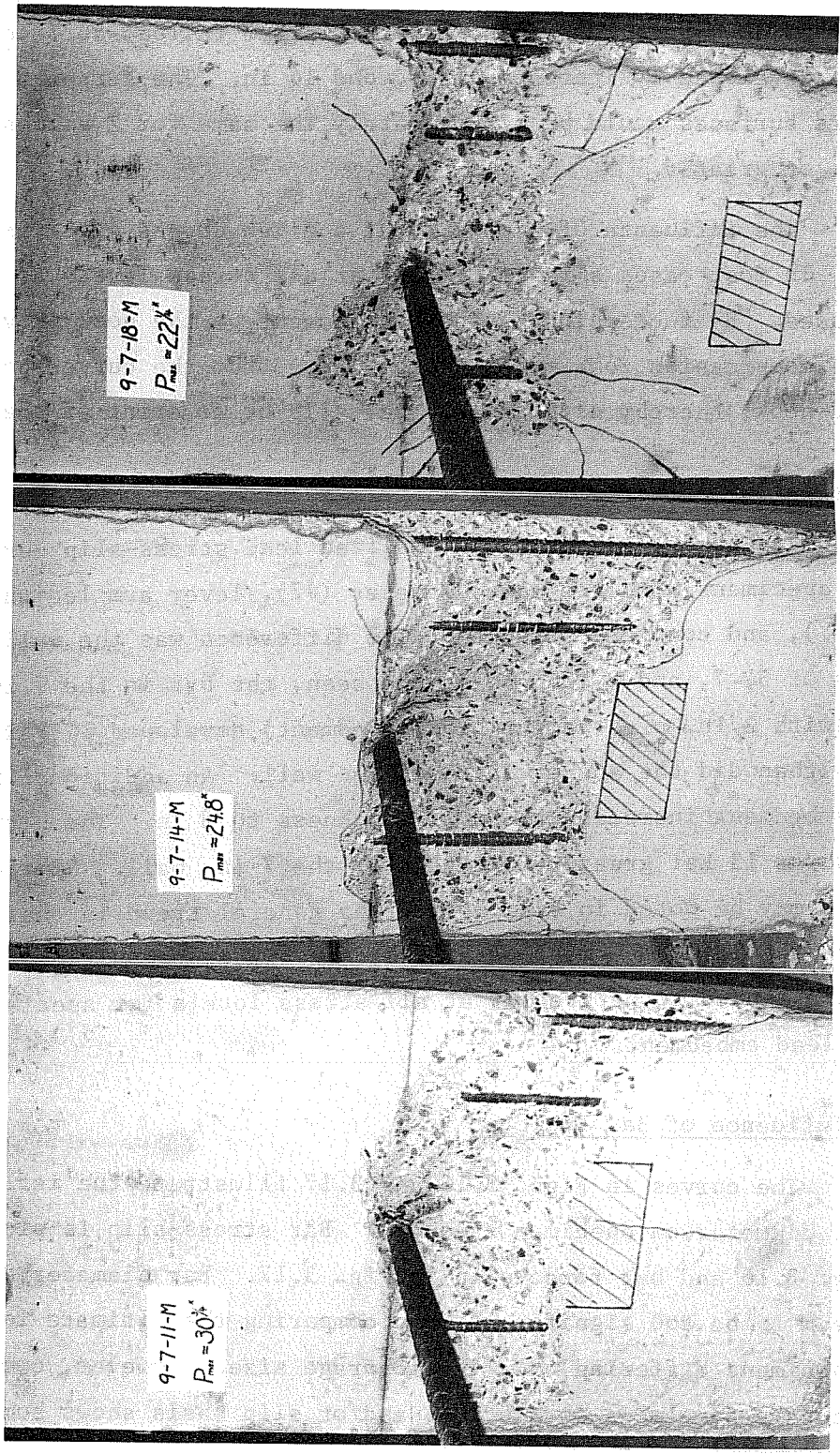
Fig. 3.13 Influence of lever arm on failure patterns, #9 bars

9-7-18-M does not extend entirely to the compression area. For the #9 hooked anchorage in a 7 in. wall, a larger failure surface could not be developed by increasing Z beyond 14 in. The strength and failure surfaces would be approximately the same for Z values 14 in. or greater.

The influence of Z on slip at a given stress level is evident. In most cases slip is greater at all stress levels as Z is increased. By increasing Z, the confinement on the hook provided by the compression zone moves further away from the curved portion of the hook, thereby allowing greater slip or movement of the hook.

3.5 Influence of Lead Embedment (Wall Thickness)

Figure 3.14 shows the normalized lead stress-slip curves of three specimens with the same diameter (#7), lever arm length (14 in.), and concrete strength. The difference was the wall thicknesses of 5, 7, and 8 in. As can be seen, the bar in the 7 in. wall (with 2 in. of straight lead embedment) developed 14 ksi more stress than did the anchor in the 5 in. wall. An additional inch of lead embedment increased the wall thickness to 8 in. The ultimate stress was 13 ksi greater than that of the 7 in. wall. Similar results may be noted in Fig. 3.15. The general trend is that the greater the lead embedment of a hook, the higher the ultimate capacity. The slip tended to be greater at all stress levels for specimens with short lead embedment.

3.6 Influence of Bar Diameter

The curves in Figs. 3.16 and 3.17 illustrate the influence of bar diameter on specimen strength. Bar stress-slip is plotted in Fig. 3.16 and bar force-slip in Fig. 3.17. Bar diameter does not seem to be too significant when comparing the ultimate loads of two specimens differing only in anchorage size. However, comparison of the same specimens on a stress and/or slip basis shows some
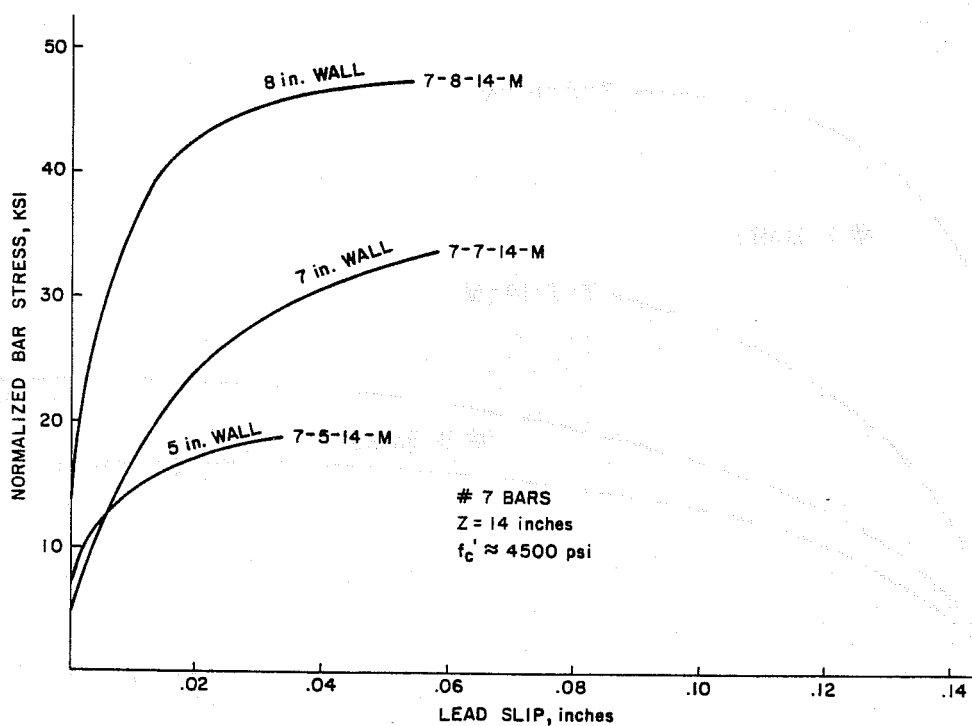
Fig. 3.14   Influence of lead embedment on wall thickness,
#7 bars
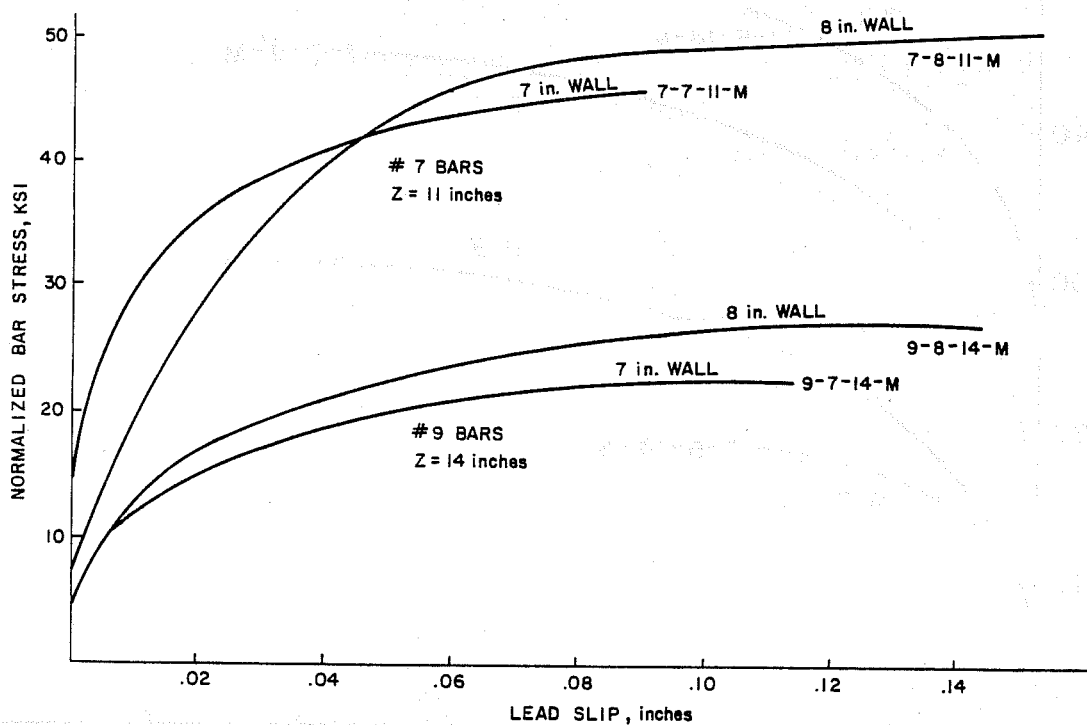
Fig. 3.15   Influence of lead embedment or wall thickness,
#7 and #9 bars
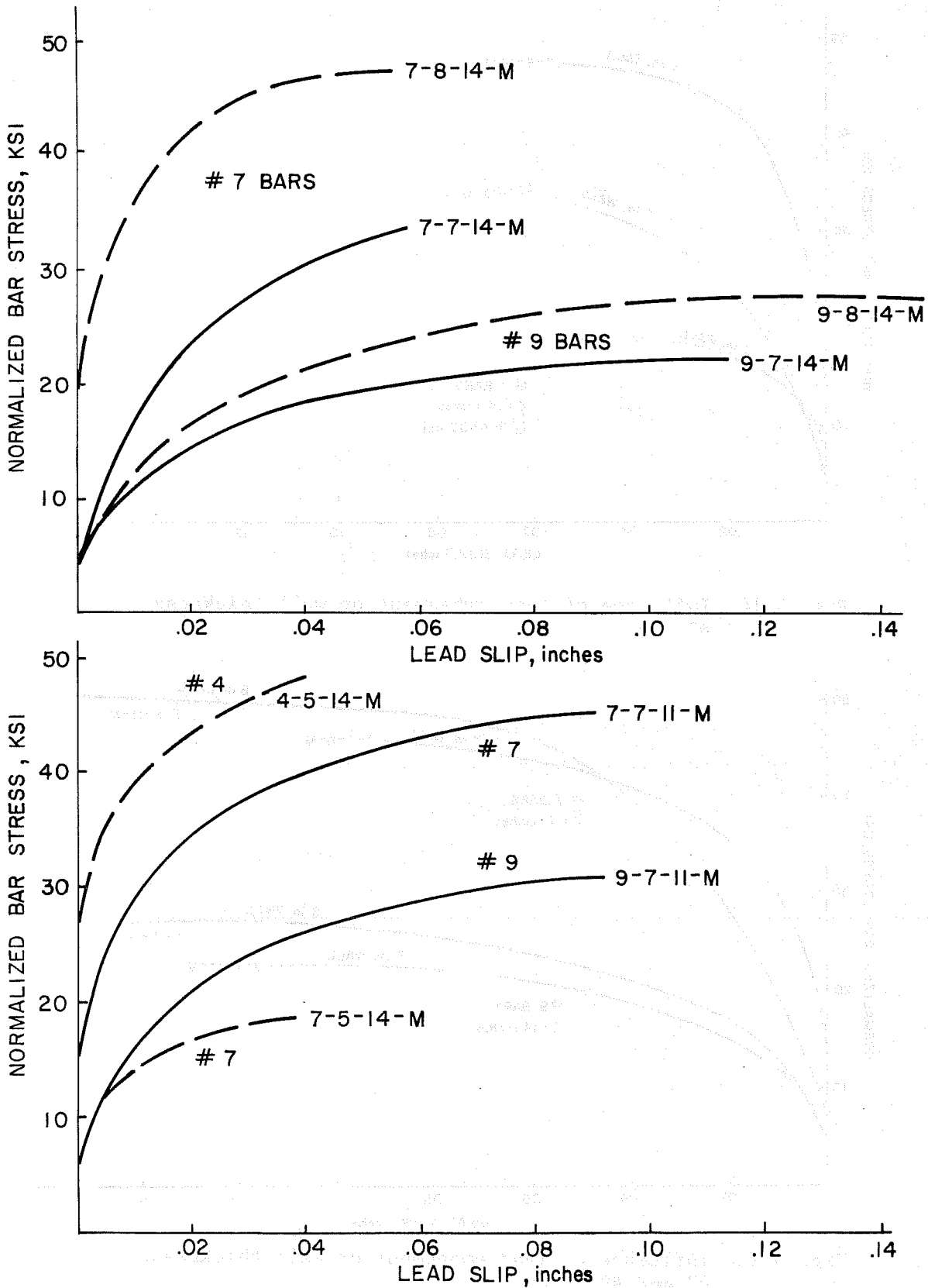
Fig. 3.16 Influence of bar size (stress-slip)
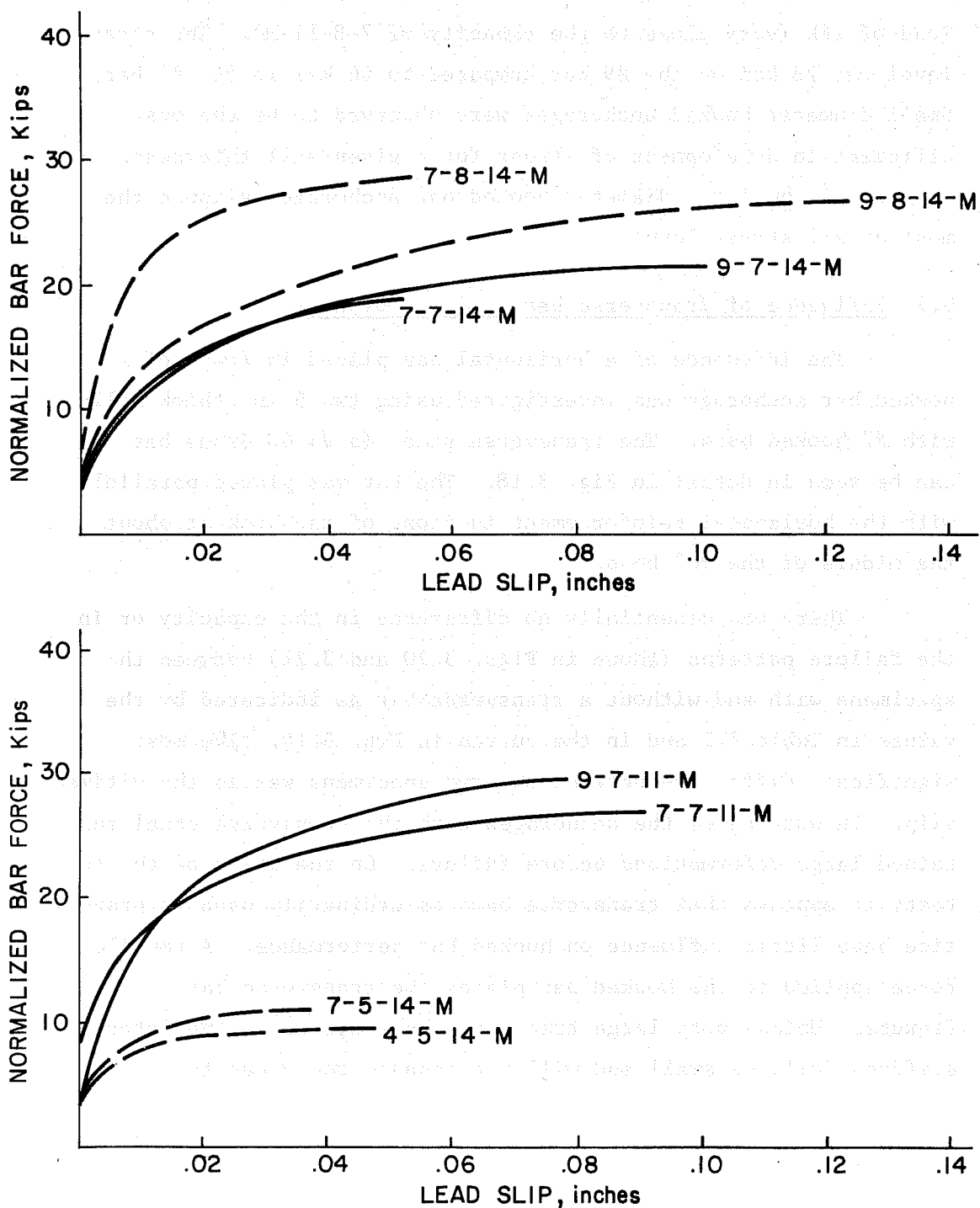
Fig. 3.17   Influence of bar size (load-slip)

interesting trends. For instance, Specimen 7-8-14-M failed at a normalized load of 27.8k. Specimen 9-8-14-M failed at a normalized load of 28k (very close to the capacity of 7-8-14-M). The stress level was 28 ksi on the #9 bar compared to 46 ksi in the #7 bar. Small diameter hooked anchorages were observed to be the most efficient in development of stress for a given wall thickness. In general the large diameter hooked bar anchorages slipped the most at all stress levels.

3.7   Influence of Transverse bar in Front of Hook

The influence of a horizontal bar placed in front of a hooked bar anchorage was investigated using two 5 in. thick walls with #7 hooked bars. The transverse steel (a #4 60 Grade bar) can be seen in detail in Fig. 3.18. The bar was placed parallel with the horizontal reinforcement in front of the hook at about the middle of the 90° bend.

There was essentially no difference in the capacity or in the failure patterns (shown in Figs. 3.20 and 3.21) between the specimens with and without a transverse bar as indicated by the values in Table 3.1 and in the curves in Fig. 3.19. The most significant difference between the two specimens was in the ultimate slip. In both cases the anchorages with the transverse steel sustained large deformations before failure. On the basis of the two tests it appears that transverse bars as ordinarily used in practice have little influence on hooked bar performance. A tensile force applied to the hooked bar places the transverse bar in flexure. Unless very large transverse bars are used, the lateral stiffness will be small and will not enhance the capacity.

TRANSVERSE BAR

VERTICAL REINF.

SIDE
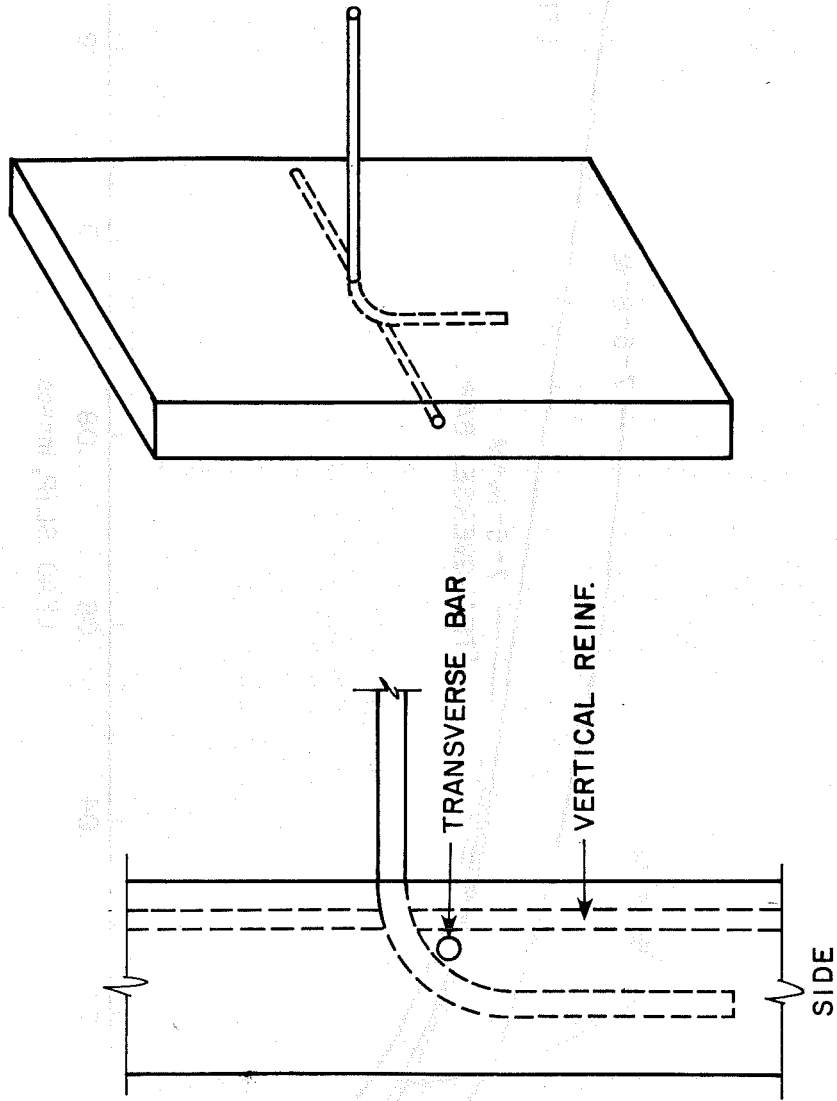
Fig. 3.18 Location of transverse bar
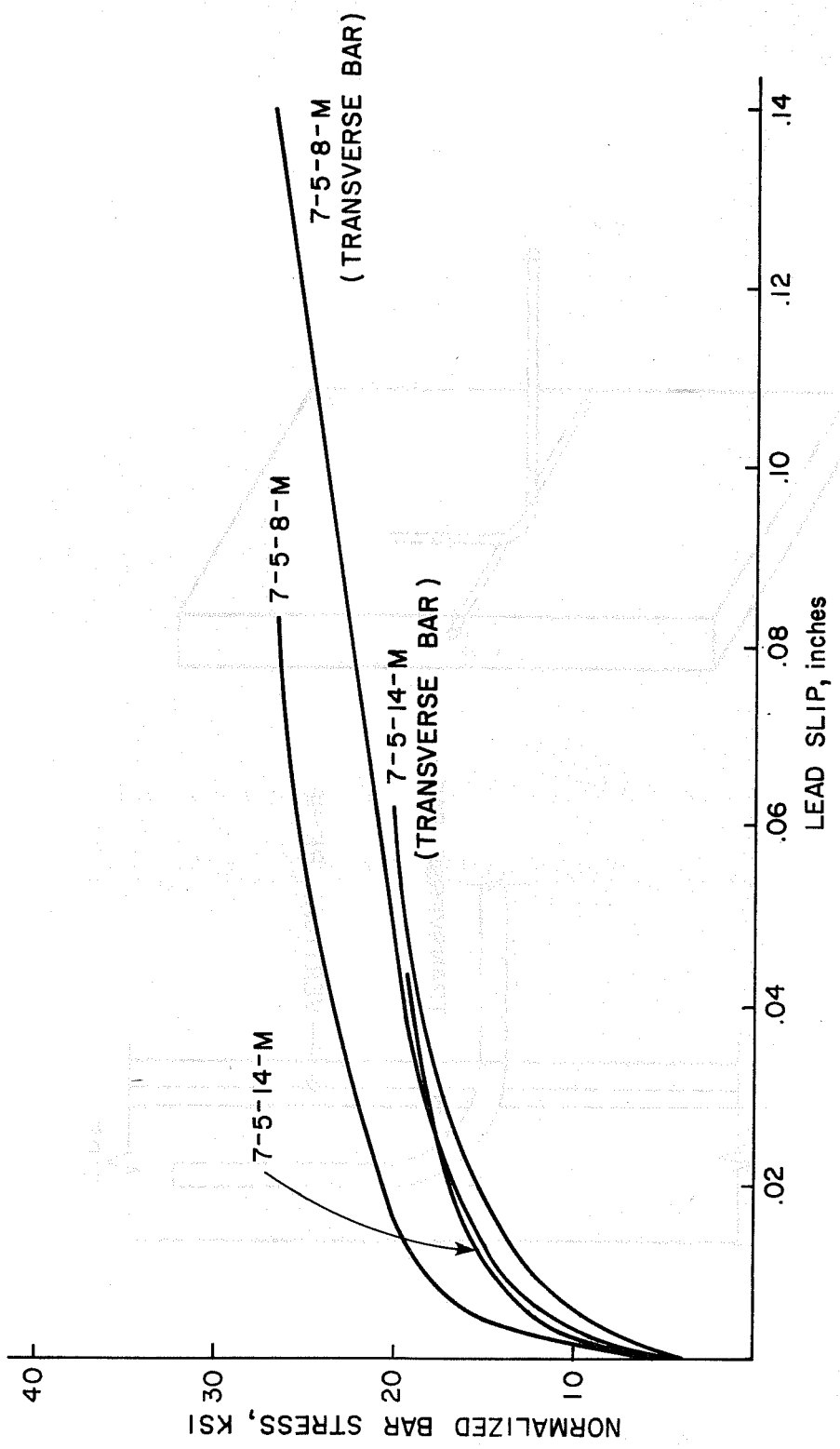
Fig. 3.19   Influence of transverse bar
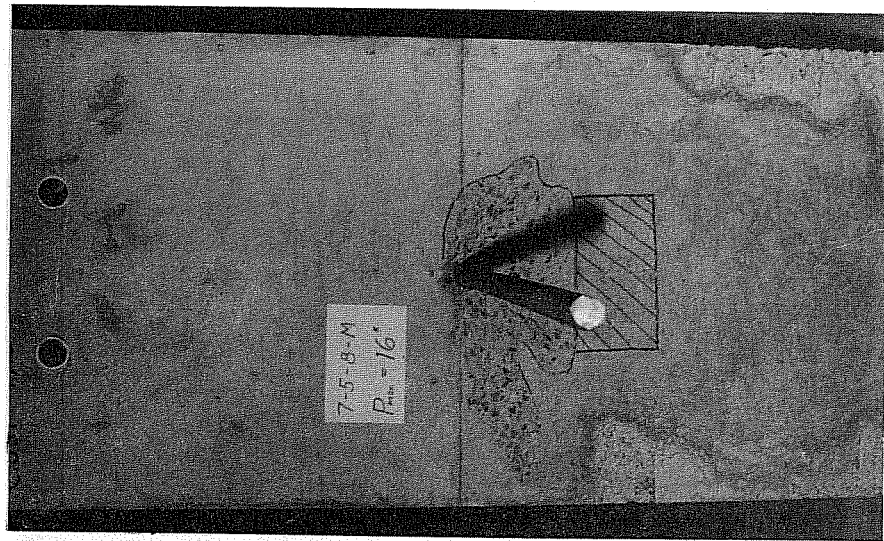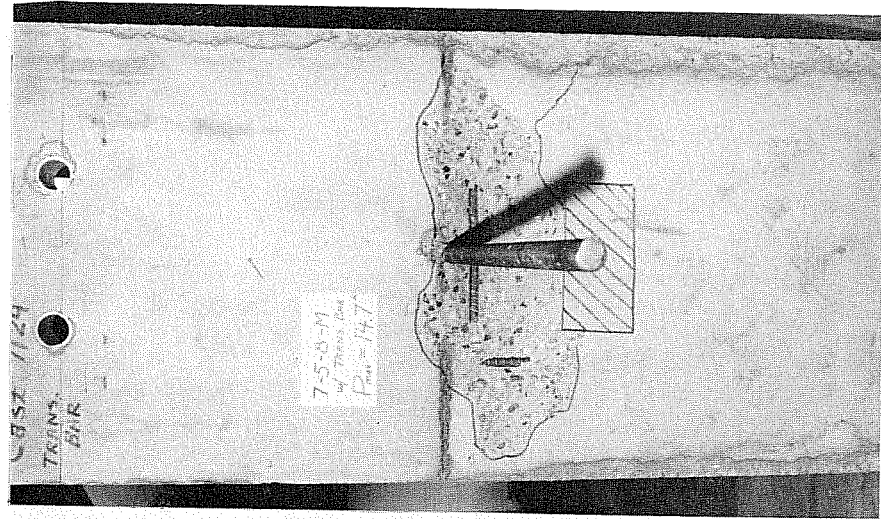
Fig. 3.20 Failure patterns of companion specimens with and without a transverse bar, Z = 8 in.
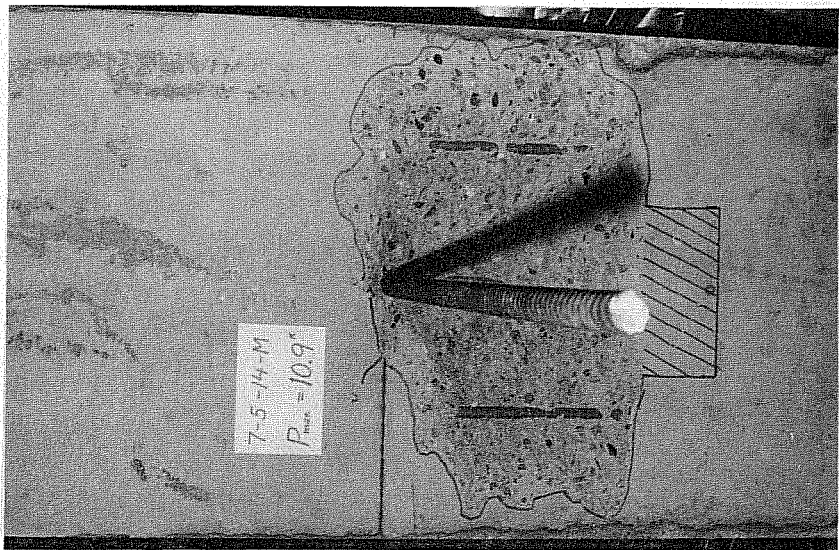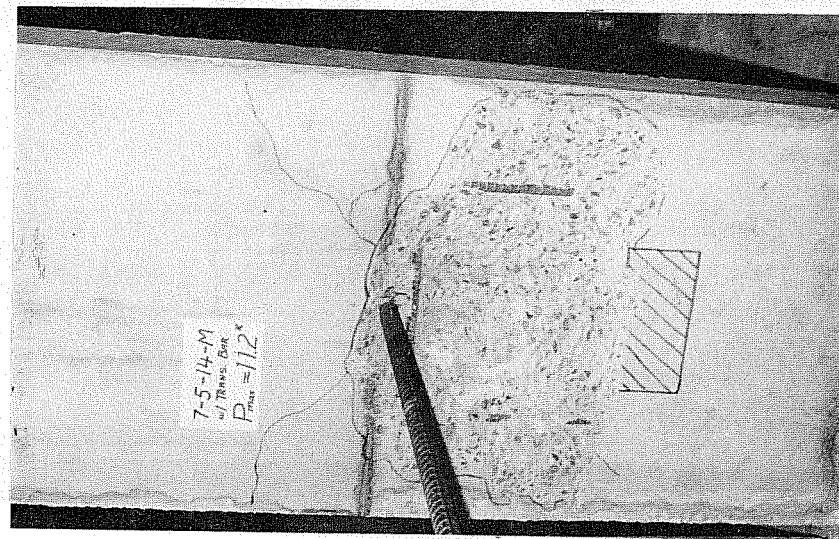
Fig. 3.21 Failure patterns of companion specimens with and without a transverse bar, Z = 14 in.

3.8 Influence of an Unbonded Straight Lead Length

A series of 8 in. thick walls with #7 hooked bar anchorages was studied to determine the influence of lead length between the hook and the face of the wall. In these tests 3 in. of straight lead embedment ahead of the hook were provided. The bar was bonded to the concrete along the 3 in. straight lead length in two specimens and was left unbonded in the other two specimens by placing a sheath over the bar during casting.

The curves in Fig. 3.22 show no significant difference in the ultimate stress capacity between the bonded and unbonded companion specimens. The unbonded Specimen 7-8-14-M had a lower stiffness (stress/slip) in comparison with the bonded Specimen 7-8-14-M. As bond along the straight lead length was destroyed, the entire stress was transferred to the hook leaving the 3 in. lead length essentially unbonded as in the case where a sheath was provided. Little difference was found in ultimate stress, total slip at failure, or failure surface (see Figs. 3.23 and 3.24) between the bonded and unbonded companion specimens.

3.9 Influence of Bar Spacing

A very wide beam or a slab framing into a wall generally requires anchoring a number of bars into the wall. A lower strength might be expected when the bars are closely spaced than when a single bar or widely spaced bars are anchored. To study this possibility several three-bar specimens were tested.

The anchorages of multiple bar Specimen 11-8.5-11-M, with s = 11 in., failed simultaneously while the other multiple bar specimens were characterized by bars failing at slightly different normalized load levels. The right bar in Specimen 7-7-11-L (Fig. 3.26) failed when all bars were loaded to 22k. The left bar
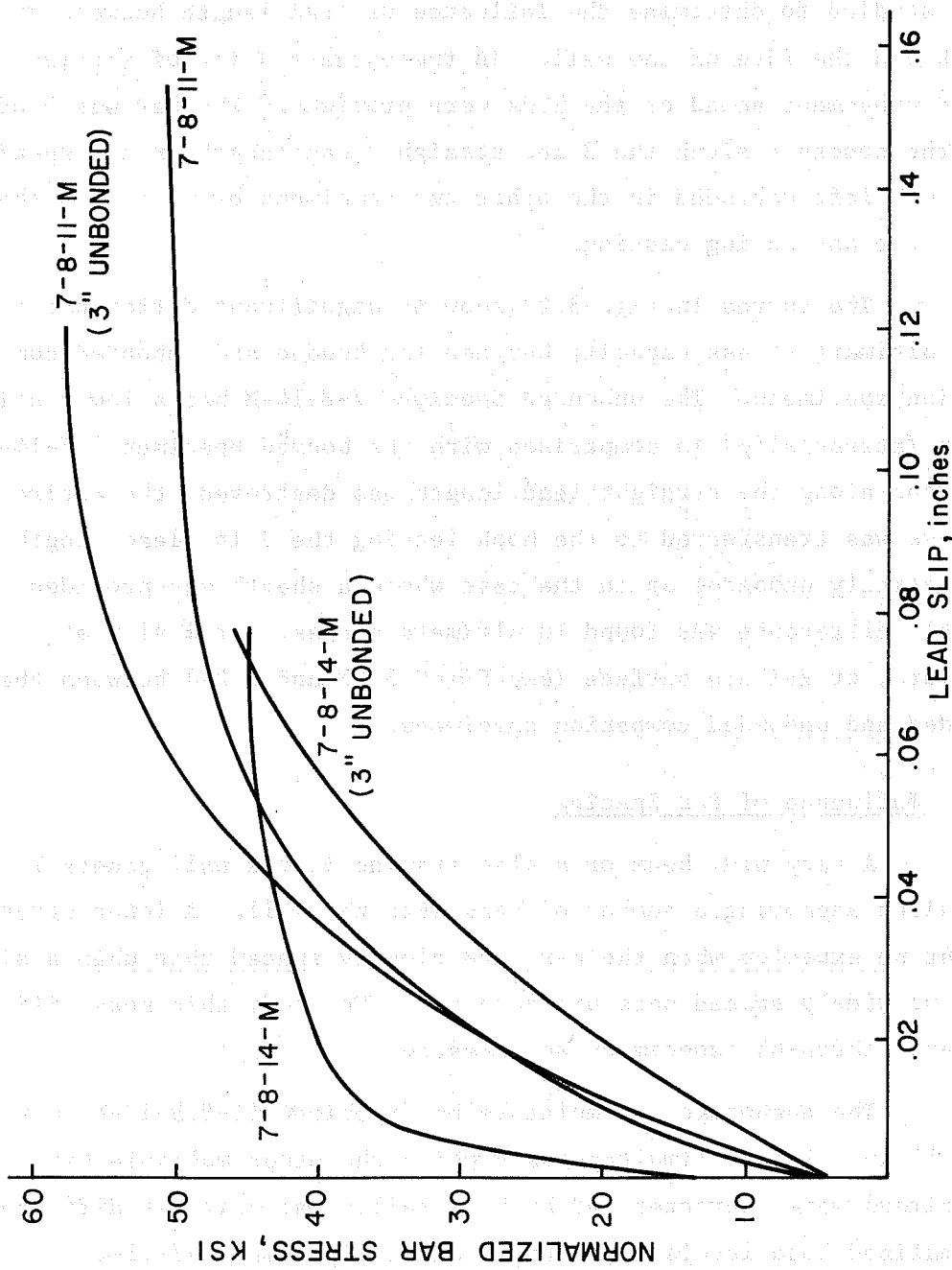
Fig. 3.22 Influence of unbonded lead length
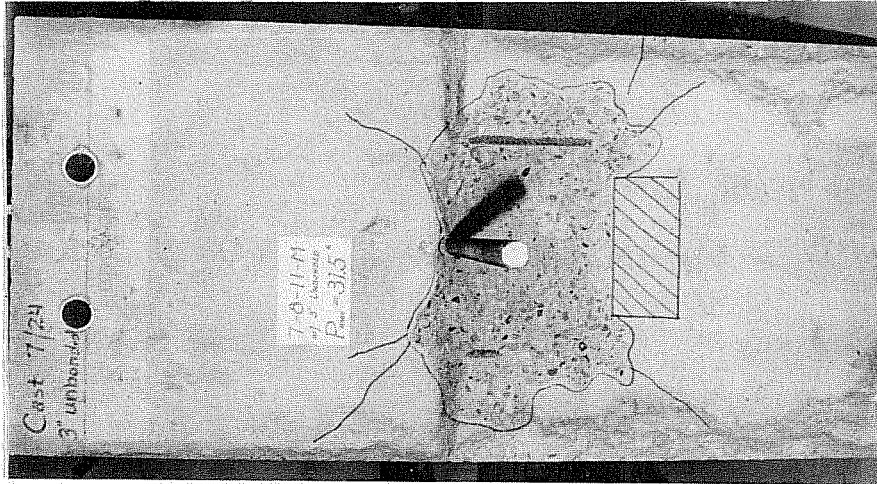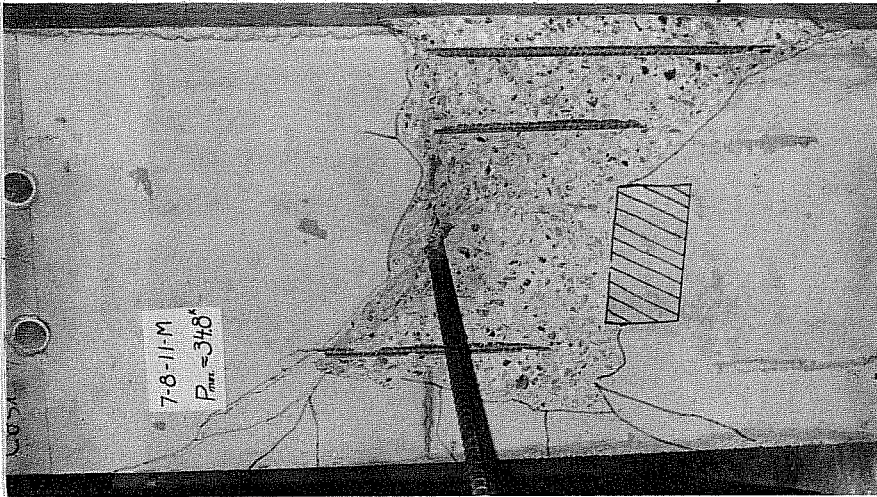
Bonded   Unbonded

Fig. 3.23 Failure Patterns of companion bonded and unbonded specimens, Z = 11 in.

58
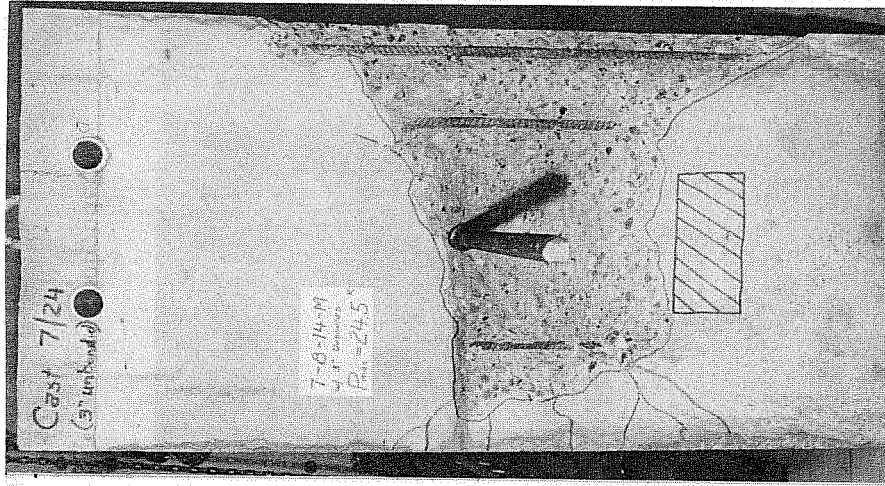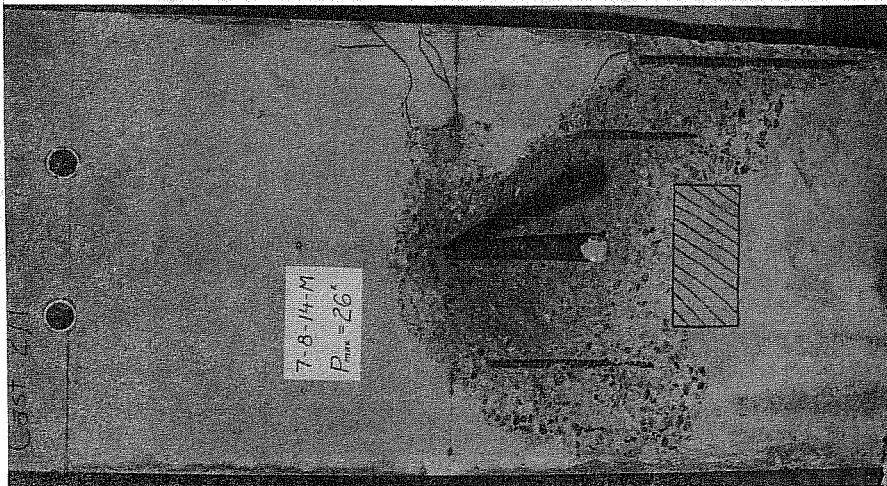
Unbonded

Bonded

Fig. 3.24 Failure patterns of companion bonded and unbonded specimens,
Z = 14 in.
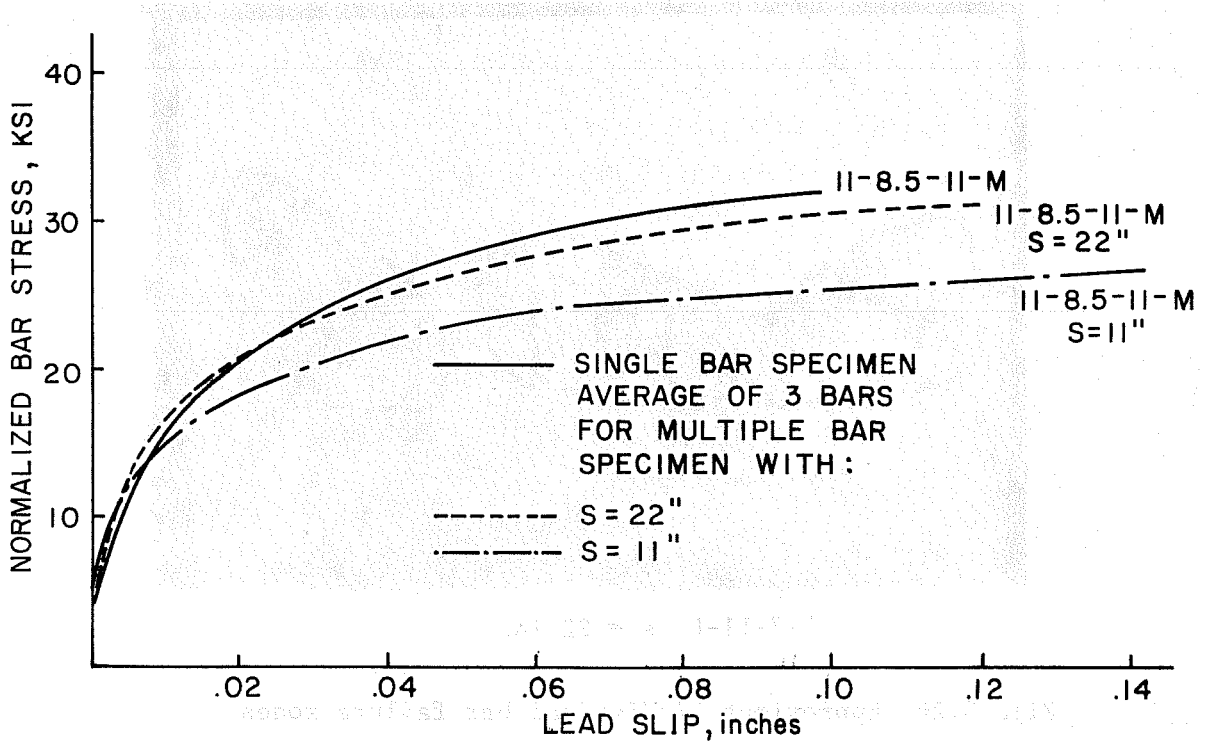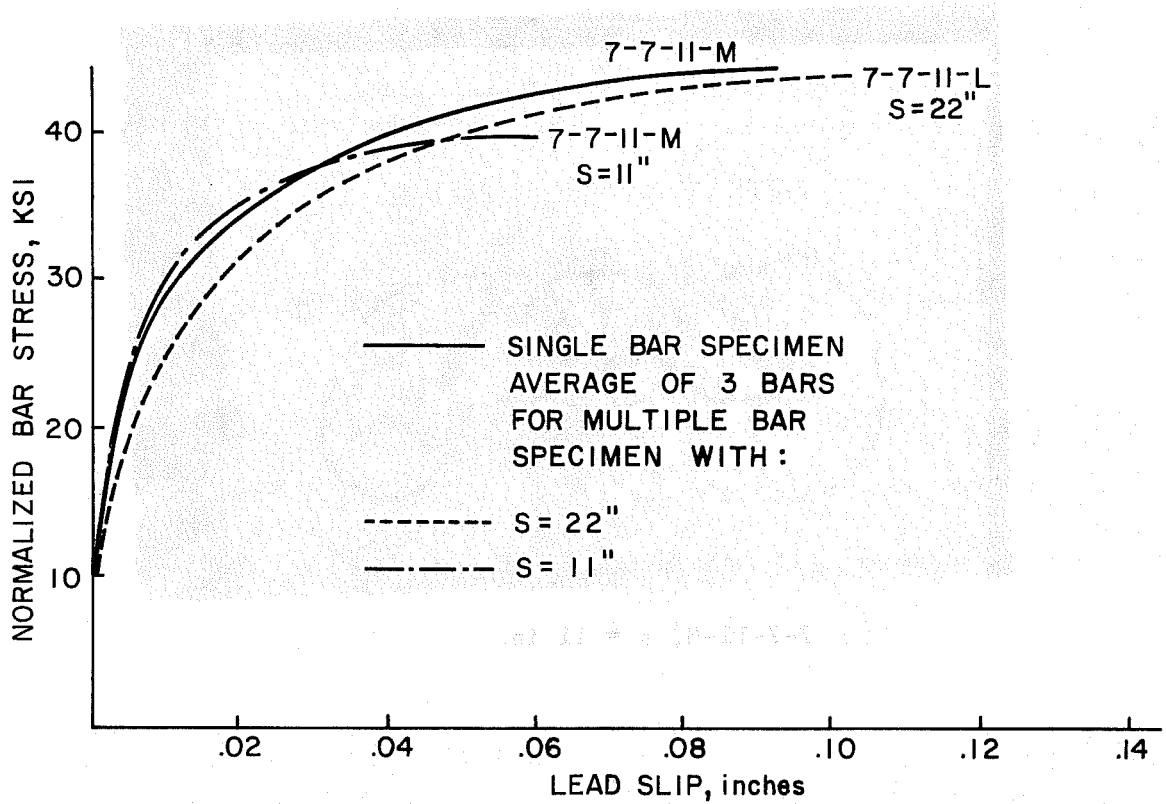
Fig. 3.25 Influence of bar spacing
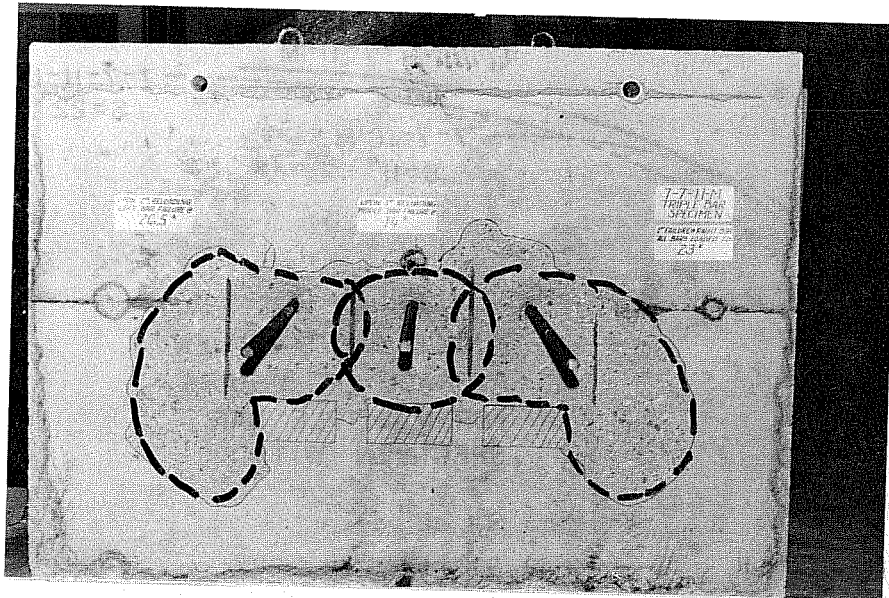
7-7-11-M, s = 11 in.
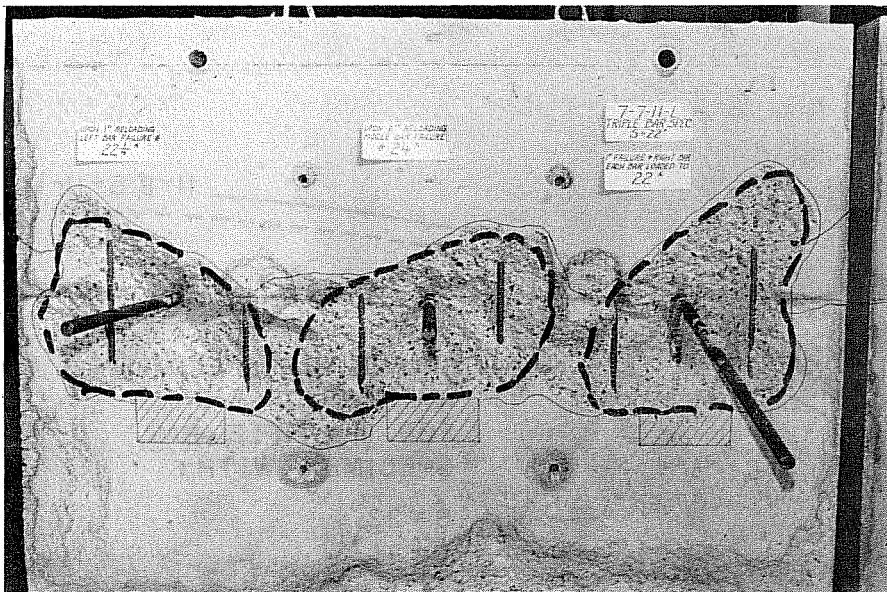
7-7-11-L, s = 22 in.

Fig. 3.26 Approximate individual bar failure zones

failed at 22.25k and the middle bar developed a maximum load of 24k. Both the right and middle bars of Specimen 7-7-11-M (Fig. 3.26) failed at nearly the same load level. The concrete around the right bar fractured first at 23k and upon reloading the middle bar could only carry 14k, indicating that it had failed at the previous 23k load level. The multiple bar specimens in 8.5 in. walls are shown in Fig. 3.27. A bar spacing of 11 in. produced normalized anchorage capacities of 41.4k, while anchorages spaced at 22 in. developed normalized loads of 47.8k, 56.3k, and 44.0k.

Figure 3.25 provides a comparison of stress-slip curves for the multiple bar specimens and companion single bar specimens. Each multiple bar stress-slip curve is the average of three curves. The anchorages spaced at 11 in. developed the lowest stress in each case. By increasing the spacing to 22 in., bars in each multiple bar specimen reached stress and slip levels very near to those of the respective companion single bar specimen. A specimen with a spacing greater than 22 in. would most likely have resulted in the same stress-slip data as for the single bar specimen. The two curves for s = 11 in. indicate a loss of about 5 ksi in ultimate strength due to the interaction of the closely spaced bars. A further decrease in stress capacity would likely occur with further decrease in bar spacing.

The failure surface for each multiple bar specimen is shown in Figs. 3.26 and 3.27. Dashed lines have been added to indicate the approximate zone of failure for each bar. Note the overlap of fracture zones in the cases involving closely spaced bars. Even though the concrete has spalled between each of the bars spaced at 22 in., the spalling is very shallow and indicates very little interaction between failure zones.

62
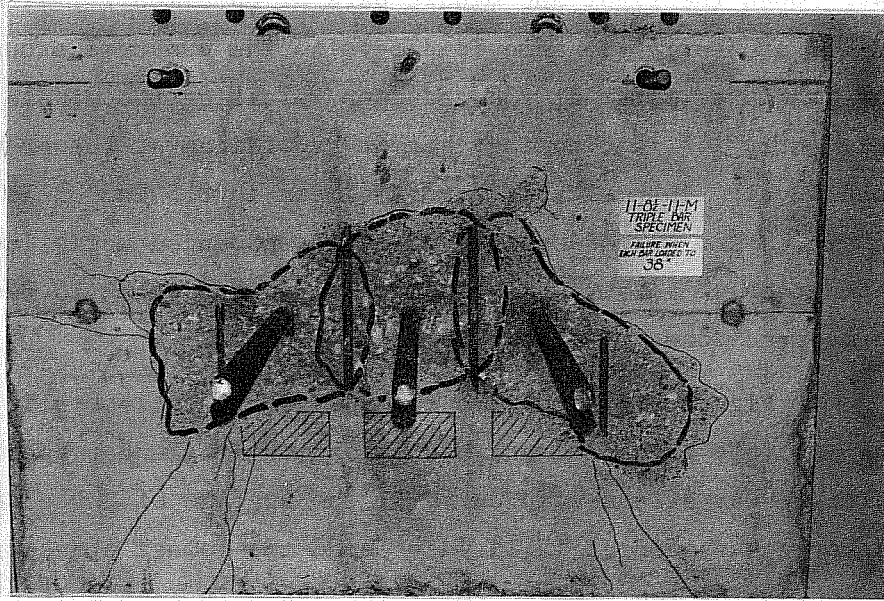
11-8.5-11-M, s = 11 in.
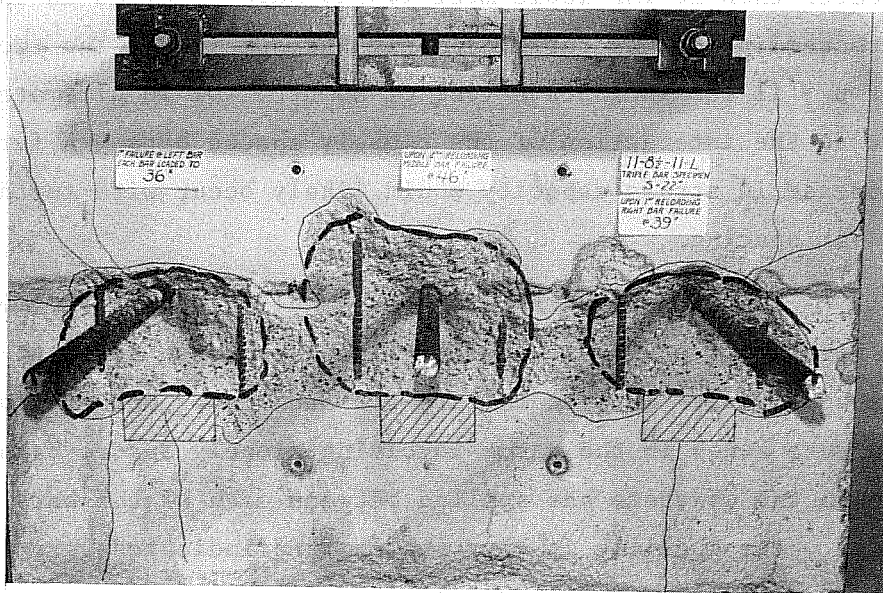
11-8.5-11-L, s = 22 in.

Fig. 3.27 Approximate individual bar failure zones

3.10 A Failure Hypothesis for Hooked Bars with Short Lead Embedment

In the two previous hooked bar investigations it was concluded that the failure of a hooked bar is governed primarily by a loss of cover rather than pulling out [2,3]. In the beam-wall joint cases of this study, fracture and spalling of the concrete in front of the hook produced failure. Failure zones which could be described as "pullout cones" resulted in each case.

As a hook is pulled forward, large compressive stresses develop on the inside of the bend. These stresses must be resisted by diagonal tension in the face cover zone. As the cover splits and fractures, a cone-type failure similar to that observed in tension tests of anchor bolts or headed studs is produced. A reduction in the internal lever arm length (Z) provides greater restraint to the face-splitting stresses, thereby allowing the anchorage to develop a greater capacity. Also, the internal lever arm length seems to control the failure surface and the extent of spalling, as shown in Fig. 3.28.

The interaction of stresses on common areas of concrete between closely spaced bars generally leads to a lower ultimate capacity of each bar. As the bars are placed closer together, the fracture surfaces overlap, resulting in earlier anchorage failure.

Transverse steel in front of a hook provides some initial restraint against splitting, allowing for greater deformations, but does not increase capacity. Tension on the hooked bar places the transverse bar in flexure so that small bars having very little lateral stiffness cannot offer the hook any additional restraint at ultimate. The use of very large transverse bars might lead to greater ultimate capacity but were not considered in this investigation.
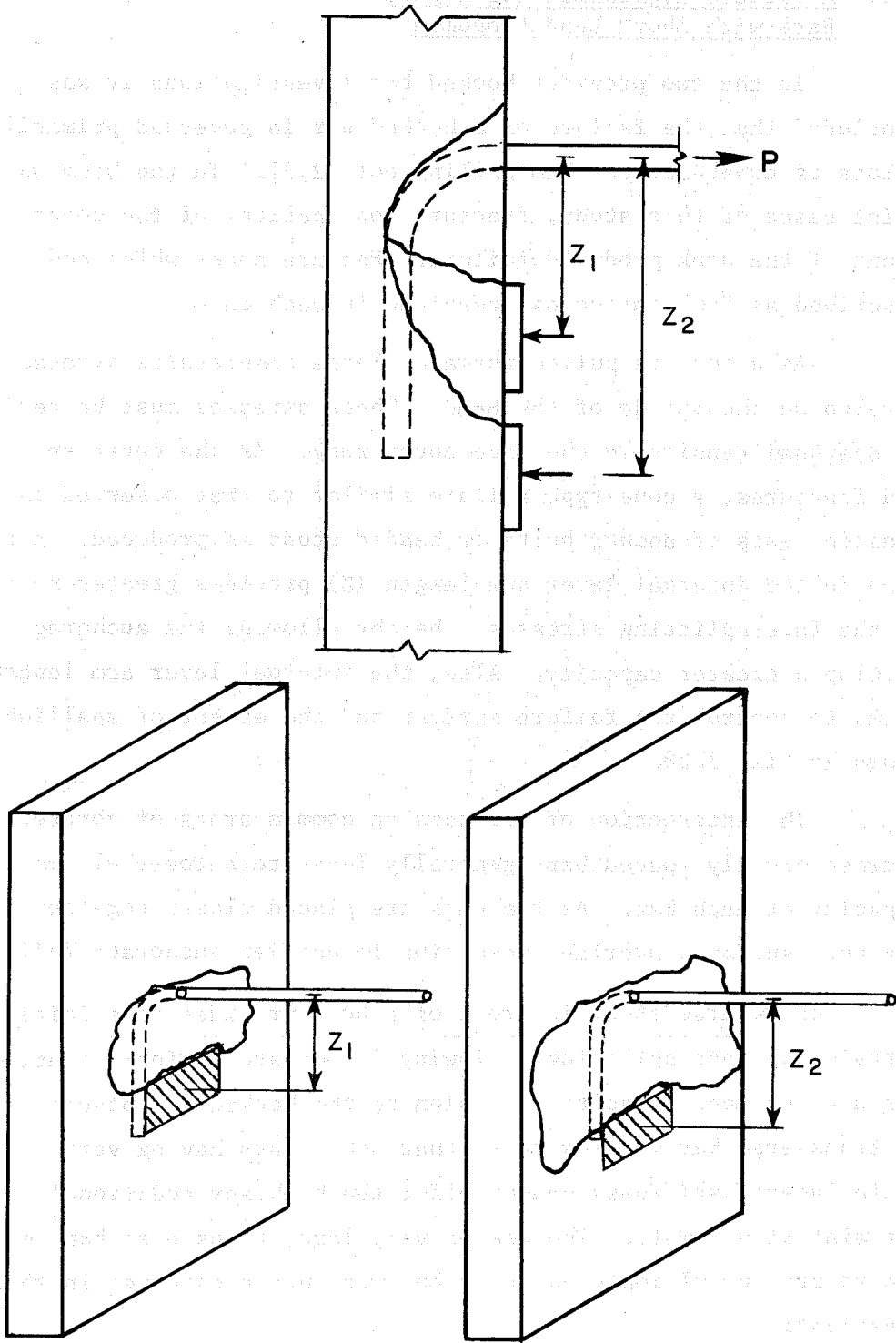
Fig. 3.28 Influence of lever arm (Z) on failure zone

The diameter of the hooked bar is very important in determining the efficiency of the anchorage. Two bars, differing in diameter but having the same embedment length will develop approximately the same load. This indicates the relative insignificance of bar diameter compared to hook embedment length. In terms of the failure mechanism postulated above, for a given hook embedment there is a certain amount of concrete in front of the hook that will resist the pullout force, regardless of bar diameter and straight lead embedment. The unbonded specimens showed the insignificance of bond over the straight lead length. Therefore, the efficiency of a small bar in relation to a large bar for this type of anchorage is seen by comparing the capacity and the pullout stiffness (stress/slip). For a given load, small diameter bars are stressed to a higher level and generally slip less at all stress levels.

4. IMPLICATION OF TEST RESULTS ON DESIGN PROCEDURES

4.1 Introduction

The design provisions in ACI 318-77 for standard hooks in tension offer limited guidance for the design of such hooks in practice. Recent investigations of the strength of hooked bars in structural applications (beam-column joints) resulted in the basic development length equation for hooked bars given by Eq. 1.1. This equation provides a simpler and more accurate method of determining hooked bar anchorage capacity by accounting for variables such as side cover on the hook and the amount of transverse reinforcement. However, the requirement that the basic development length of a hook (straight lead embedment plus bend radius plus one bar diameter) be at least $8d_b$ or 6 in., whichever is greater, was imposed because there was virtually no data on the strength of hooks with very short straight lead embedments. Therefore, the tests reported herein were directed toward filling this gap by investigating hooks with short embedments. Observations of the failure patterns of such short hook embedments show a striking similarity to the failures resulting from anchor bolts or studs under tension and imply that a method similar to that used to predict headed stud or anchor bolt tension capacity might be employed for short hooked bar anchorages.

4.2 Measured vs Computed Strength

ACI 318-77 Design Provisions. Section 12.5 of ACI 318-77 states that standard hooks in tension be considered to develop a stress given by:

$$f_h = \xi \sqrt{f'_c} \tag{4.1}$$

67

Values of ξ are provided in Table 12.5.1 and depend on bar size, grade of steel, and the classification of the bar as a "top bar" or "other bar". The basis for the ξ values as well as for the "top bar" or "other bar" classifications are ambiguous. In addition, a footnote to Table 12.5.1 permits an increase of 30 percent in ξ if "enclosure" perpendicular to the plane of the hook is provided. However, "enclosure" is not defined. Therefore, "top cast" and "other bar" hook capacities were calculated for each specimen in this study neglecting effects of "enclosure". In some instances it was necessary to determine the stress developed by straight lead embedment using the basic equation for development length, ACI Sec. 12.2, and solving for f_ℓ in terms of a known straight lead length.

$$f_\ell = \frac{l_\ell \sqrt{f'_c}}{0.04A_b} \tag{4.2}$$

where l_ℓ = straight lead length

A_b = area of bar

For straight lead lengths with more than 12 in. of concrete cast below the bar, f_ℓ is multiplied by $1/1.4 = 0.71$. The capacity of the anchorage using ACI 318-77 was determined by Eqs. 4.3 and 4.4 for "top cast" and "other bars".

$$\text{ACI (Top Cast)} \quad f_s = f_{h\ top} + f_\ell/1.4 \tag{4.3}$$

$$\text{ACI (Other Bars)} \quad f_s = f_{h\ other} + f_\ell \tag{4.4}$$

Measured anchorage capacities (which have been normalized using $\sqrt{f'_c/45000}$) are tabulated along with calculated ACI hook capacities (top bars and other bars) in Table 4.1 and plotted in Fig. 4.1.

ACI recommendations for "other bars" generally overestimate strength of short hooked bar embedments. The difference depends to a large extent on the internal lever arm length (Z). An

TABLE 4.1 MEASURED CAPACITY VS ACI 318-77 AND COMMITTEE 408 RECOMMENDATIONS

Specimen	Meas. Capacity (normalized)* P(meas) kips	Meas. Stress (normalized)* f_s(meas) ksi	ACI 318-77* Top bars f_s, ksi	ACI 318-77* Other bars f_s, ksi	ACI 408* f_s, ksi	ACI 318-77 $\dfrac{f_s(\text{meas})}{f_s(\text{top})}$	ACI 318-77 $\dfrac{f_s(\text{meas})}{f_s(\text{other})}$	ACI 408 $\dfrac{f_s(\text{meas})}{f_s(408)}$
4-3.5-8-M	3.80	19.0	36.2	36.2	17.0	0.52	0.52	1.12
4-5-11-M	12.00	60.0	45.2	48.8	29.8	1.32	1.23	2.01
4-5-14-M	9.80	49.0	45.2	48.8	"	1.08	1.00	1.64
7-5-8-L	17.44	29.0	24.1	36.2	17.0	1.20	0.80	1.71
7-5-8-M	16.50	27.5	"	"	"	1.14	0.76	1.62
7-5-8-H	17.80	29.7	"	"	"	1.23	0.82	1.75
7-5-14-L	11.40	19.0	"	"	"	0.79	0.52	1.12
7-5-14-M	11.73	19.6	"	"	"	0.81	0.54	1.15
7-5-14-H	10.90	18.2	"	"	"	0.75	0.50	1.07
7-7-8-M	32.00	53.3	27.9	41.3	26.7	1.91	1.29	2.00
7-7-11-M	27.00	45.0	"	"	"	1.61	1.09	1.69
7-7-14-M	20.00	33.3	"	"	"	1.19	0.81	1.25
9-7-11-M	30.80	30.8	24.1	36.2	20.9	1.28	0.85	1.47
9-7-14-M	22.63	22.6	"	"	"	0.94	0.63	1.08
9-7-18-M	22.20	22.2	"	"	"	0.92	0.61	1.06
7-8-11-M	31.77	53.0	30.1	44.6	31.6	1.76	1.19	1.59
7-8-14-M	27.76	46.3	"	"	"	1.54	1.04	1.47
9-8-14-M	28.00	28.0	25.3	37.9	24.7	1.11	0.74	1.13
11-8.5-11-L	49.60	31.8	24.2	28.2	21.1	1.32	1.13	1.51
11-8.5-11-M	49.90	32.0	"	"	"	1.32	1.14	1.52
11-8.5-11-H	50.00	32.0	"	"	"	1.32	1.14	1.52
11-8.5-14-L	41.60	26.7	"	"	"	1.10	0.95	1.27
11-8.5-14-M	38.00	24.4	"	"	"	1.01	0.86	1.16
11-8.5-14-H	41.50	26.6	"	"	"	1.10	0.94	1.26
Average						1.18	0.88	1.42**
σ_n						0.31	0.24	0.29

*Based on f'_c = 4500 psi   **Avg. is 1.78 if ϕ = 0.8 is used in ACI 408 approach.
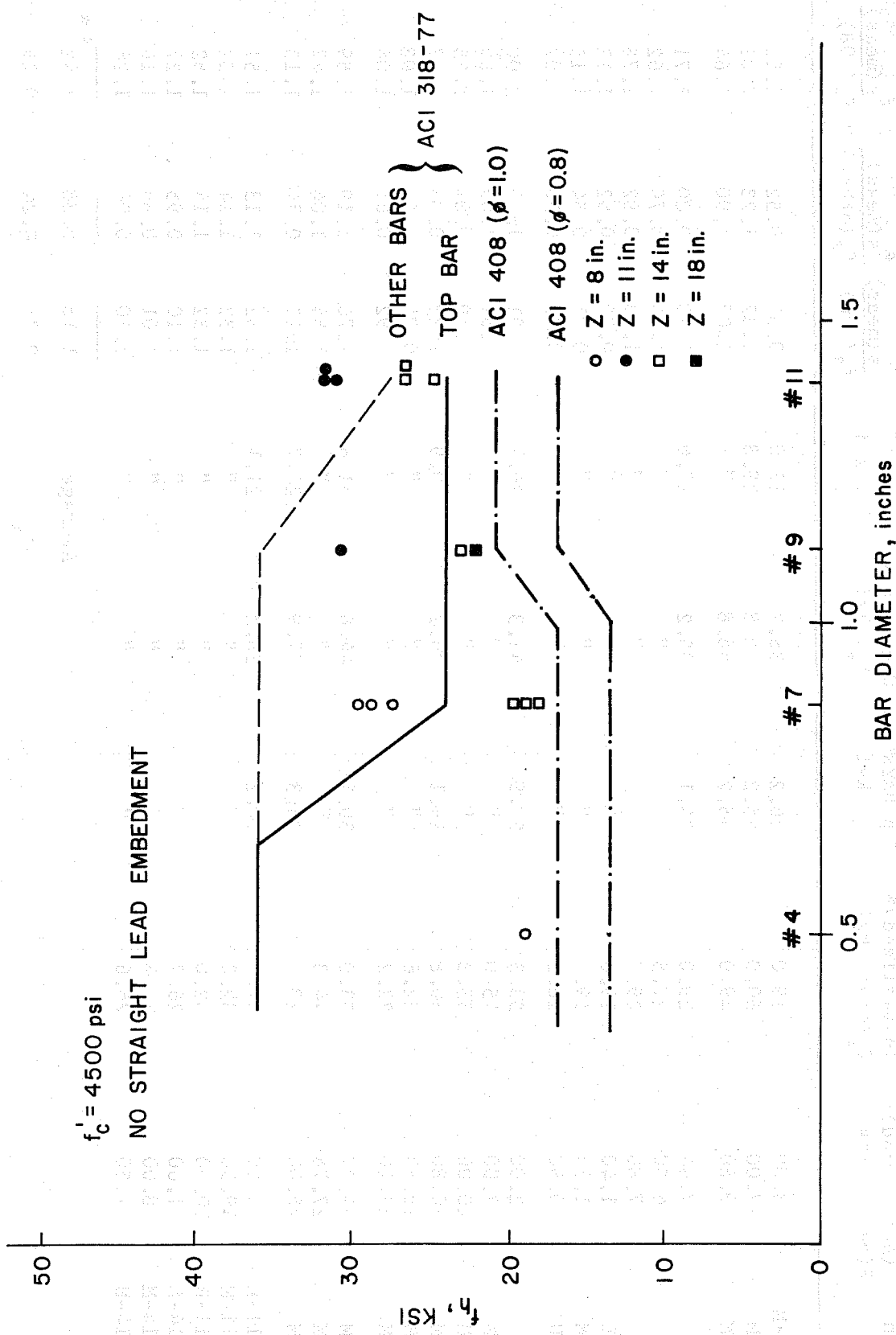
Fig. 4.1 Comparison of measured and computed hook capacity

increase in the lever arm length decreases hook capacity, thereby
increasing the difference between measured values and ACI values.
Table 4.1 provides ratios of measured to computed hook capacity. The
average for f_s(meas)/f_s(other) is 0.88, with a standard deviation of
0.24. This means that on the average, short hooked anchorages in
this study had 12 percent less capacity than computed using
ACI 318-77 for "other bars".

ACI hook recommendations for "top bars" provide somewhat
better results. Generally about half of the specimens showed a
strength in excess of that predicted by ACI 318-77 (for "top bars"),
while half held less load than estimated. The average for f_s(meas)/
f_s(top) of 1.18 (standard deviation = 0.31) appears to be acceptable
for design; however, use of ACI recommendations for hooks with short
embedment could easily result in failure at low stresses in some
cases. The overestimation of load capacity using ACI provisions
for specimens with large internal moment arms raises serious ques-
tions regarding the adequacy of ACI 318-77 for hooked bar capacity.

Design Recommendations of ACI Committee 408. The two
previous hooked bar investigations supported by Reinforced Concrete
Research Council Project 33 [2,3] led to the following basic embed-
ment length equation for standard hooks in tension.

$$\ell_{dh} = \frac{0.02 \cdot d_b \cdot f_h}{\psi \sqrt{f'_c}}$$ (4.5)

where ℓ_{dh} = embedment length of hooked bar in tension (includes
straight lead embedment + bend radius + one bar
diameter)

        $\geq 8d_b$ or 6 in., whichever greater

     ψ = one or a combination of the factors (described in
Chapter 1) as applicable

It should be noted that a prime objective of this study was to
examine the validity of the $8d_b$ or 6 in. limitation.

To state Eq. 4.5 in a form similar to that of other development length equations, ACI Committee 408 provided the following recommendations:

$$\ell_{dh} = \ell_{hb} \cdot \text{(applicable factors)} \tag{4.6}$$

where ℓ_{dh} = development length of a deformed bar in tension terminating in a standard hook

ℓ_{hb} = basic development length of a standard hook

$$= \frac{0.02 \cdot d_b \cdot f_y}{\sqrt{f'_c}}$$

$$= \frac{0.02 \cdot d_b \cdot 60000}{\sqrt{f'_c}} \cdot \frac{0.8}{\phi} \quad \text{where } \phi = 0.8$$

$$\ell_{hb} = \frac{960 \cdot d_b}{\phi \cdot \sqrt{f'_c}} \tag{4.7}$$

and the applicable factors are

$f_y/60000$ - for reinforcement having yield strength other than 60000 psi.

0.7 - for #11 bars or smaller with side cover normal to the plane of the hooked bar not less than 2.5 in. and cover on the tail extension of 90° hooks not less than 2 in.

0.8 - for additional confinement by closed stirrups or hoops at a spacing of $3d_b$ or less.

1.25- for lightweight concrete replacing all or a portion of the aggregate

A_{sr}/A_{sp} - for reinforcement in flexural members (not subjected to seismic loads) in excess of that required.

Equations 4.5 and 4.6 may appear to be different but are simply two forms of the same equation. The value of ψ for each specimen of this study is 1.0. By rearranging the terms in Eq. 4.7, the hook

capacity for any given embedment length can be determined:

$$f_h = \frac{63\phi\ell_{dh}f'_c}{d_b} \qquad (4.8)$$

An estimation of anchorage capacity for each specimen using Eq. 4.8 (with ϕ = 1.0) is tabulated in Table 4.1. Also, a curve representing the Committee 408 proposal for hooks with no straight lead embedment is shown in Fig. 4.1.

It is interesting to note that none of the test results fall below the curve representing the Committee 408 proposal. The ACI 408 proposed approach approximates the results quite well. The ratios of measured-to-computed hook capacities range from a low of 1.07 to a high of 2.0. The average for f_s(meas)/f_s(408) is 1.42 with ϕ = 1.0. With ϕ = 0.8, the average ratio increases to 1.78. The results indicate that the Committee 408 proposal can be safely extended into the short hook embedment range of $8d_b$, 6 in., or less. In some cases, Eq. 4.8 may be too conservative. Bar size and lever arm length seem to be the variables which account for the conservative estimate of strength using the Committee 408 proposal. For instance, as can be seen in Fig. 4.1, a #7 hooked bar embedded in a 5 in. wall exhibits greater strength when the lever arm distance is reduced from 14 in. to 8 in. A #9 hooked bar embedded in a 7 in. wall begins to show large strength increases when Z is decreased to 11 in. or less. In general, the Committee 408 proposal provides a lower bound which can be used to estimate short hook embedment capacity. Adjustments for lever arm (beam depth) appear to be unnecessary. The range of Z values considered in this study appear to bracket values expected in practical structures.

Anchor Bolt or Stud, Stress Cone-Type Failures. The proposed addition to "Code Requirements for Nuclear Safety Related Concrete Structures (ACI 349-76) [6], recommends that a 45° stress cone radiating from the head of an anchor bolt or stud embedment to the surface, as shown in Fig. 4.2, be considered as the failure surface.
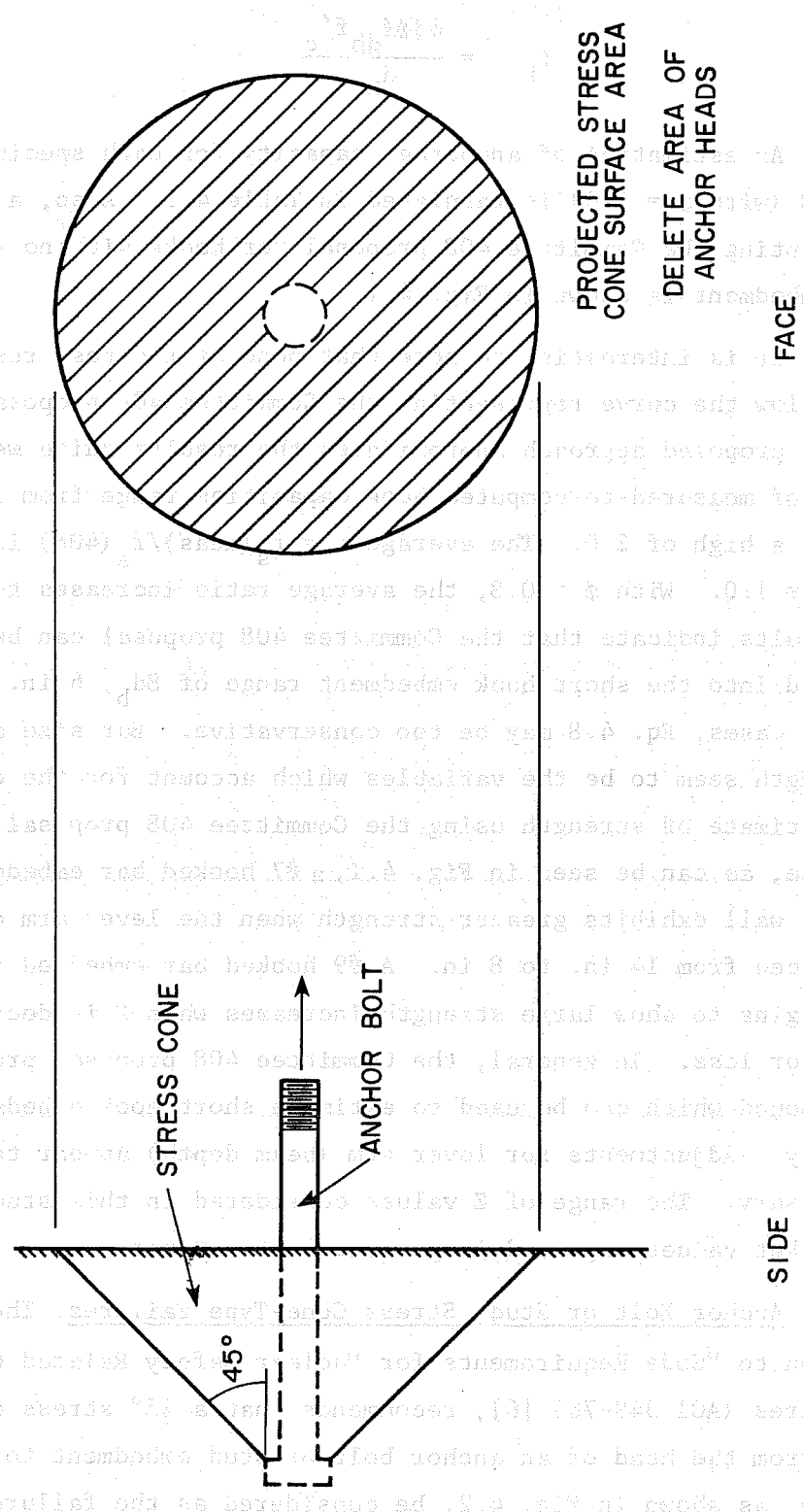
Fig. 4.2 Committee 349 recommendation for a single steel embedment

A tensile stress capacity of $4\sqrt{f'_c}$ is applied to the projected stress cone surface area in determining anchorage tensile load capacity.

Since all the specimens of this investigation resulted in a cone-type fracture, it was felt that a procedure similar to the ACI 349 recommendation for anchorage capacity might apply to hooked bars with short embedment. A 45° cone beginning at the tail point of tangency of the hook was assumed for each wall thickness and the projected stress cone area was determined as indicated in Fig. 4.3. Bar size was neglected in the calculations. The same concrete tensile stress capacity, $4\sqrt{f'_c}$, recommended by Committee 349 was applied to the projected stress cone area for each wall thickness of this study. In order to base these calculations on the same material strength as the normalized observed results, a concrete strength of 4500 psi was used. The curve in Fig. 4.4 represents the estimated loads for the wall thicknesses of this study using the stress cone approach. The test data (based on wall thickness, bar size, and internal beam lever arm) have been added for comparison. It is interesting that the curve is perhaps the best fit through the data points. Specimens with lever arm lengths 11 in. or less generally fall on or above the curve while specimens with larger lever arm lengths of 14 and 18 in. fall below. For small internal lever arms the capacity is underestimated and for large internal lever arms it is overestimated.

In evaluating the data two factors tend to complicate any explanation. A small internal beam lever arm results in greater confinement on the hook and a smaller failure surface area. In reality more confinement will result in greater load capacity while a smaller failure surface area is generally connected with a smaller load capacity since less concrete actually fractures. Apparently, confinement outweighs the influence of failure surface area, since all tests show more load capacity as Z decreases.
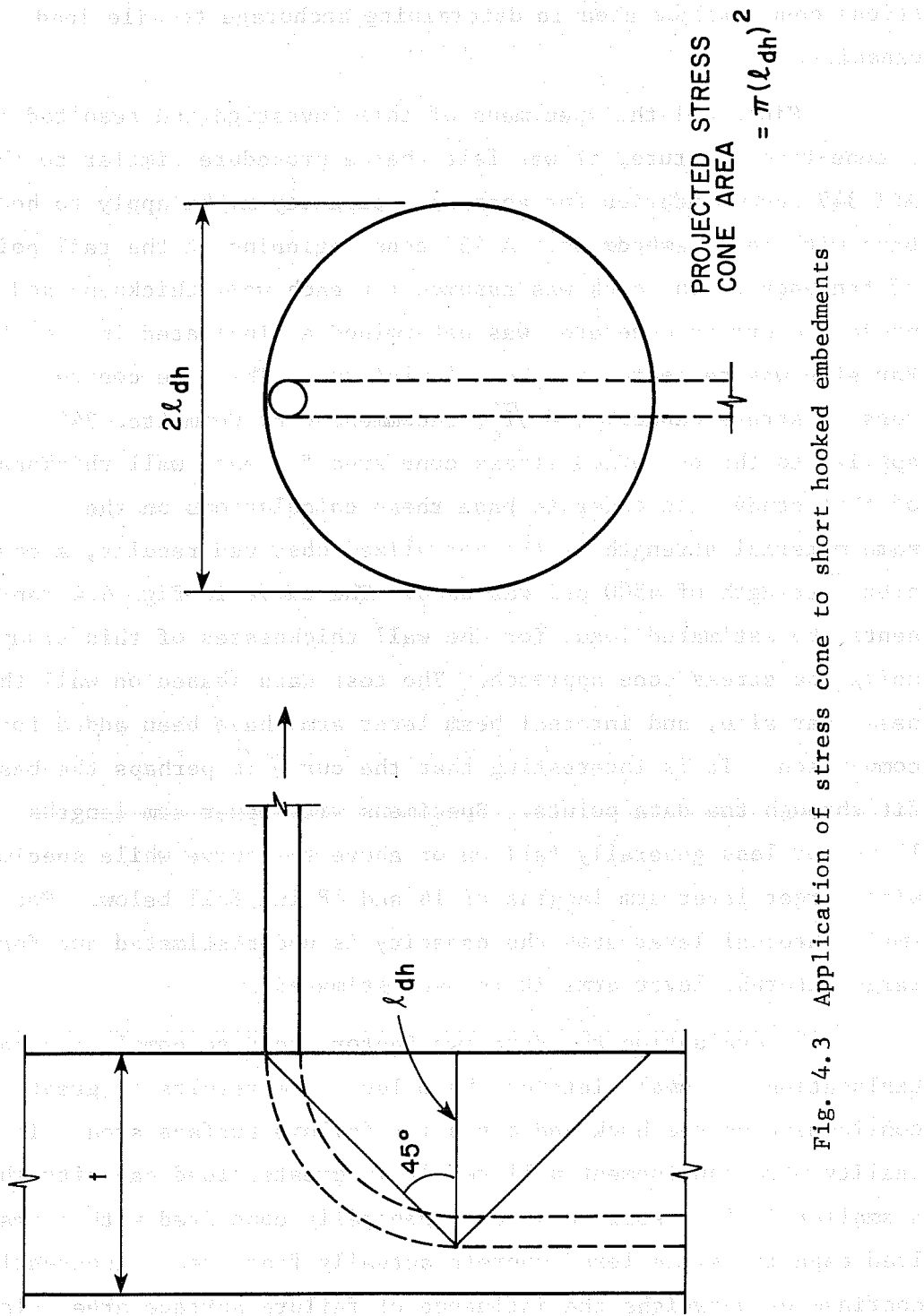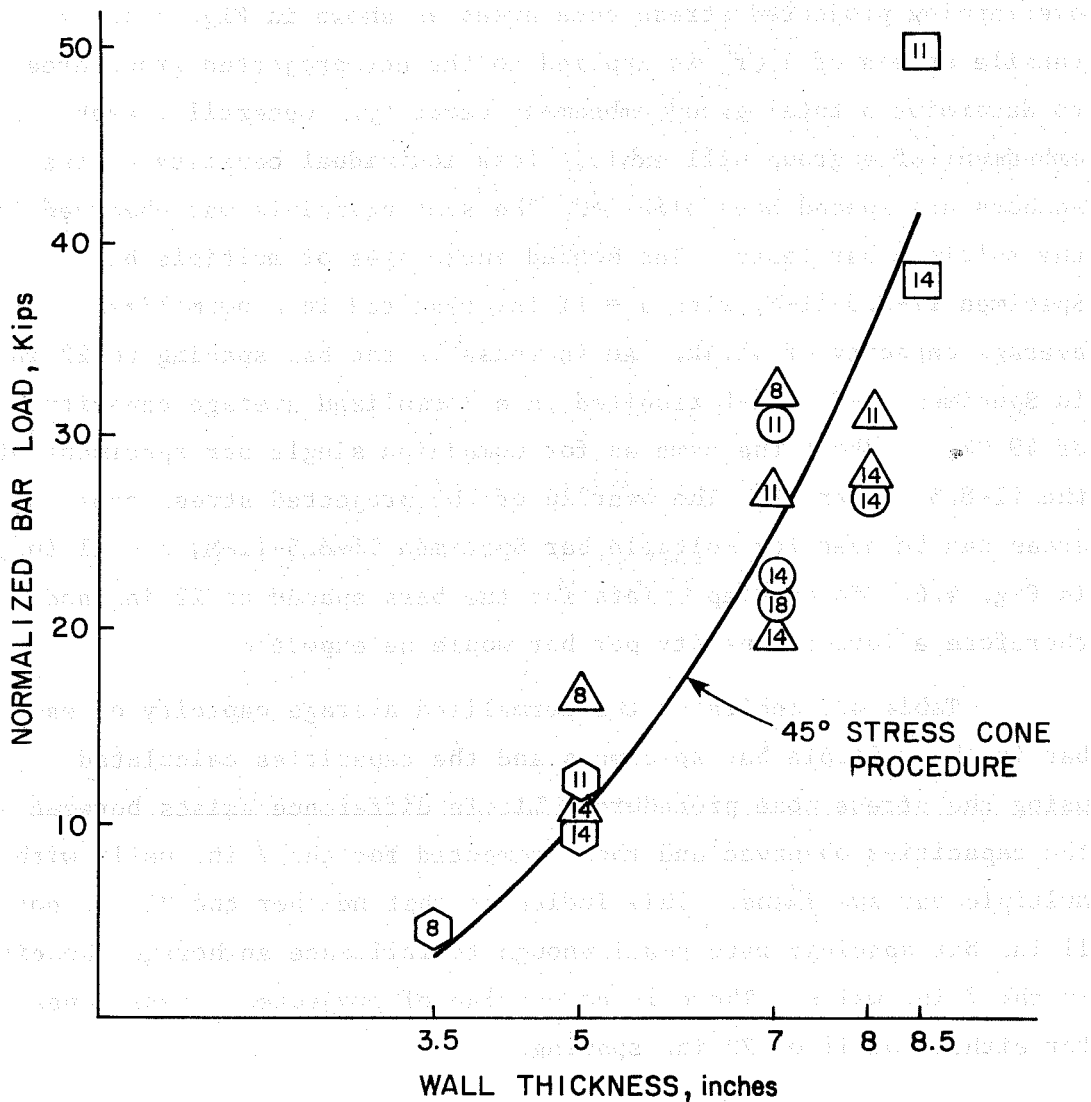
PROJECTED STRESS CONE AREA $= \pi(\ell_{dh})^2$

$2\ell_{dh}$

ℓ_{dh}

$45°$

t

Fig. 4.3 Application of stress cone to short hooked embedments

Fig. 4.4 Measured vs stress cone estimated hook capacities

The Committee 349 report also recommends a method of determining the effective capacity of grouped steel embedments with overlapping projected stress cone areas as shown in Fig. 4.5. A tensile stress of $4\sqrt{f'_c}$ is applied to the net projected group area to determine a total group embedment capacity. Generally, each embedment of a group will exhibit less individual capacity as the anchors are spaced more closely. The same principle was observed in the multiple bar tests. The hooked anchorages of multiple bar Specimen 11-8.5-11-M, with s = 11 in., resulted in a normalized average capacity of 41.4k. An increase in the bar spacing to 22 in. in Specimen 11-8.5-11-L resulted in a normalized average capacity of 49.0k, or about the same as for companion single bar specimens of the 11-8.5-11 series. The overlap of the projected stress cone areas can be seen for multiple bar Specimen 11-8.5-11-M, s = 11 in., in Fig. 4.6. No overlap exists for the bars spaced at 22 in. and therefore a larger capacity per bar would be expected.

Table 4.2 indicates the normalized average capacity of each bar in the multiple bar specimens and the capacities calculated using the stress cone procedure. Little difference exists between the capacities observed and those computed for the 7 in. walls with multiple bar specimens. This indicates that neither the 22 in. nor 11 in. bar spacings were small enough to influence anchorage capacity in the 7 in. walls. There is no overlap of projected stress cones for either the 11 or 22 in. spacing.

OVERLAPPING
PROJECTED
AREAS

DELETE AREA OF
ANCHOR HEADS

FACE

STRESS CONE

2 CLOSELY SPACED
ANCHOR BOLTS

STRESS CONE

45°

45°

SIDE
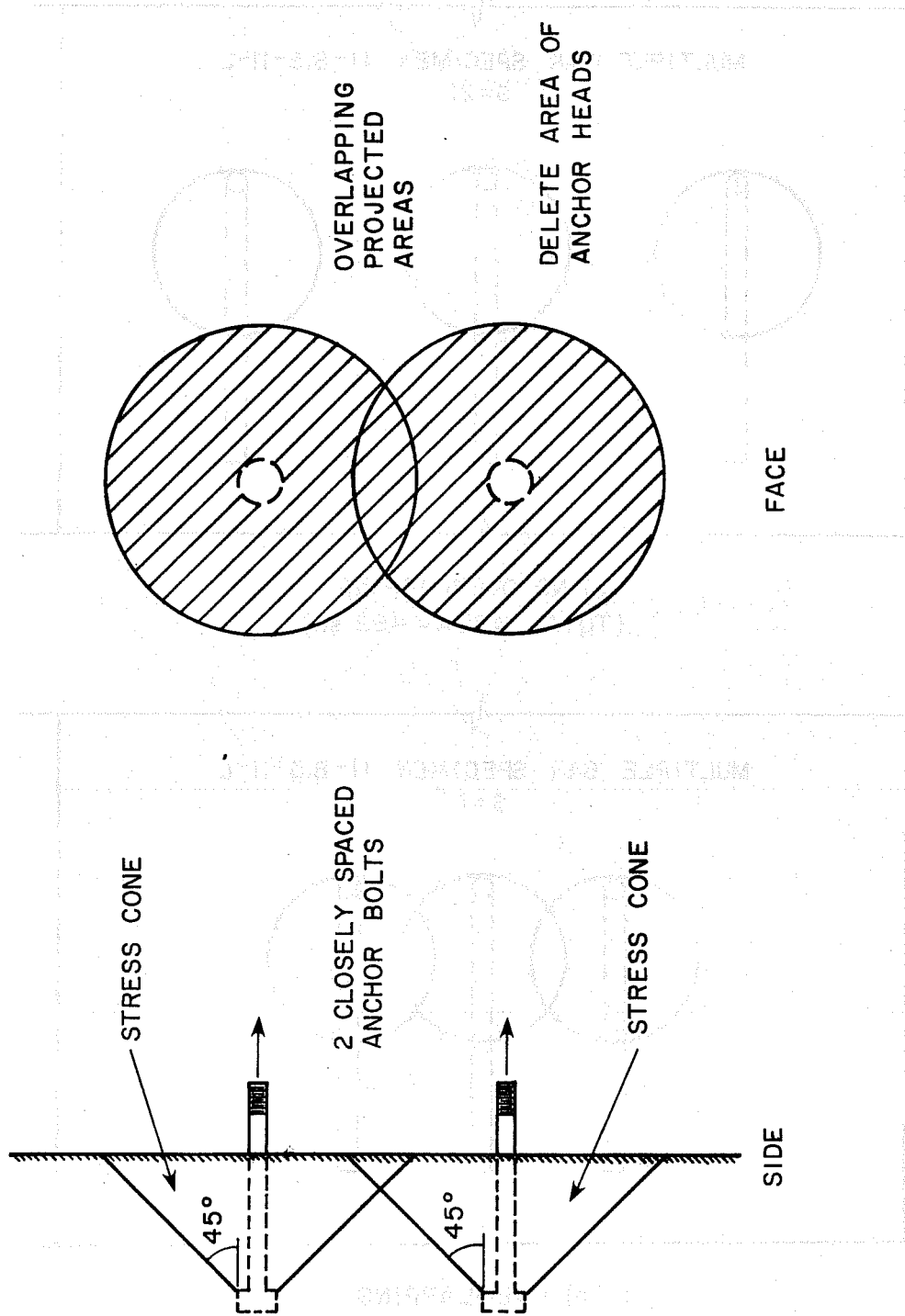
Fig. 4.5 Committee 349 recommendation for closely spaced embedments

MULTIPLE BAR SPECIMEN II-8.5-II-L
S=22"

a) NO OVERLAPPING
(TOTAL AREA = 462 si.)

MULTIPLE BAR SPECIMEN II-8.5-II-L
S=II"

b) OVERLAPPING
(TOTAL AREA = 421 si.)
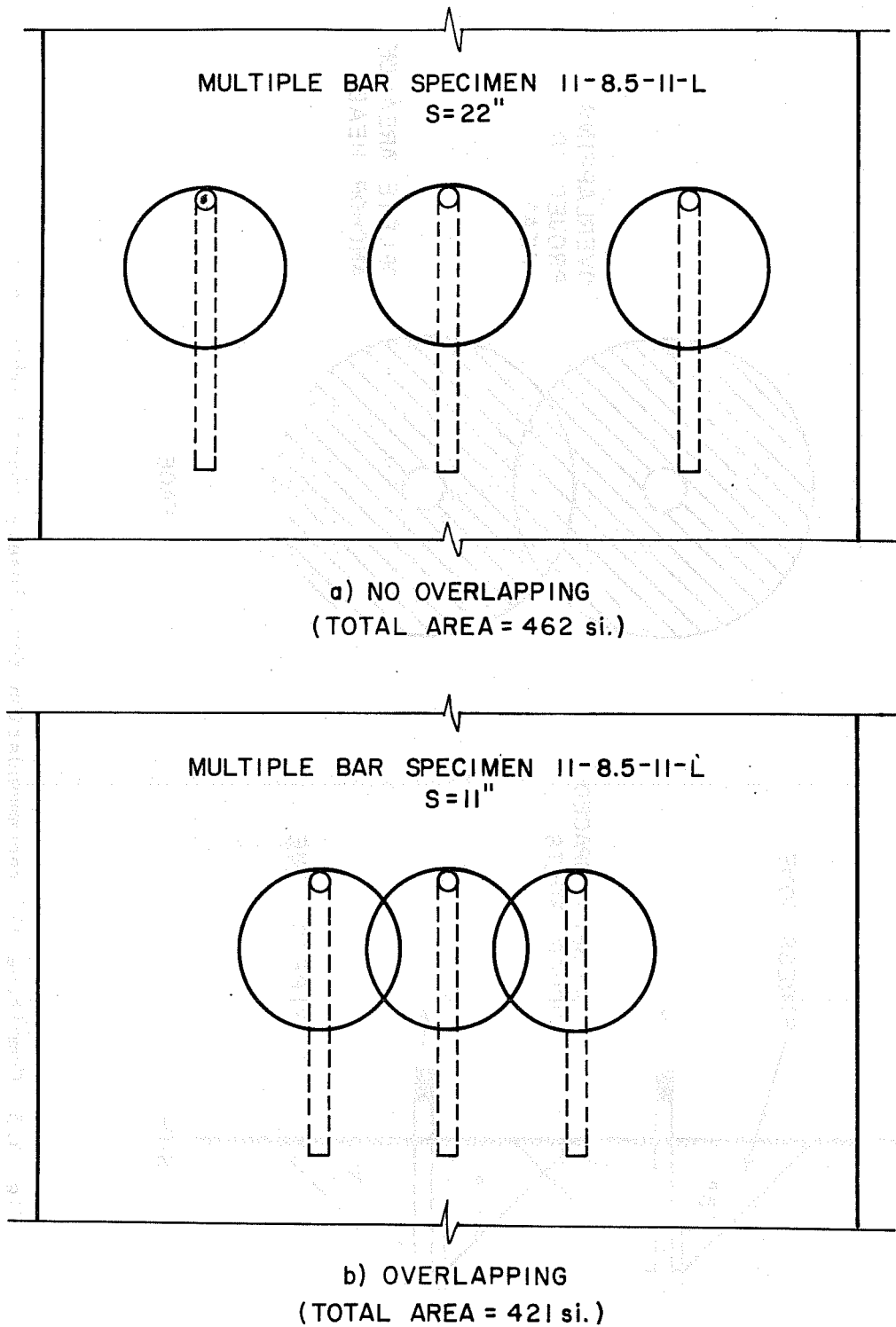
Fig. 4.6   Stress cone projected surface areas - #11 bars

TABLE 4.2 MEASURED VS STRESS CONE ESTIMATED CAPACITIES FOR THE MULTIPLE
           BAR SPECIMENS

| Specimen | Multiple Bar Specimens | | | Single Bar Specimen Capacity |
	Spacing (in.)	Avg. Normalized Bar Capacity (kips/bar)	Stress Cone* Est. Bar Capacity (kips/bar)	
7-7-11-M	11	26.0	25.5	
7-7-11-L	22	27.8	25.5	27.1k
11-8.5-11-M	11	41.4	37.7	
11-8.5-11-L	22	49.0	41.3	50.0k

*Based on f'_c = 4500 psi.

5. PROPOSED DESIGN RECOMMENDATIONS

5.1 Introduction

Because of the significant influence of beam depth on short hooked anchorage capacity, two approaches for the design of hooked bar anchorages with short embedment will be discussed. Approach A is the ACI Committee 408 proposal with added conditions. Approach B follows the same principles recommended for headed studs or anchor bolts by ACI Committee 349.

5.2 Design Recommendations

Approach A. The ACI Committee 408 proposal for the design of hooked bar anchorages can safely be extended into the short embedment range of $8d_b$, 6 in., or less under the following conditions:

(1) Only Standard 90° Hooks are to be used.

(2) An embedment beginning at the start of the hook shall be considered as minimum.

(3) #14 and #18 bars are excluded from these recommendations.

(4) The spacing between hooked bars must be $\geq 12d_b$.

(5) No reduction in anchorage length for confinement effects.

These conditions stem from the range of variables of this investigation. No short hooked bar anchorages larger than #11 were investigated because of the unrealistic nature of their use in thin walls. Condition (4) is suggested in order to exclude hooked bar spacings smaller than examined in this study. The stress developed by a standard hook with an embedment of ℓ_{dh} is given by Eq. 4.8.

Figure 4.1 indicated the generally conservative nature of the Committee 408 proposal in regard to short hooked bar anchorages. It should be noted that in the use of this approach the benefit of

extra capacity due to increased hook confinement resulting from a small beam depth is not taken into account. However, the simplicity, speed, and conservative nature of the ACI 408 proposal make it an excellent approach for use in situations where it is not critical that the designer determine the maximum capacity of a short hooked anchorage.

Approach B. The headed stud or anchor bolt stress cone failure procedure provides a more accurate estimate of hook capacity in beam-wall joints. Figure 4.4 shows that the results using this procedure fall on a curve that is perhaps the best fit through the data points of this study. Depending upon the internal lever arm length, the use of the single curve shown in Fig. 4.4 would be satisfactory for hooked bars in beams or slabs with effective depth of around 12 in. or less framing into thin walls.

A decrease in beam depth results in more confinement on the hook and provides greater anchorage capacity while an increase in beam depth reduces the capacity of the hooked bar. To reflect these conditions, upper and lower bounds based on Z are proposed as shown in Fig. 5.1. The upper bound represents the capacity of short hooked bar anchorages in walls where Z is 8 in. or less, and was determined by applying a factor of 11/8 to the curve in Fig. 4.4. The lower bound represents hook capacity for beam-wall joints where Z is 18 in. or greater, and was determined by applying a factor of 11/18 to the same curve in Fig. 4.4. The linear adjustments are simple and represent the data very well. Using linear interpolation between the upper and lower bounds, short hooked bar anchorage capacity can be determined. However, it should be noted that these curves apply only to hooked bars with no overlapping projected stress cones from adjacent anchorages. The recommended equation for such short hooked bar anchorages
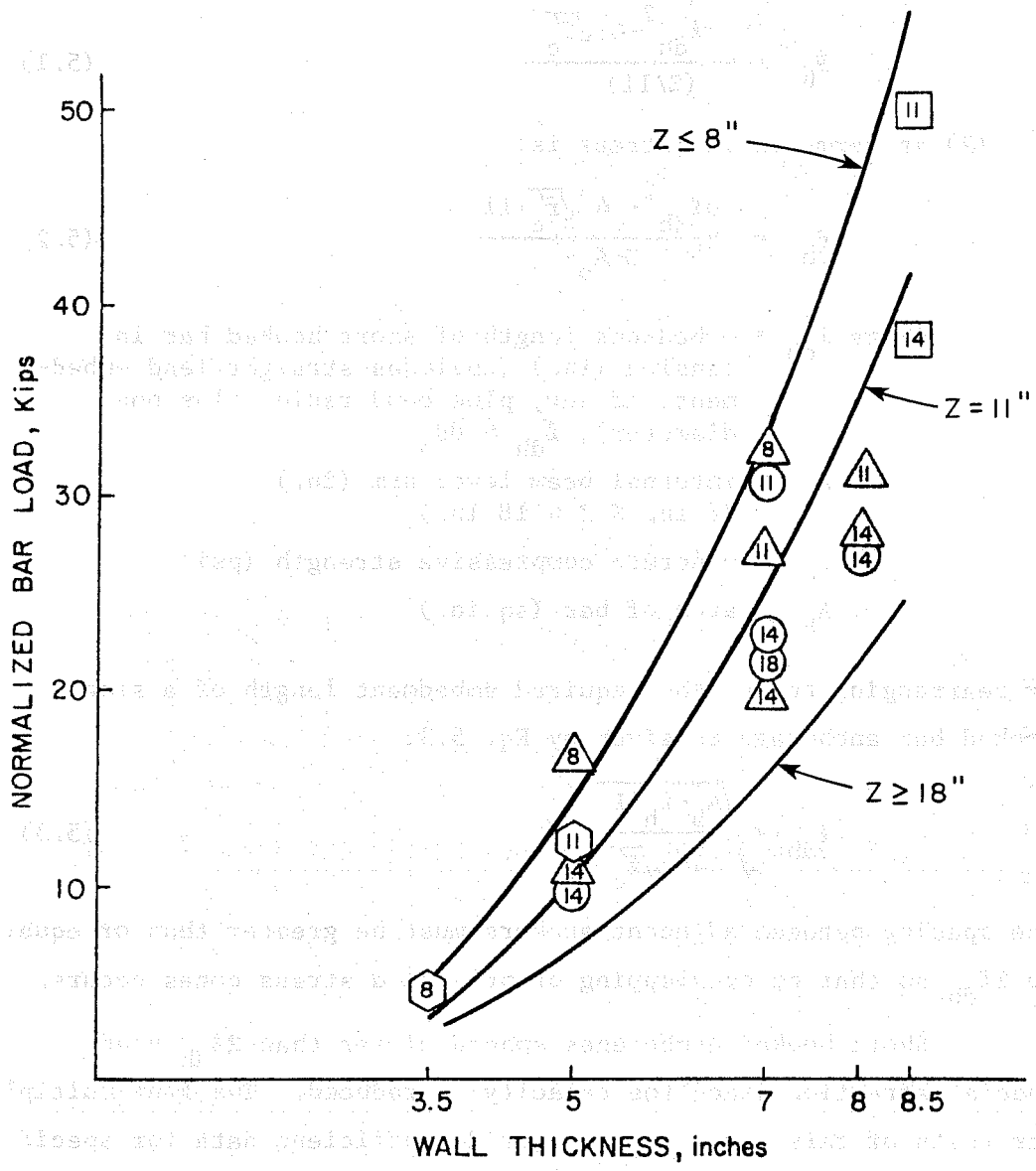
Fig. 5.1 Proposed stress cone upper and lower bounds

(1) in terms of bar load is:

$$P_h = \frac{\pi \ell_{dh}^2 \cdot 4 \sqrt{f_c'}}{(Z/11)}$$
(5.1)

(2) in terms of bar stress is:

$$f_h = \frac{\pi \ell_{dh}^2 \cdot 4 \sqrt{f_c'} \cdot 11}{Z \cdot A_b}$$
(5.2)

where ℓ_{dh} = embedment length of short hooked bar in tension (in.) (includes straight lead embedment, if any, plus bend radius plus one diameter), $\ell_{dh} \leq 8d_b$

Z = internal beam lever arm (in.) (8 in. $\leq Z \leq$ 18 in.)

f_c' = concrete compressive strength (psi)

A_b = area of bar (sq in.)

By rearranging terms, the required embedment length of a single hooked bar anchorage is given by Eq. 5.3:

$$\ell_{dh} = \sqrt{\frac{A_b \cdot f_h \cdot Z}{44\pi \sqrt{f_c'}}}$$
(5.3)

The spacing between adjacent anchors must be greater than or equal to $2\ell_{dh}$ so that no overlapping of projected stress cones occurs.

Short hooked anchorages spaced closer than $2\ell_{dh}$ need special attention since the capacity is reduced. The four multiple bar tests of this study do not provide sufficient data for specific recommendations to be made. However, as Table 4.2 indicated, considering the overlap of stress cone groups provided conservative estimates of hook capacity for each of the multiple bar specimens of this study. Perhaps the most tedious part of the stress cone group procedure is determining the total area of the overlapping stress cones. Figure 5.2 is a graphic representation of three

hooked bar anchorages. Fig. 5.2 depicts a spacing of 11 in. The

total projected area of the three overlapping cylinders (total

bearing area for equation ...) ... their areas for Zone ...

... cylinders (using an ...) ... equation ... projected area

to determine the area ... ... a given ...

$2\ell_{dh}$

11" 11"

1 **2** **3**
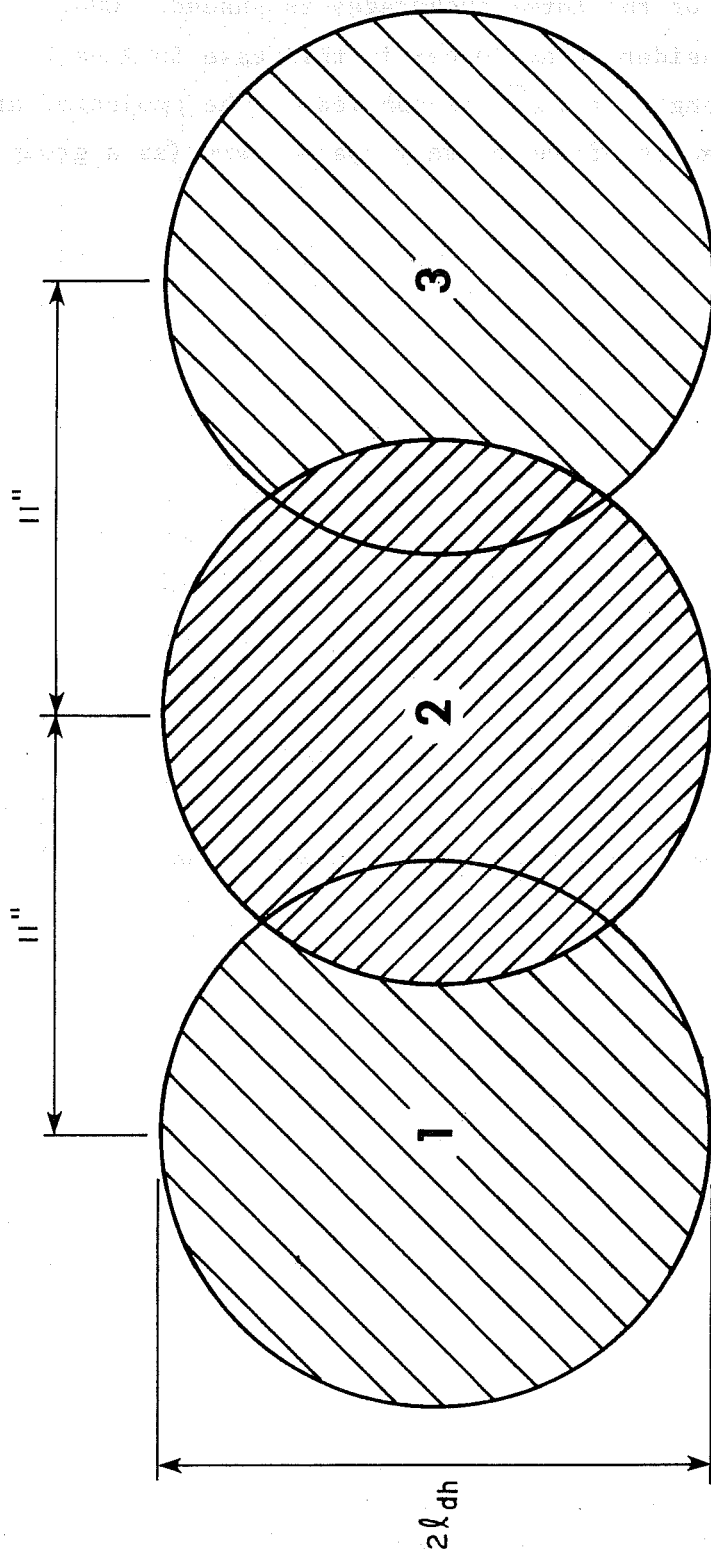
TOTAL PROJECTED AREA = AREAS 1 + 2 + 3

Fig. 5.2   Graphic representation of the projected stress cone area of
three hooked bars, ℓ_{dh} = 7 in., s = 11 in.

88

hooked bar anchorages, ℓ_{dh} = 7 in., at a spacing of 11 in. The
total projected area of the three anchorages is shaded. Over-
lapping areas are considered only once--in this case in Area 2. A
concrete tensile strength of $4\sqrt{f'_c}$ is applied to the projected area
to determine the capacity of the closely spaced bars (as a group).
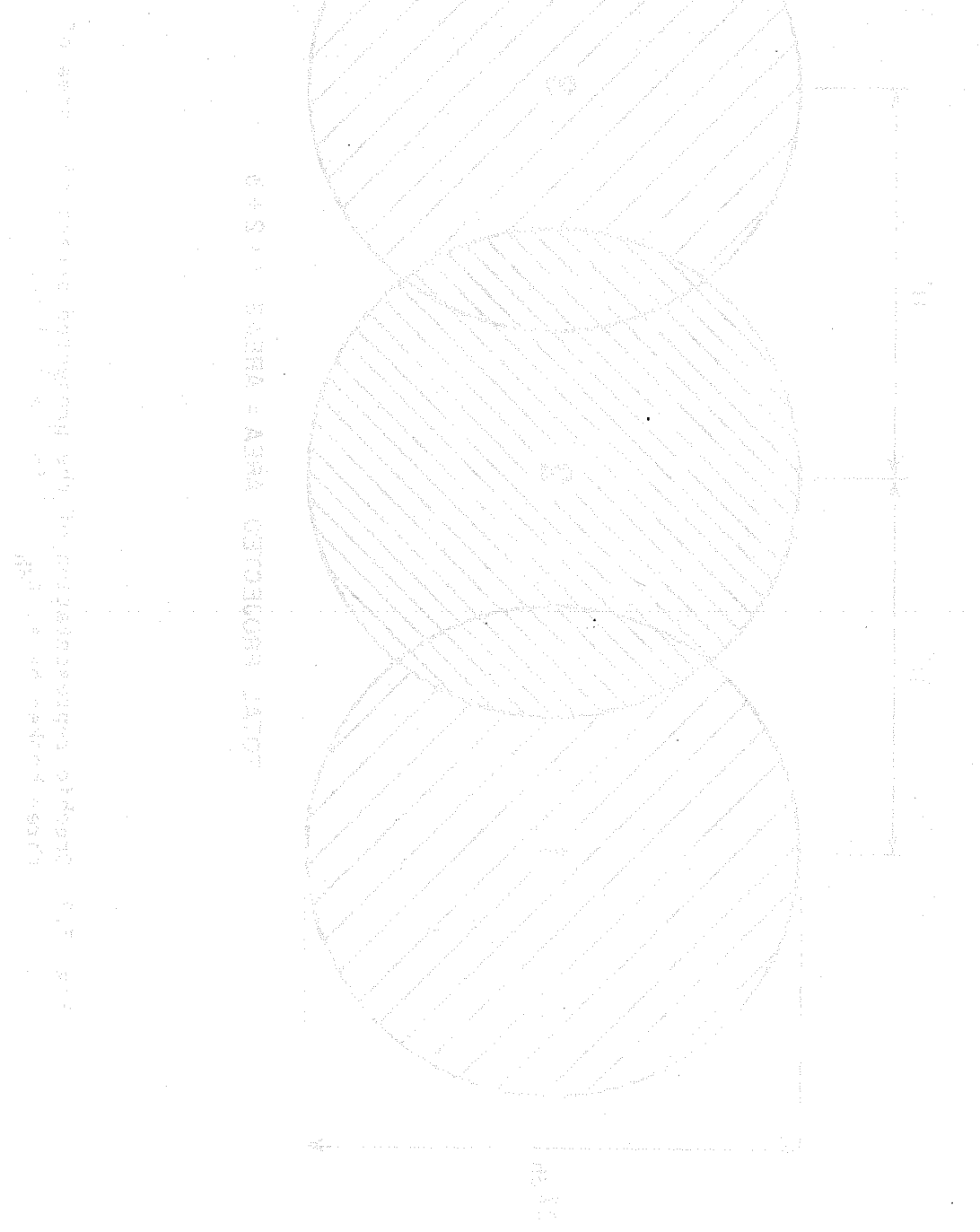
6. SUMMARY AND CONCLUSIONS

6.1 Experimental Program

In order to examine the behavior and evaluate the capacity of hooked bar anchorages with short embedment lengths, thirty-six specimens were tested. The program extended two previous hooked bar investigations from which changes in design procedures were proposed. The specimens were full-scale models of typical beam or slab wall joints. The effect of bar diameter, concrete strength, beam depth, lead embedment, transverse reinforcement, unbonded straight lead lengths, and spacing between hooked bars on hook capacity and mode of failure were examined. The slip of the hooked bar with respect to the concrete was measured during each test.

6.2 Summary of Behavior

Based on the test results of this investigation combined with an evaluation of previous hooked bar studies, the behavior of hooked bars with short embedment can be summarized as follows:

(1) Failure of a short (embedment $\leq 7d_b$) hooked bar anchorage in a wall is governed by a loss of cover in front of the hook, rather than pulling out or side splitting (as in beam-column joints).

(2) The characteristic cone-type of failure is similar to that observed in tensile tests of headed studs or anchor bolts.

(3) The capacity of hooked bar anchorages is directly proportional to $\sqrt{f'_c}$ for the range of concrete strength considered (2.5 - 5.5 ksi).

(4) The principal factor affecting the capacity of short hooked anchorages in beam-wall joints is beam depth. The anchorage

89

capacity is inversely proportional to beam or slab depth for effective beam depths from 8 to 18 in.

(5) Hooked bar strength and stiffness (stress/slip) increase as lead embedment increases.

(6) Small diameter hooked bars are the most efficient in developing stress for given wall thickness.

(7) A transverse bar placed in front of the hook has little, if any, influence on ultimate anchorage capacity. However, the anchorage appears to slip more before failure.

(8) Bond along the straight lead embedment has no influence on ultimate capacity.

(9) Hooked bars at small spacings show a decrease in ultimate capacity. However, more research is needed in this area.

6.3 Design Implications

Based on the test results, the following approaches are suggested for designing short hooked bar embedments:

Approach A: The equations

$$f_h = \frac{\ell_{dh}\sqrt{f'_c}\,\phi}{0.016d_b} \quad \text{or} \quad 63\,\frac{\phi\ell_{dh}}{d_b}\sqrt{f'_c} \tag{6.1}$$

$$\text{and} \quad \ell_{dh} = \frac{0.016\cdot d_b\cdot f_h}{\sqrt{f'_c}\,\phi} \tag{6.2}$$

are different forms of the same equation recommended for hooked bars by ACI Committee 408 and can be safely extended into the short embedment range of $\ell_{dh} = 8d_b$, 6 in., or less. (Embedment beginning at the start of the hook is minimum; spacing between hooks is $\geq 12d_b$, and ϕ is taken as 0.8.) However, since hook confinement is not accounted for by these equations, this approach may underestimate the capacity. It should also be noted that no reduction is needed to account for beam depth using this approach.

Approach B: The equations

$$f_h = \frac{140\ \ell d_h^2\ \sqrt{f'_c}}{Z} \tag{6.3}$$

and

$$\ell_{dh} = \sqrt{\frac{A_b \cdot f_h \cdot Z}{140\ \sqrt{f'_c}}} \tag{6.4}$$

similar to the recommendations of ACI Committee 349 for anchor bolt and other steel embedments, provide the best method of estimating short hooked anchorage capacity (where the effective depth Z is 8 in. $\leq$ Z $\leq$ 18 in. and spacing between adjacent hooked bars $\geq 2\ell_{dh}$.) ϕ has been omitted in this approach, but could be easily incorporated.

Short hooked bar anchorages spaced closer than $2\ell_{dh}$ should be evaluated considering the overlapping of failure surfaces. Approach B, stress cone procedure, can be easily adapted to account for the decrease in capacity.

REFERENCES

1. Minor, J., and Jirsa, J. O., "A Study of Bent-Bar Anchorages," Structural Research at Rice University, Report No. 9, Rice University, Houston, Texas, March 1971.

2. Marques, J. L. G., and Jirsa, J. O., "A Study of Hooked Bar Anchorages in Beam-Column Joints," Structural Research at Rice University, Report prepared at The University of Texas at Austin, Austin, Texas, July 1972.

3. Pinc, R. L., Watkins, M. D., and Jirsa, J. O., "Strength of Hooked Bar Anchorages in Beam-Column Joints," Structural Research at The University of Texas at Austin, CESRL Report No. 77-3, The University of Texas at Austin, Texas, November 1977.

4. ACI Committee 318, Building Code Requirements for Reinforced Concrete (ACI 318-77), American Concrete Institute, Detroit, Michigan, 1977.

5. ACI Committee 318, Commentary on Building Code Requirements for Reinforced Concrete (ACI 318-77), American Concrete Institute, Detroit, Michigan, 1977.

6. ACI Committee 349, Proposed Addition to: Code Requirements for Nuclear Safety Related Concrete Structures (ACI 349-76), American Concrete Institute, Detroit, Michigan, 1978.

7. ACI Committee 408, "Suggested Development, Splice, and Standard Hook Provisions for Deformed Bars in Tension," Concrete International, Vol. 1, No. 7, July 1979, pp. 44-61.